

IN PLANTA CHARACTERIZATION OF *Magnaporthe oryzae* BIOTROPHY-
ASSOCIATED SECRETED (BAS) PROTEINS AND KEY SECRETION
COMPONENTS

by

MARTHA CECILIA GIRALDO

B.Sc., Universidad del Valle, Cali, Colombia, 1996

AN ABSTRACT OF A DISSERTATION

submitted in partial fulfillment of the requirements for the degree

DOCTOR OF PHILOSOPHY

Department of Plant Pathology
College of Agriculture

KANSAS STATE UNIVERSITY
Manhattan, Kansas

2010

Abstract

Rice blast caused by the ascomycetous fungus *Magnaporthe oryzae* remains a threat to global sustainable agriculture and food security. This pathogen infects staple cereal crops such as rice, wheat, barley and millets, as well as turf grasses, in a distinct way among fungal plant pathogens, which we described in the first chapter. In addition to economical importance, rice blast is a model pathosystem for difficult-to-study biotrophic fungi and fungal-plant interactions. We are studying proteins that fungi secrete inside living cells to block plant defenses and control host cell processes; these proteins are called effectors. To date mechanisms for secretion and delivery of effectors inside host cells during disease establishment remain unknown. This step is critical to ensure the successful infection. So far, the only commonality found among all unique small-secreted blast effector proteins is their accumulation in a novel *in planta* structure called the biotrophic-interfacial complex (BIC). Identifying effectors and understanding how they function inside rice cells are important for attaining durable disease control. In the second chapter, we presented one approach to address this challenge. We characterized four candidate effector genes that were highly expressed specifically during the rice cell invasion. Using transgenic fungi that secrete fluorescently-labeled versions of each protein allowed me to follow them during invasion *in vivo* by live cell imaging. These candidates show distinct secretion patterns suggesting a spatially-segregated secretion mechanism for effectors. Results revealed a BIC-located strong candidate cytoplasmic blast effector, two putative cell-to-cell movement proteins and a putative extrainvasive hyphal membrane (EIHM)-matrix protein, which has become a valuable tool for assessing successful infection sites. In the third chapter, we test if normal secretion components of filamentous fungi are involved in accumulation of effectors into BICs. We report localization studies with *M. oryzae* orthologs of conserved secretion machinery components to investigate secretion mechanisms for effectors showing preferential BIC accumulation and for non-BIC proteins such as BAS4. Especially bright fluorescence adjacent to BICs from Mlc1p (Myosin Light Chain, a Spitzenkörper marker), from Snc1p (a secretory vesicle marker), and from Yup1p (a putative t-SNARE endosomal protein) suggest secretion actively occurs in the BIC-associated cells. Localization of Spa2p (a polarisome marker), as a distinct spot at the tips of the bulbous invasive hyphae (IH) *in planta*, suggests the existence of two secretion complexes after the fungus switches growth from the polarized filamentous primary hyphae to bulbous IH. In the final chapter on future perspectives, we present some strategies towards the molecular understanding of the *M. oryzae* secretion mechanism during biotrophic invasion, which will lead to novel strategies for disease control.

IN PLANTA CHARACTERIZATION OF *Magnaporthe oryzae* BIOTROPHY-
ASSOCIATED SECRETED (BAS) PROTEINS AND KEY SECRETION
COMPONENTS

by

MARTHA CECILIA GIRALDO

B.Sc., Universidad del Valle, Cali, Colombia, 1996

A DISSERTATION

submitted in partial fulfillment of the requirements for the degree

DOCTOR OF PHILOSOPHY

Department of Plant Pathology
College of Agriculture

KANSAS STATE UNIVERSITY
Manhattan, Kansas

2010

Approved by:

Major Professor
Dr. Barbara Valent

Copyright

MARTHA CECILIA GIRALDO

2010

Abstract

Rice blast caused by the ascomycetous fungus *Magnaporthe oryzae* remains a threat to global sustainable agriculture and food security. This pathogen infects staple cereal crops such as rice, wheat, barley and millets, as well as turf grasses, in a distinct way among fungal plant pathogens, which we described in the first chapter. In addition to economical importance, rice blast is a model pathosystem for difficult-to-study biotrophic fungi and fungal-plant interactions. We are studying proteins that fungi secrete inside living cells to block plant defenses and control host cell processes; these proteins are called effectors. To date mechanisms for secretion and delivery of effectors inside host cells during disease establishment remain unknown. This step is critical to ensure the successful infection. So far, the only commonality found among all unique small-secreted blast effector proteins is their accumulation in a novel *in planta* structure called the biotrophic-interfacial complex (BIC). Identifying effectors and understanding how they function inside rice cells are important for attaining durable disease control. In the second chapter, we presented one approach to address this challenge. We characterized four candidate effector genes that were highly expressed specifically during the rice cell invasion. Using transgenic fungi that secrete fluorescently-labeled versions of each protein allowed me to follow them during invasion *in vivo* by live cell imaging. These candidates show distinct secretion patterns suggesting a spatially-segregated secretion mechanism for effectors. Results revealed a BIC-located strong candidate cytoplasmic blast effector, two putative cell-to-cell movement proteins and a putative extrainvasive hyphal membrane (EIHM)-matrix protein, which has become a valuable tool for assessing successful infection sites. In the third chapter, we test if normal secretion components of filamentous fungi are involved in accumulation of effectors into BICs. We report localization studies with *M. oryzae* orthologs of conserved secretion machinery components to investigate secretion mechanisms for effectors showing preferential BIC accumulation and for non-BIC proteins such as BAS4. Especially bright fluorescence adjacent to BICs from Mlc1p (Myosin Light Chain, a Spitzenkörper marker), from Snc1p (a secretory vesicle marker), and from Yup1p (a putative t-SNARE endosomal protein) suggest secretion actively occurs in the BIC-associated cells. Localization of Spa2p (a polarisome marker), as a distinct spot at the tips of the bulbous invasive hyphae (IH) *in planta*, suggests the existence of two secretion complexes after the fungus switches growth from the polarized filamentous primary hyphae to bulbous IH. In the final chapter on future perspectives, we present some strategies towards the molecular understanding of the *M. oryzae* secretion mechanism during biotrophic invasion, which will lead to novel strategies for disease control.

Table of Contents

List of Figures	ix
List of Tables	xi
List of Supplemental Videos.....	xii
Acknowledgements.....	xiii
Dedication	xiv
Chapter 1 - Features of Live Rice Cell Invasion by the Blast Fungus <i>Magnaporthe oryzae</i>	1
Introduction.....	1
Fungal Effector Proteins	2
Diversity of Fungal Effectors.....	2
Detection of Effectors by Plant Cells.....	4
Evidence for Effector Delivery inside Living Plant Cells	5
Secretion Mechanism in Filamentous Fungi	8
<i>M. oryzae</i> : Glowing Inside Rice Cells.....	10
BIC Pattern: Secretion and Translocation of Effectors.....	11
Cell Boundaries: Trespassing the Borders Avoiding Detection	13
Dimorphism during Successful Biotrophic Interaction	14
Chapter 2 - <i>In Planta</i> Characterization of Candidate Blast Effector Proteins during Live Rice	
Cell Invasion by <i>Magnaporthe oryzae</i>	22
Abstract.....	22
Introduction.....	22
Results.....	25
Biotrophy-Associated Secreted Proteins in Rice Blast Disease	25
A BAS Protein that Accumulates in BICs and is Translocated into the Rice Cytoplasm	26
BAS Proteins with a Potential Role in Cell-to-Cell Movement.....	27
A BAS Protein that Outlines Invasive Hyphae Inside Rice Cells.....	29
Differential Expression of BAS Proteins in Compatible and Incompatible Interactions	30
Discussion.....	31
Biotrophy-Associated Secreted Proteins Distinctively Expressed during Compatible	
Interactions.....	31

BAS Proteins as Putative Effectors.....	33
EIHM Intactness Indicates Successful Blast Biotrophic Rice Cell Invasion at Individual Infection Sites in a Compatible Interaction.....	34
Material and Methods	35
Preparation of Infected Tissue and Live Cell Imaging.....	35
Assays for Growth and Plant Infection.....	36
Vector Construction, Fungal Transformation and Southern Analysis.....	36
Plasmolysis-Based Assay for Visualization of Translocated Cytoplasmic Effectors.....	38
Accession Numbers	38
Supplemental Data	38
Chapter 3 - Identification of the Spitzenkörper and Polarisome in <i>Magnaporthe oryzae</i> during Biotrophic Rice Invasion.....	60
Abstract.....	60
Introduction.....	61
Results.....	64
Candidate <i>M. oryzae</i> Orthologs of Widely Conserved Key Secretion and Cell Polarity Components	64
Localizing the Spitzenkörper (Spk) in <i>M. oryzae</i> Hyphae.....	66
Putative Endocytic Pathway Visualized by MoYup1:GFP.....	69
Labeling the <i>M. oryzae</i> Polarisome	70
Discussion.....	72
Dimorphism in <i>M. oryzae</i> during Biotrophic Invasion Labeled by Spk Markers	72
Differential Localization of the Spk and Polarisome in Bulbous IH	74
Potential Mechanism of Blast Effector Secretion to BICs.....	75
Blast Bulbous IH are Important for Live Rice Cell Invasion	75
Lessons from Localization of Fungal Secretion Components	76
Material and Methods	77
Assays for <i>M. oryzae</i> Live Cell Imaging <i>In Vitro</i> and <i>In Planta</i>	77
Fluorescence Recovery After Photobleaching – FRAP	78
Sequence analysis	78
FM4-64 staining <i>in vitro</i> and <i>in planta</i>	79

Vector Construction and Agro-mediated Fungal Transformation	79
Accession Numbers	80
Supplemental Data	80
Chapter 4 - Future Perspectives	105
Determine if the rice blast cell-to-cell movement occurs through plasmodesmata	106
Determine the protein or complex of proteins that interact with known effectors and BAS proteins <i>in planta</i>	107
References	109

List of Figures

Figure 1.1. A model of hyphal tip growth in filamentous fungi from Steinberg (2007a)	16
Figure 1.2. Pre-penetration phase of the life cycle of <i>M. oryzae</i> (Wilson and Talbot, 2009).....	17
Figure 1.3. Transmission electron microscopy (TEM) of appressorium penetration in a gentle and precisely controlled manner from Heath et al. (1992).	18
Figure 1.4. FM4-64 Stains <i>M. oryzae</i> hyphae <i>in vitro</i> but not IH <i>in planta</i>	19
Figure 1.5. Cartoon summarizing the BIC development from Khang et al. (2010).	20
Figure 1.6. Effector PWL2:mRFP translocation into invaded rice cells and movement into uninvaded rice cells, from Khang et al. (2010).	21
Figure 2.1. Constructs and expression of fluorescent chimeric proteins from <i>Agrobacterium</i> - mediated fungal transformation.	40
Figure 2.2. Distinct localization patterns of <i>M. oryzae</i> BAS proteins <i>in planta</i>	43
Figure 2.3. BAS1:mRFP secretion and co-localization with AVR-Pita:GFP proteins.....	44
Figure 2.4. BAS1:mRFP, but not BAS4:GFP, is translocated inside rice cytoplasm of invaded cells and moves into uninvaded neighbor cells.....	45
Figure 2.5. BAS2:mRFP and BAS3:mRFP accumulate at the cell wall crossing points where the fungus moves to neighbor cells.....	46
Figure 2.6. Southern blot hybridization of <i>BAS4</i> in different <i>M. oryzae</i> strains.....	47
Figure 2.7. Evidence for the <i>BAS4</i> gene knock-out (KO) mutant.	48
Figure 2.8. Restriction Enzyme Map of <i>BAS4</i> and the <i>BAS4</i> KO allele.	49
Figure 2.9. BAS proteins accumulate together with the effector PWL2 in susceptible, YT-16, but not in resistant, Yashiro-mochi, rice cells.....	50
Figure 2.10. BAS4:EYFP failed to outline IH and appeared in the host cell, indicating unsuccessful infection sites during compatible interactions.	51
Figure 3.1. Cartoon showing the criterion for selection of cellular secretion components based in their localization patterns in filamentous fungi.....	81
Figure 3.2. Phylogenetic trees of selected fungal proteins involved in secretion and the <i>M.</i> <i>oryzae</i> orthologs.....	82
Figure 3.3 FM4-64 staining of rice and <i>M. oryzae</i> membranes <i>in vitro</i> and <i>in planta</i>	86

Figure 3.4. Co-labeling of <i>M. oryzae</i> hyphae <i>in vitro</i> with MoMlc1:GFP and FM4-64	87
Figure 3.5. MoMlc1:GFP identified the Spitzenkörper during rice blast invasion.	88
Figure 3.6. Co-labeling MoMlc1:GFP and PWL2:mRFP localized the putative Spk with respect to the BIC during blast biotrophic invasion <i>in planta</i>	89
Figure 3.7. The Fluorescence Recovery After Photobleaching assay (FRAP) demonstrated continuous, stronger and faster dynamic activity of MoMlc1:GFP in the Spk of vegetative hyphae <i>in vitro</i>	90
Figure 3.8. Fluorescence Recovery After Photobleaching assay (FRAP) demonstrated continuous activity of MoMlc1:GFP at the Spitzenkörper of primary hyphae, <i>in planta</i>	91
Figure 3.9. MoSnc1p:GFP defines the Spitzenkörper <i>in vitro</i> and <i>in planta</i> at the growing hyphal tip	92
Figure 3.10. MoSnc1p:GFP in the first bulbous IH cell next to the BIC supports the hypothesis of active secretion in this cell.....	93
Figure 3.11. MoYup1:GFP co-localization with FM4-64 identified endocytic vesicles <i>in vitro</i>	94
Figure 3.12. <i>In planta</i> , a fungal strain expressing MoYup1:GFP and PWL2:mRFP showed localization of putative early endosomes and vacuoles with respect to BICs.	95
Figure 3.13 MoSpa2:GFP revealed the <i>M. oryzae</i> Polarisome <i>in vitro</i> and <i>in planta</i>	96
Figure 3.14. MoSpa2:GFP revealed <i>M. oryzae</i> Polarisome <i>in planta</i>	97
Figure 3.15. Localization of <i>M. oryzae</i> secretion components showed <i>in planta</i> differences between filamentous-polarized hyphae and bulbous invasive hyphae during compatible interactions.	98

List of Tables

Table 2.1. List of gene candidates characterized and <i>AVR</i> genes, <i>PWL2</i> and <i>AVR-Pita1</i>	52
Table 2.2. Testing candidate genes with different fluorescent proteins in different background strains.	53
Table 2.3. Primers used for KO and expression constructs of BAS proteins.	54
Table 2.4 Plasmids used for fungal transformation.	56
Table 2.5. Fungal transformant strains.	58
Table 3.1. Cellular markers for protein secretion components in filamentous fungi.	100
Table 3.2. Primers used for cloning and sequencing of cellular markers of <i>M. oryzae</i>	101
Table 3.3. Plasmids used for fungal transformation of <i>M. oryzae</i>	102
Table 3.4. Fungal transformants.	103
Table 3.5. FRAP experiment for MoMlc1:GFP recovery.	104

List of Supplemental Videos

Supplemental videos can be found with the item record for this thesis in the K-State Research Exchange (<http://krex.k-state.edu>).

- Supplemental Video 2.1. The rice leaf sheath inoculation assay.
- Supplemental Video 3.1. *In vitro*, MoMlc1:GFP labeling the Spk in *M. oryzae*.
- Supplemental Video 3.2. *In vitro*, FRAP of MoMlc1:GFP at the Spk *M. oryzae*.
- Supplemental Video 3.3. *In planta*, FRAP of MoMlc1:GFP at the Spk *M. oryzae*.
- Supplemental Video 3.4. *In planta*, MoSnc1:GFP localized in *M. oryzae* vegetative hyphae.
- Supplemental Video 3.5. *In planta*, MoYup1:GFP co-localized with PWL2:mRFP at 24 hpi.
- Supplemental Video 3.6. *In planta*, MoYup1:GFP co-localized with PWL2:mRFP at 27 hpi.
- Supplemental Video 3.7. *In vitro*, MoSpa2:GFP.
- Supplemental Video 3.8. *In planta*, MoSpa2:GFP at 22 hpi.

Acknowledgements

I wish to thank Dr. Barbara Valent for inspiring me with her work, for tutoring me day-to-day and for being a wonderful mentor. To Dr. Gloria Mosquera, Dr. Chang Hyun Khang, Dr. Guadalupe Valdovinos-Ponce, Dr. Mihwa Yi and Melinda Dalby for all their help, training, advice; for good discussions and specially groovy moments. To Diana Pavlisko, Anita Kesler, Morgan Fyffe and Jeanna Cox for all their support and for offering their generous friendship. To all the professors in the Plant Pathology Department for being available and willing to share their knowledge. To Dr. Joe Tohme for all his support and mentoring as a researcher since I began this path in 1995. To Dr. Frank White, Dr. Anna Whitfield, Dr. Gero Steinberg and Dr. Nicholas Talbot for all the vivid and rich discussions that encouraged me to improve my research skills. To Dr. James R. Nechols and Dr. Katsura Asano for their assistance and complete availability. To Dr. Philine Wangemann and Joel Sanneman for their support in confocal microscopy. And specially, to my family for all their encouragement and motivation.

Dedication

To God and to the most important people in my life; my husband Frank and our son Santiago who give me their love, support and motivation; my parents, Martha Zapata and Cesar Augusto Giraldo who taught me about faith, hard work, determination and dedication. These skills help me to reach any goal through and on behalf of God.

Chapter 1 - Features of Live Rice Cell Invasion by the Blast Fungus

Magnaporthe oryzae

Introduction

The challenge that humanity will face in 2035 to ensure sustainable agriculture will be to produce more food on reduced land with less availability of water, for a population that grows exponentially (FAO, 2003; Khush, 2005; FAO, 2009; Gerbens-Leenesa et al., 2009). Among the biotic factors that limit us in overcoming this challenge are plant pathogens that annually and worldwide cause extensive yield losses on staple crops. Rice production does not increase at the same speed as the demanding population, although rice is a staple crop on which more than half of the global population depends (Khush, 2005; FAO, 2006, 2009). Globally, considerable yield losses in rice are caused by the “cereal killer” (Talbot, 2003; Khush, 2005) *Magnaporthe oryzae* B. Couch, anamorph *Pyricularia oryzae* (Couch and Kohn, 2002; Dean et al., 2005; Ebbole, 2007).

Live-cell imaging of the ascomycetous fungus *M. oryzae* using rice leaf sheaths, a methodology for clear cytological observations, first described by Sakamoto (1949) and more recently by Koga et al. (2004), revealed unique features displayed by this fungal plant pathogen during biotrophic invasion (Bourett et al., 2002; Czymbek et al., 2002; Kankanala et al., 2007; Mosquera et al., 2009; Khang et al., 2010). After recognition of appropriate surface conditions, the blast fungus forms specialized structures called appressoria to enter into first host cells (Howard and Valent, 1996; Talbot, 2003). After an unnoticed penetration, the fungus first grows inside live rice cells as polarized-specialized invasive hyphae (IH), called primary hyphae, which are enclosed by a plant-derived membrane called extrainvasive hyphal membrane (EIHM) (Kankanala et al., 2007). In a compatible interaction, this filamentous IH turns into a bulbous IH, which completely packs the first invaded cell and switches again to a polarized IH to cross to neighbor cells (Heath et al., 1990a; Kankanala et al., 2007; Veses and Gow, 2009). For successful infection, biotrophic fungi that invade living plant cells must block plant defenses to sustain healthy rice cells during the invasion. Effector proteins are predicted to be delivered into the cytoplasm of susceptible plant cells to enable a compatible interaction. When rice-blast resistance (*R*) gene products target predicted cytoplasmic effectors, also called avirulence (*AVR*)

gene products, the plant resistance response is induced, eliciting an incompatible interaction by which the fungus is disabled in invading new cells (Flor, 1971; Jia et al., 2000; Hulbert et al., 2001). Among all known blast cytoplasmic effector proteins, which are unique small-secreted proteins, the single commonality found is their accumulation in a novel *in planta* structure called the biotrophic-interfacial complex (BIC) (Khang et al., 2010). How effector proteins cross the EIHM to reach the rice cytoplasm and influence the plant defenses is still unknown. We present a review of the most remarkable findings in the biology of the *M. oryzae* biotrophic interaction in the context of what is known about fungal effectors and the secretion mechanism in filamentous fungi. A better understanding of this intimate relationship can guide us to proficient strategies of disease control.

Fungal Effector Proteins

Knowledge of pathogenicity in fungi was limited to development of specialized infection structures, secretion of enzymes and production of toxins, but new findings suggest that filamentous pathogens as well as bacterial pathogens secrete an arsenal of effector proteins that modulate plant innate immunity, manipulate plant cells and promote disease. Interest in effector proteins increases as genome sequences become available for numerous filamentous pathogens, resulting in genome-wide catalogs of effector secretomes. Biotrophic and hemibiotrophic plant pathogens establish intimate contact with their host's cytoplasm by inserting specialized infection structures as intracellular hyphae or haustoria. For the establishment of disease, delivery of effectors specifically, avirulence (AVR) proteins plays a critical role. However, little is known about their delivery and their interaction inside the host cells. To understand the mechanism used by these pathogens to secrete effectors into the host cytoplasm, we need to understand their structure and biochemistry. In that direction, it is also important understand their function and their interaction with the corresponding plant resistance (R) proteins.

Diversity of Fungal Effectors

Known fungal effectors display a diverse protein structure and composition that makes the task of finding additional effectors challenging. Fungal effectors are typically small proteins, less than 200 amino acids, and some present avirulence (AVR) activity. AVR effector proteins activate host defenses via recognition by their specific host resistance protein. Because of the

different strategies of invasion, intracellular or extracellular, fungal AVR proteins can be recognized as cytoplasmic or apoplastic effector proteins. In general, fungal effector proteins are distinguished by small size, the presence of a signal peptide that directs them to be secreted, and the lack of a known enzymatic role (Rep et al., 2004; Kamoun, 2007; de Wit et al., 2009). In addition to these characteristics, the apoplastic effectors of extracellular fungal pathogens are typically cysteine (cys)-rich.

These few characteristics have been extensively used to identify new AVR fungal proteins. Based on their ability to trigger a host hypersensitive response (HR), effectors from different fungal plant pathogens were identified via map-based cloning as follows: from *Melampsora lini*, flax rust AvrL567 (Dodds et al., 2004); from *M. oryzae*, rice blast AvrPita, PWL1 and PWL2 (Sweigard et al., 1995; Orbach et al., 2000; Bryan et al., 2000b; Jia et al., 2004); and from *Blumeria graminis*, powdery mildew Avra10 and AvrK1 (Ridout et al., 2006).

Based on their infection-specific expression, identification of expressed sequence tags (ESTs), led to the identification of effectors and putative effectors from *Uromyces fabae*, rust haustoria UfRTP1 (Hahn et al., 1997; Catanzariti et al., 2006); from *M. oryzae*, rice blast BAS1-4 (Mosquera et al., 2009); from *M. lini*, flax rust AvrM, AvrP4, and AvrP123 (Catanzariti et al., 2010); and from *Ustilago maydis*, corn smut MIG1 and MIG2 (Basse et al., 2000; Basse et al., 2002). In silico prediction generated a list of candidate effector genes from *M. oryzae* (Dean et al., 2005) and *U. maydis* (Kämper et al., 2006). Moreover, genome sequencing and association genetics using two isolates of *M. oryzae* led to the identification of three blast AVR effector genes, *AVRPia*, *AVRPii*, and *AVRPik/km/kp* (Ballini et al., 2008; Yoshida et al., 2009).

Although many effector genes from different fungal plant pathogens have been identified, no common motifs have been found that help in the search for new effector proteins. However, efforts to find new fungal effector proteins revealed they have in common a high diversity of protein sequence, small size and avirulence activity, and cys-rich characteristics for apoplastic effectors, as the only commonalities among them.

Regarding the main characteristics defined for fungal effector proteins, outliers can be found. Some avirulence proteins are not typical secreted effector proteins, as in *M. oryzae*, where the gene encoding avirulence conferring enzyme1 (ACE1) is specifically recognized by rice (*Oryza sativa*) cultivars carrying the resistance gene *Pi33*. ACE1 encodes a putative hybrid between a polyketide synthase (PKS) and a nonribosomal peptide synthetase (NRPS), which are

two distinct classes of enzymes involved in the production of secondary metabolites. Ace1 biosynthetic activity is required for avirulence and detection, suggesting that a small secondary metabolite molecule is recognized by the Pi33 protein (Böhnert et al., 2004).

At least two more cases are found for filamentous plant pathogens in which virulence proteins are not restricted to those that contain a predicted signal peptide for secretion and targeting to host cells. In the barley powdery mildew fungus *Blumeria graminis* f. sp. *hordei* (Bgh), *AVRk1* and *AVRa10*, the first identified candidate effector genes (cloned by positional cloning), are not predicted to contain signal peptides for secretion via ER (Ridout et al., 2006). Ridout et al. (2006) demonstrated that AVRk1 and AVRa10 are functional inside the cytoplasm of barley cells carrying *Mkk1* and *Mla10* resistance genes, respectively. As well, transient expression experiments of AVRa10 and AVRk1 in susceptible barley cells indicated that these effectors enhance the virulence phenotype.

Other outliers with characteristics of transcription factors are encoded by the *Phytophthora infestans* *Avr3b-Avr10-Avr11* locus, the candidate avirulence gene *pi3.4*, which controls avirulence to three potato resistance genes *R3b*, *R10*, and *R11* (Jiang et al., 2006). This avirulence gene encodes the largest fungal AVR protein with 1956 amino acids and an N-terminal WD40 regulatory domain. At the C-terminus it has a nuclear localization signal, an acidic domain and a leucine zipper. Analysis of the gene sequence from *P. infestans* field isolates revealed that the *pi3.4* amplification correlated with avirulence; isolates virulent on R3b, R10, and R11 plants lack the amplified gene cluster. The function of *Pi3.4* is unknown, but the combination of a NLS, an acidic domain, and a leucine zipper often occurs in transcription factors (Jiang et al., 2006).

Detection of Effectors by Plant Cells

Detection of effector proteins by the plant cells can be extracellular or intracellular (Hulbert et al., 2001; Chisholm et al., 2006; Jones and Dangl, 2006; de Wit et al., 2009). Structures involved in intracellular effector delivery are: the invasive hyphal structure in *M. oryzae*, and the form-specialized feeding structures called haustoria that penetrate the host plant cell walls while extracellular hyphae continue growing in the extracellular compartment (Perfect and Green, 2001; de Wit et al., 2009; Valent and Khang, 2010). Haustoria, which remain separated from the host cytoplasm by a double membrane, are produced by filamentous fungi

such as rust and powdery mildew fungi, and by oomycetes such as downy mildews and *Phytophthora* species (Birch et al., 2006; Catanzariti et al., 2006; Kamoun, 2007). The majority of known resistance proteins to fungal and oomycete pathogens are cytoplasmic nucleotide binding site/leucine-rich repeat (NBS-LRR) proteins, just as they are for bacterial pathogens. Oomycete avirulence proteins have been shown to enter the host cell in a two-step process involving signal peptide-mediated secretion followed by host cell uptake mediated by a second signal, the RxLR-EER motif that is involved in host cell targeting.

Some filamentous plant-pathogens secrete a diverse family of inhibitors into the plant apoplast, which presents a protease-rich environment in which proteases are integral components of the plant defense response. In the apoplast, membrane-spanning R proteins similar to extracellular receptors recognize these inhibitors. During infection, *Cladosporium fulvum* secretes Avr2 into the apoplast of tomato leaves where it binds and inhibits the extracellular tomato cysteine protease Rcr3 and forms a complex that enables the Cf-2 protein to activate the host hypersensitive response (HR) (Rooney et al., 2005). In *P. infestans*, Kazal-like (conserved Kazal domain motifs) extracellular protease inhibitors (EPI), EPI1 and EPI10 are multidomain-secreted serine protease inhibitors that bind and inhibit the pathogenesis-related protein P69B, a subtilisin-like serine protease pathogenicity related (PR) protein of tomato (Tian et al., 2005). *P. infestans* also secretes EPIC1 to EPIC4, a new family of secreted proteins with similarity to cystatin-like protease inhibitor domains. EPIC2B interacts with and inhibits a novel papain-like extracellular Cys protease, termed *Phytophthora* Inhibited Protease 1 (PIP1). PIP1 is a PR protein closely related to Rcr3, a tomato apoplastic Cys protease that functions in fungal resistance and is targeted by the protease inhibitor Avr2 of *C. fulvum* (Tian et al., 2007).

Evidence for Effector Delivery inside Living Plant Cells

One of the few examples of direct interaction between R and AVR proteins is the interaction between the first cloned pair of blast resistance–*Avr* genes, the rice Pita resistance protein and the secreted AVR-Pita protein from the rice blast fungus, *M. oryzae*. Pita is a NBS-LRR protein, a member of the largest class of R gene products (Bryan et al., 2000a; Bryan et al., 2000b; Jones and Dangl, 2006), and *AVR-Pita* from the rice blast fungus encodes a putative zinc-dependent metalloprotease that is not essential for pathogenicity (Jia et al., 2000; Orbach et al., 2000). By circumstantial evidence using yeast two-hybrid and *in vitro* membrane-binding

systems, Jia et al. (2000) demonstrated that transient expression of this AVR effector protein in the cytoplasm of rice cells with Pita triggers HR, suggesting that this Avr protein enters the plant cell.

In the flax rust fungus *Melampsora lini*, Catanzariti et al. (2006) identified genes encoding haustorially-expressed secreted proteins (HESPs) by screening a flax rust haustorium-specific cDNA library. Avirulence activity was confirmed for some of these proteins by transient expression assays in flax, which induced resistance gene-mediated cell death with the appropriate specificity. HESPs, AvrL567, AvrM, AvrP123 and AvrP4, induce cell death when expressed intracellularly in flax rust varieties with the corresponding *R* gene products, suggesting their translocation into plant cells during infection (Dodds et al., 2004; Catanzariti et al., 2006). Direct interaction was proven for the variable flax rust AvrL567 proteins and the flax L5, L6, and L7 resistance proteins by a yeast two-hybrid assay (Dodds et al., 2006). Recently, Catanzariti et al. (2010) showed direct interaction of AvrM with the M protein in yeast and also demonstrate that the C-terminal domain of AvrM is essential for M-dependent hypersensitive response.

Kemen et al. (2005) demonstrated the secretion of a rust haustorial-secreted protein into the infected plant cell. The rust transferred protein 1 from *Uromyces fabae* (Uf-RTP1p) has a unique feature, a bipartite nuclear localization signal (NLS), RQHHKR[X9]HRRHK, in addition to the classical signal peptide. Direct evidence that this protein is translocated into host cell was presented by expression of GFP-Uf-RTP1 fusion protein in tobacco protoplasts and by immunofluorescence and electron microscopy in bean plants. The GFP-Uf-RTP1 protein was detected in the nuclei, and at the host parasite interface in the extrahaustorial matrix.

For oomycete effector proteins, functional analysis described a conserved dual peptide motif RxLR-EER required for delivery inside host cells (Armstrong et al., 2005; Rehmany et al., 2005; Birch et al., 2006; Whisson et al., 2007). More than 400 genes encode potential secreted RxLR-EER effectors and many are up-regulated during infection (Whisson et al., 2007). These motifs contain shared RxLR sequences (for arginine, any amino acid, leucine, and arginine) located downstream of the signal peptide. Many also have an EER sequence (for double glutamic acid and arginine) occurring within 25 amino acids of the RxLR. Both motifs have been implicated in host translocation (Birch et al., 2006). The RxLR motif of oomycetes resembles the PEXEL motif (RxLxE/D/Q) found in the human malarial pathogen *Plasmodium*

falciparum, which belong to apicomplexa, a group of protists-animal parasites. The apicomplexa parasite occupies the parasitophorous vacuole after entering the erythrocyte, and the effectors are secreted into the vacuole. The PEXEL motif-containing proteins are then selectively delivered into the erythrocyte cytoplasm (Bhattacharjee et al., 2006).

Bhattacharjee et al. (2006) provided the first visual evidence of translocation of *Plasmodium* effectors into the erythrocytes mediated by this motif. Using the PEXEL motif from *P. falciparum* as a control, they demonstrated that the oomycete motif operates as the host-cell-targeting signal in *P. falciparum*, suggesting that there might be a common delivery mechanism for both pathogens. Whisson et al. (2007) used cell biology to demonstrate that the RxLR-EER effector, AVR3a, is secreted from haustoria and translocated from the extrahaustorial matrix to the plant cells. The replacement of RxLR-EER with alanine residues, or with the sequence KMIK-DDK that more closely maintained the native structure of the Avr3a protein, proved that this motif is required for its translocation into the host cell. Transformants expressing Avr3a-mRFP failed to demonstrate translocation into the host cytoplasm. Confirmation of the delivery of a plant pathogen effector into the host cell was presented by fusion of Avr3a with a gene encoding β -glucuronidase (GUS), a cytoplasmic enzyme that is reported to be inactive in the apoplast (Denecke et al., 1990; Yan et al., 1997). Under the assumption that the GUS reporter is only expressed after delivery to the host cytoplasm, we would say that they present the first evidence of RxLR-EER for a host cell targeting sequence. Unlike plasmodium and oomycetes, the most recent case in the same phylum apicomplexa parasite, *Theileria*, no specific signal has yet been targeted for introduction into the host cell (Ravindran and Boothroyd, 2008). Their sporozoites can enter host cells in any orientation and in a process that does not depend on the actin cytoskeleton of the parasite. The host secretory organelles are not thought to be involved in parasite binding and entry into the host cell, but somehow in parasite escape from host plasma membrane and subsequent polymerization of free microtubules around the parasite. The host membrane surrounding *Theileria* breaks down immediately upon invagination and the released parasite differentiates into the multinucleated stage that lives directly in the host cytoplasm rather than in a parasitophorous vacuole (PV). This facilitates the parasite proteins to interact with and modify the host cell, in contrast to plasmodium proteins that need to cross a PV membrane (Ravindran and Boothroyd, 2008).

Results from Khang et al. (2010) provided the first visual evidence of *M. oryzae* effector translocation into the rice cells, using both plasmolysis-based and nuclear targeting-based translocation assays. This work focused on PWL2, a blast AVR effector that prevents pathogenicity towards weeping lovegrass (*Eragrostis curvula*), and accumulates as other known blast effectors in the biotrophic-interfacial complex (BIC). Use of constructs containing a nuclear localization signal fused to the fluorescent effector enhanced visualization of its translocation inside the rice nuclei of the invaded cell as well as ahead in uninvaded neighbor cells. For *M. oryzae*, no motif sequence is known to be responsible for the effector translocation.

Secretion Mechanism in Filamentous Fungi

The secretory pathway of eukaryotic organisms, in general, begins with free ribosomes in the cytosol where the synthesis of most secretory proteins occurs. All nuclear-encoded mRNA are translated on cytosolic ribosomes. Ribosomes synthesizing nascent proteins in the secretory pathway are directed to the rough endoplasmic reticulum (ER) by an ER signal sequence. After the proteins are completely translated in the ER, they move via transport vesicles to the Golgi complex, Golgi transport vesicles and Golgi cisternae. From there, the proteins are further sorted to several destinations, secretory or transport vesicles, lysosomes, or the plasma membrane (Lodish et al., 2008).

Small transport vesicles bud off from the ER and fuse to form the cis-Golgi reticulum. By cisternal migration, cis-Golgi vesicles with their luminal protein cargo move through the Golgi complex to the trans-Golgi reticulum. Proteins are retrieved from the cis-Golgi to the ER and from later Golgi cisternae to earlier ones by small retrograde transport vesicles (Lodish et al., 2008). Since secretory proteins are synthesized in association with the ER membrane, some signal-sequence recognition mechanism must target them there.

A typical eukaryotic signal peptide contains a positive charge at the N-terminus, a highly hydrophobic core, and a hydrophilic C-terminus. After this C-terminus is where the likely cleavage site occurs, enabling the protein to either to be secreted or to become a membrane component (Sweigard et al., 1995). In general, signal peptide refers to the sequence of 20 to 30 amino acids that interacts with the signal recognition particle and directs the ribosome to the endoplasmic reticulum where co-translational insertion takes place. However, signal peptide can also refer to sequences that direct posttranslational uptake by organelles. The signal sequence is

normally removed from the growing peptide by a specific protease located on the cisternal face of the ER. The protein continues to form and is constricted into the ER lumen by the translocon. The remaining C-terminus of the secreted protein is drawn into the ER lumen, the translocon gate closes, and the secreted protein assumes specific conformation for its final destination (Lodish et al., 2008).

Fluorescently-labeled proteins have been used to characterize the secretory pathway in eukaryotes *in vivo*. These studies facilitated the identification of the main compartments and proteins-markers of the secretory pathway (Drees et al., 2001; Sudbery and Court, 2007; Shivas et al., 2010). Different functional analyses in *Neurospora*, *Aspergillus*, *Saccharomyces* and *Ustilago*, mainly using temperature sensitive mutants, provided a conserved model for the secretion mechanism in filamentous fungi, as described by Steinberg (2007) and Shoji et al. (2008) and summarized in Figure 1.1.

The review of Shoji et al. (2008) on molecular progress in understanding of the vesicular trafficking in filamentous fungi with a high secretion capability, presented a model for the secretion pathway with four main steps: (1) Newly synthesized secreted proteins enter ER, where they are folded and glycosylated, (2) These proteins are delivered to the Golgi apparatus by vesicular trafficking mediated by soluble N-ethylmaleimide-sensitive factor attachment protein receptor (SNARE) proteins, (3) After additional glycosylation in the Golgi, the proteins are secreted at hyphal tips, (4) Unfolded proteins are sorted in the ER, and targeted to either proteasomes or to vacuoles for degradation. This model operates by molecular mechanisms of membrane fusion, conserved between ER-Golgi, Golgi-plasma membrane and Golgi-vacuole transport, achieved by the fusion of SNARE proteins on secretory vesicles (v-SNAREs) specifically to t-SNAREs on the target membrane (Söllner et al., 1993). Protein secretion is believed to mainly occur at hyphal apices, but some secretion also appears to occur at tubular networks close to the plasma membrane of subapical regions and along newly-formed septa (Maruyama et al., 2006; Valkonen et al., 2007; Shoji et al., 2008).

Studies based on the fungal model systems *Neurospora*, *Aspergillus* and *Saccharomyces* support evidence for differences in organization of the secretory pathway between filamentous fungi and budding yeast, supporting the model of two secretion pathways, regulated and constitutive exocytosis. Filamentous fungi, known for their high secretory capacity, may have required an expansion in the number of the secretion related small GTPases, a monomeric class

of guanine nucleotide-binding proteins. Small GTP-binding proteins, *cdc42* and *Rho3*, members of the Rho family play a critical role in *M. oryzae* morphogenesis during pathogenicity (Zheng et al., 2007; Zheng et al., 2009). Secretion-related small GTPases like Rab/Ypt (*Ras* genes from rat brain/yeast protein transport) and ARF (ADP-ribosylation factor) that diverge from the Ras superfamily viruses (Harvey and Kirsten rat sarcoma) play critical roles during secretory and endocytic trafficking (Conesa et al., 2001; Punt et al., 2001; Talbot, 2003; Shoji et al., 2008). The *M. oryzae* database contains ~ 116 GTPase-like and 53 Ras-like proteins (http://www.broadinstitute.org/annotation/genome/magnaporthe_grisea/MultiHome.html). In contrast, nine genes encode Ypt proteins in yeast that have a role in exocytosis (Segev, 2001).

Not all secretory proteins in filamentous pathogens have signal peptides (SP) that allow them follow the classical or default pathway, through endoplasmic reticulum (ER) and Golgi. Those few proteins that are secreted without a SP are assumed to follow an undescribed non-classical pathway. Even though pathways are identified and a general model for secretion in filamentous fungi is illustrated, the fungal effector secretion mechanism is not clear.

***M. oryzae*: Glowing Inside Rice Cells**

Under moist environmental conditions on the rice leaf surface, an *M. oryzae* spore lands on a leaf and attaches by a mucilage at the spore tip. This mucilage is deposited at the spore apex and is called spore tip mucilage (Figure 1.2) (Hamer et al., 1988; Bourett and Howard, 1990; Koga and Nakayachi, 2004). In presence of the right physical properties, a hydrophobic hard surface, appressorium development is stimulated at the tip of the germination tube. Appresoria are dome-shaped structures that are highly melanized and that accumulate significant levels of glycerol (Chumley and Valent, 1990; Howard and Valent, 1996; Talbot, 2003). To enter into the first rice cell, the spore undergoes autophagocytosis, redeploying nutrients to generate the turgor pressure (deJong et al., 1997) (~80 atmospheres of pressure) that the appressorium needs to penetrate; but this entry occurs in a gentle and precisely controlled manner without disrupting the rice plasma membrane (Figure 1.3) (Howard et al., 1991; Heath et al., 1992; deJong et al., 1997; Talbot, 2003; Ebbole, 2007; Wilson and Talbot, 2009). After appressorium penetration, the penetration peg develops to form a filamentous invasive hypha (IH) called the primary hypha (Heath et al., 1990a). At the first entry, the following events reveal an astounding biotrophic invasion strategy.

To understand the state of this interaction *in planta*, studies applying FM4-64, an endocytic marker dye, present the first evidence of this close relationship. After addition of FM4-64, it is quickly incorporated into the plant plasma membrane. The dye is only internalized in living cells by endocytosis, through which it labels small organelles and finally vacuoles (Figure 1.4 A, B) (Fischer-Parton et al., 2000; Atkinson et al., 2002; Bolte et al., 2004). In contrast to *M. oryzae* hyphae *in vitro*, IH growing *in planta* did not internalize FM4-64; Spitzenkörper, septa or organelles of the blast IH inside rice cells are not labeled by FM4-64 (Figure 1.4 C, D, E) (Kankanala et al., 2007), although they normally stain under *in vitro* conditions within 15 minutes of dyeing (Fischer-Parton et al., 2000; Atkinson et al., 2002). Via FM4-64 endocytic dye experiments and transmission electron microscopy using high-pressure freezing and freeze substitution to preserve the membranes, Kankanala et al. (2007) proved that in a compatible interaction a plant-derived membrane, called the extrainvasive hyphal membrane (EIHM), encloses biotrophic IH. Kankanala et al. (2007) revealed several key steps in the process of biotrophic invasion: (1) IH are enclosed by the EIHM that prevents FM4-64 from reaching fungal membranes; (2) After penetration, filamentous IH change into bulbous IH that grow to fill the invaded cells, and then switch again to filamentous IH when crossing into neighbor cells; and (3) When IH find the specific location to cross into a new rice cell, they swell moderately at the tip and then undergo extreme constriction while crossing the cell wall.

BIC Pattern: Secretion and Translocation of Effectors

In contrast to plasmodium or oomycete effectors, rice blast effectors do not share any sequences such as the RxLxE/Q/D or RXLR-dEER motifs that permit *in silico* searches for candidate effectors (Bhattacharjee et al., 2006; Dou et al., 2008). Except for small size of the protein and presence of a cleavage site for secretion in the N-terminal region, sequence motifs are missing for finding candidate effectors in the *Magnaporthe* genome database. Live cell imaging of fluorescently-labeled cytoplasmic-effector proteins, AVR-Pita, PWL1 and PWL2, provided us a distinctive commonality among them: specific secretion *in planta* and accumulation into a novel structure called the biotrophic interfacial complex (BIC) (Khang et al., 2010). This opened a novel way to search, *in vivo*, for candidate blast effector proteins. Khang et al. (2010) discovered and extensively described the development of BICs *in planta* during blast invasion in susceptible rice plants (Figure 1.5). This research supports results of Kankanala

et al. (2007) in which EIHMs enclosed membrane caps at the primary hyphal tips as well as at the filamentous IH tips after cell wall crossing. Khang et al. (2010) presented the first evidence and provided a sensitive *in planta* assay system to demonstrate blast effector translocation into the rice cytoplasm. Additionally, they showed that effector proteins advance ahead of where the fungus is invading, as if preparing the new cells for further invasion (Figure 1.6). No specific sequence signature responsible for the BIC localization (secretion) and/or translocation of blast effectors *in planta* has been yet found. However, advances in understanding secretion have been achieved by Gilbert et al. (2006) showing that *MgApt2*, a P-type ATPase-encoding gene, has a role in exocytosis specifically for plant infection. Recently, Khang et al. (2010), suggested that targeted effector secretion involves promoter and signal peptide sequences; and Yi et al. (2009) demonstrated an ER-dependent mechanism for effector secretion into BICs and pathogenicity.

Different results support the hypothesis that effector accumulation in BICs is a product of a regulated and dynamic secretion mechanism. (1) Yi et al. (2009) showed that deficiency in MoLHS1, an ER chaperone required for ER-dependent secretion, impairs AVR-Pita accumulation in BICs in compatible interactions and impairs the plant resistance response during incompatible interactions. They proposed that blast effector BIC localization occurs by a normal ER-mediated secretion mechanism. (2) Khang et al. (2010) illustrated how fluorescently-labeled PWL2:GFP accumulated at the BIC is able to recover from photobleaching (FRAP) as IH continue growing in the cell. Results from this FRAP analysis suggested that fluorescent effector proteins are continuously synthesized and secreted to BICs although IH keep growing at other points in the host cell.

Gene expression analysis of blast-invaded rice cells during a compatible interaction at 36 hours post inoculation (hpi) was an effective approach to enrich for IH RNA presented by Mosquera (2007) and Mosquera et al. (2009). Fungal strains that expressed cytoplasmic enhanced yellow fluorescent protein (EYFP) facilitated the selection of only heavily invaded rice leaf sheaths and cleaning of spores and mycelia on the surface of the sheath tissue ensured that the fungal RNA was derived by IH inside host cells. This analysis provided a high-quality candidate inventory of blast effector genes and rice susceptibility genes; this list included known blast effectors.

Cell Boundaries: Trespassing the Borders Avoiding Detection

To initiate a biotrophic interaction, the rice blast fungus must enter living rice cells without damaging them and avoid recognition by the plant defense components to enable colonization and growth on live rice cells. For delivery of *M. oryzae* effector proteins into the rice cytoplasm, those effector proteins must cross the EIHM or directly interact with plant components in BICs. During blast biotrophic invasion two control points of entry are critical for the blast fungus to succeed: (1) at the appressorial penetration site where the fungus must stealthily enter inside rice cells without perturbing them; and (2) at the crossing points in the cell wall where IH move from one cell to another. If blast IH pass through plasmodesmata as hypothesized by Kankanala et al. (2007), the fungus must to modify the plasmodesmatal size to pass without disrupting the rice cell wall and membranes. In this direction, understanding the function of secreted cytoplasmic effector proteins will give us answers regarding the mechanism used by rice blast for efficiently avoiding plant recognition. The blast fungus approximately spends 12 hours in the first invaded rice cell indicating that there is a regulated process, which agreed with the dynamic and regulated translocation of effectors to the first cell and into the neighboring uninvaded cells. Advance preparation of neighboring cells would explain why subsequent invasions require a shorter period, about 2 hours per cell (Oparka et al., 1999; Kankanala et al., 2007; Khang et al., 2010).

Plant viruses require virus-encoded movement proteins for cell-to-cell movement, which can or cannot modify the size exclusion limit (SEL) of the plasmodesmata (Oparka et al., 1997; Krishnamurthy et al., 2003). Then it is reasonable to hypothesize that plant fungal biotrophs must have a special mechanism to enable the IH to cross without damaging the rice cells. Thus, virus-encoded movement proteins with different mechanisms of plasmodesmata modifications (Fedorkin et al., 2001) represent an additional resource to understand the strategy(s) used by *M. oryzae* for sequentially invading rice cells without detection. In viruses, intracellular movement is accompanied by plant morphological changes. Rice blast could use intercellular communication pathways such as the actin or microtubule cytoskeleton, for intracellular transport of endogenous plant components (Waigmann et al., 1994; Boyko et al., 2000).

Dimorphism during Successful Biotrophic Interaction

Filamentous fungi are characterized by a highly polarized growth and they require the concentration of secretory vesicles and their fusion with the plasma membrane in the place of active growth. A complex of secretory vesicles, the vesicle supply center (VSC) or the Spitzenkörper (Spk), is typically localized at the apex of filamentous fungal hyphae. The Spk is responsible for the extension and polarized direction of growing hyphal tips (Lopez-Franco et al., 1994; Bartnicki-Garcia et al., 1995; Harris et al., 2005 ; Steinberg, 2007b). Budding yeast, *Saccharomyces cerevisiae*, and fission yeast, *Schizosaccharomyces pombe*, have been objects of extensive studies on molecular mechanisms of polarized growth, from which almost all the motors, cytoskeleton components and other protein component markers have been identified. A difference between filamentous fungal and budding yeast polarization depends on the polarisome, a complex of proteins, Pea2, Spa2 and Bud6, at the hyphal tip. The polarisome nucleates actin cables for the motion of secretory vesicles to the emergent tip and Cdc42 controls the formation and activity of the polarisome (Lew and Reed, 1995; Sheu et al., 1998; Read and Hickey, 2001). *Candida albicans* grows in three distinct morphological patterns: yeast, pseudohyphae and hyphae, which is key for its pathogenicity and is useful for the identification of different complexes involved in each form of growth (Crampin et al., 2005). Actin cables along with the myosin regulatory light chain, Mlc1, moves secretory vesicles towards the growing bud in *S. cerevisiae* (Johnston et al., 1991). Labeling Mlc1:YFP in *C. albicans* hyphae and co-localization with FM4-64 revealed the Spitzenkörper as a distinct dot at the hyphal tip. However, Spk were not observed in yeast or pseudohyphae cells (Crampin et al., 2005).

Exocytosis and endocytosis are the main pathways that sustain growth of filamentous hyphae. Early endosomes (EE) couple both processes by fusion and fission with the plasma membrane in a bidirectional movement. Using temperature-sensitive mutants in *U. maydis*, it was found that a putative endosomal t-SNARE, Yup1, was able to label early endosomes and vacuolar membranes when fluorescently tagged (Wedlich-Soldner et al., 2000). Early endosomes support exocytosis and recycling of critical proteins to maintain growth, regulate signaling and promote pathogenicity (Wedlich-Soldner et al., 2000; Steinberg, 2007a). Recent work by Berepiki et al. (2010), provided a high-resolution live-cell imaging technique using fluorescent protein fusions to allow visualization of actin patches, cables and microtubule cytoskeletons in filamentous fungi with no alteration of cellular functions. *In vitro* localization

of actin cables in *Neurospora crassa* and *M. oryzae* filamentous hyphae, labeled sites of active growth, where a dynamic endocytic pathway occurred (Berepiki et al., 2010; Patkar et al., 2010). Patkar et al. (2010) showed that in *M. oryzae*, polarization is essential for appressorium formation and pathogenicity. These new tools will provide a better understanding of the blast-effector secretion mechanism used by *M. oryzae in planta* and the switch in growth form that is critical for biotrophic invasion of live rice cells.

As in *C. albicans* and *Ustilago maydis*, *M. oryzae* undergoes a dimorphic developmental switch that is critical for pathogenicity, switching its growth from filamentous to bulbous IH *in planta* (Heath et al., 1990b; Kankanala et al., 2007; Giraldo and Valent, Unpublished).

Our research objectives were to solve part of these questions about *M. oryzae* secretion and translocation, studying effector secretion *in planta* with high-quality candidate effector proteins. In the second chapter, we will present the results from my first objective where we tested candidate effector proteins for specific secretion *in planta*, determined accumulation in BICs resembling known effectors AVR-Pita, PWL1 and PWL2, and evaluated translocation into rice cells. In the third chapter, we will present results using live cell imaging to begin to dissect the mechanism of protein secretion into BICs. In the last chapter, I will present future perspectives that can be addressed from the results obtained in this project.

Figures and Tables

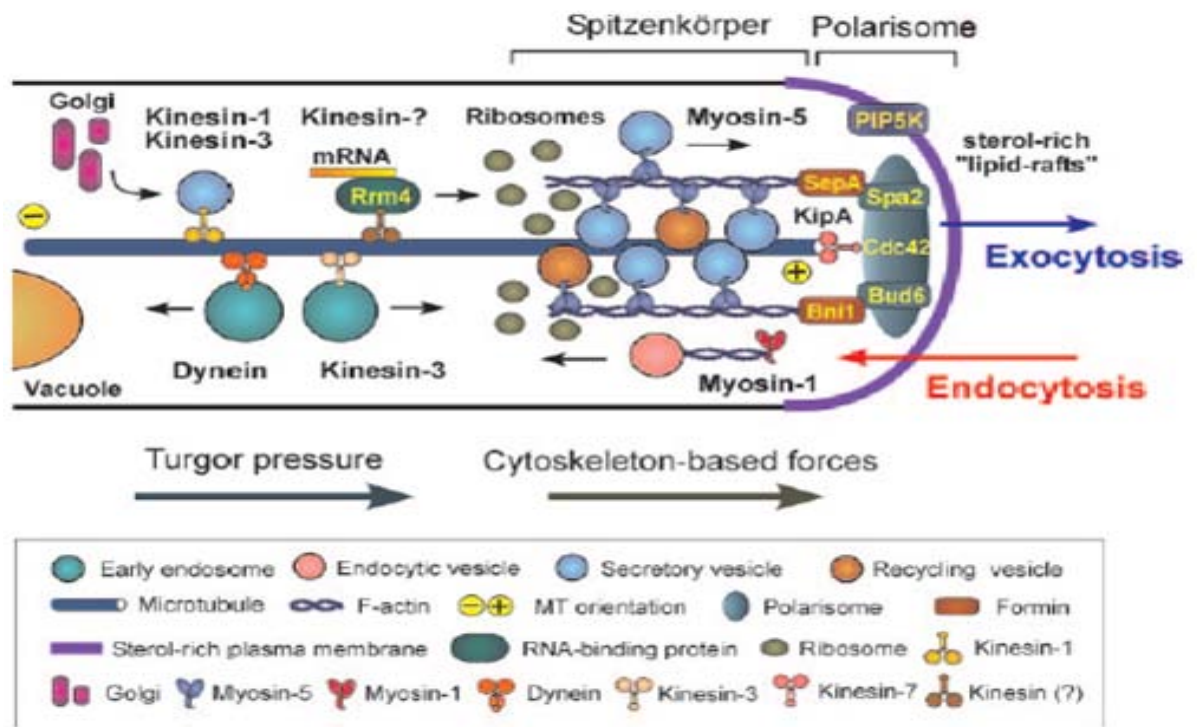


Figure 1.1. A model of hyphal tip growth in filamentous fungi from Steinberg (2007a)

This model is based on model systems including *Fusarium acuminatum*, *S. cerevisiae*, *Ashbya gossypii*, *A. nidulans*, *C. albicans*, and *U. maydis*. Sterol-rich membrane domains or lipid-rafts containing phosphatidylinositol-4-phosphate-5-kinase (PIP5K) that are located at the hyphal tip, where they might assist exocytosis. Myosin-1 takes part in initial steps of endocytosis by polymerizing actin, sending vesicles away from the membrane. In the tip are located components of the polarisome, Bud6, Spa2 and Cdc42. Spa2 and Bud6 bind formins that contribute in nucleation and polarization of the F-actin cytoskeleton, making possible the tipward delivery of exocytic vesicles. Microtubules (MTs) might be fixed at the tip via kinesin-motors for long-distance. Kinesin-1 and kinesin-3, which deliver vesicles, also might move mRNA to the tip. Short-distance transport might be mediated by myosin-5 motors. Vesicles are stored in the Spitzenkörper, which determines hyphal growth by controlled exocytosis at the growing hyphal tip.

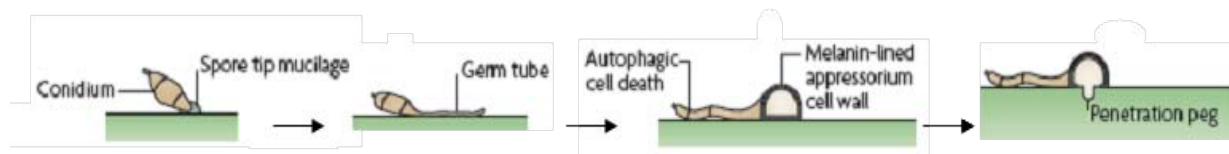


Figure 1.2. Pre-penetration phase of the life cycle of *M. oryzae* (Wilson and Talbot, 2009).

The rice blast fungus starts its infection cycle when a three-celled spore lands on the rice leaf surface. The spore attaches to the hydrophobic cuticle, germinates and produces a germ tube that subsequently differentiates into an appressorium. The single-celled appressorium matures and the three-celled spore undergoes autophagocytosis to mobilize spore components into the appressorium. The melanized appressorium develops significant turgor pressure that powers a penetration peg to penetrate the cuticle and allow access into the rice epidermal cell.

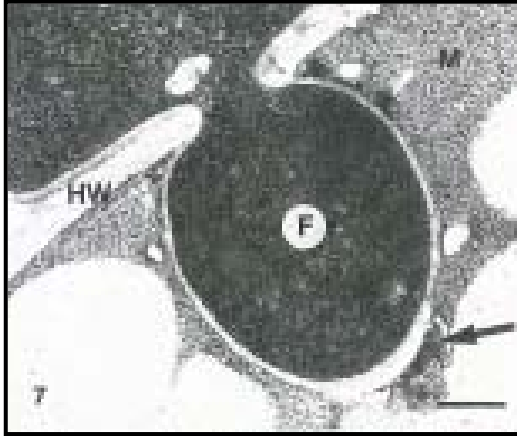


Figure 1.3. Transmission electron microscopy (TEM) of appressorium penetration in a gentle and precisely controlled manner from Heath et al. (1992).

Inoculation of weeping lovegrass with *M. oryzae* strain 4091-5-8, 46 hpi. Bar=500nm. Host cell and fungus appeared ultrastructurally normal. There was no visible response to the fungus (F) inside the mesophyll cell (M) and no visible distortion of the host cell wall (HW) at the penetration site. Note the elaborations of the plant membrane at the tip of the enclosed hypha (arrow).

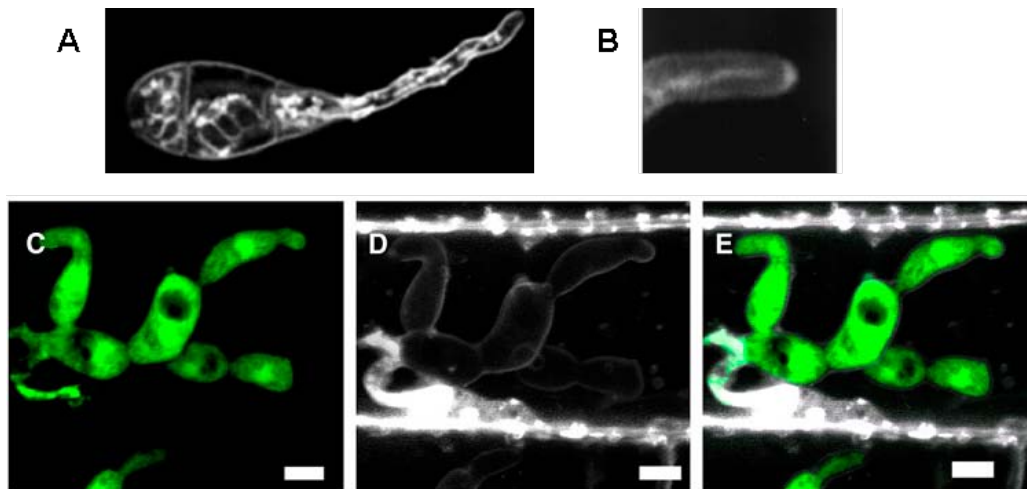


Figure 1.4. FM4-64 Stains *M. oryzae* hyphae *in vitro* but not IH *in planta*.

(A) Atkinson et al. (2002) showed the FM4-64 staining of internal organelles and vacuoles of a germinated spore of *M. oryzae in vitro*. (B) Fischer-Parton et al. (2000) used FM4-64 to show the Spitzenkörper at the tip of a *M. oryzae* germination tube. (C, D, E) FM4-64 staining of rice blast infection sites during IH invasion *in planta* from Kankanala et al. (2007) showed that the dye outlines IH but is not internalized. (C) The fungal IH (green) was expressing a cytoplasmic enhanced yellow fluorescent protein (EYFP). (D) FM4-64 fluorescence, shown in white, labeled the rice plasma membrane and small plant organelles. The IH is precisely outlined by the dye. The absence of dye in the fungal septa and vacuolar membranes showed that the dye was excluded from the IH membranes. (E) Merge EYFP and FM4-64 channels. Bars = 5 μm .

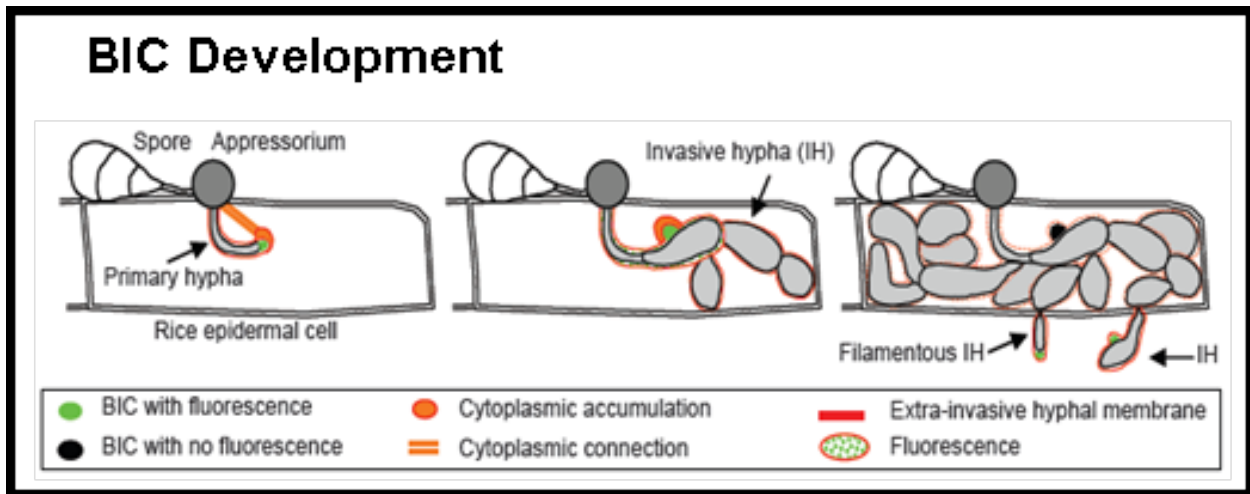


Figure 1.5. Cartoon summarizing the BIC development from Khang et al. (2010).

Development of the Biotic Interfacial Complex (BIC) required interaction between the pathogen and host. The primary fluorescent BIC appeared at the primary hyphal tip inside the first-invaded cell and then remained near by next to the first differentiated cell as bulbous IH continued to grow. After completely packing the first-invaded cells, IH undergo extreme constriction to cross the plant cell wall into the neighbor cell, and then grow as in the first cell. Once IH had moved into neighboring cells, fluorescence normally disappeared in the first-invaded cell and was detected at the tips of the filamentous IH in newly invaded cells, called secondary BICs. BIC development is repeated by every hypha that succeeds in biotrophic invasion, and is associated with differentiation of filamentous IH into bulbous IH.

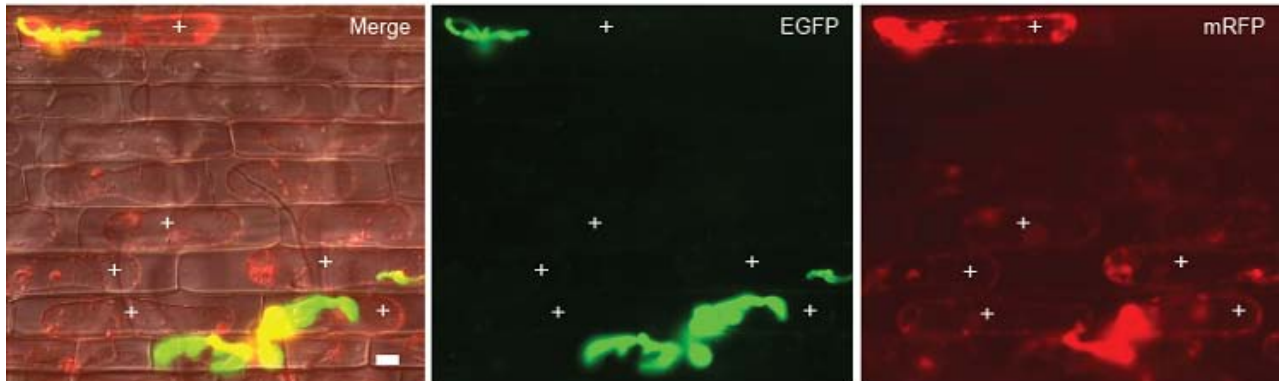


Figure 1.6. Effector PWL2:mRFP translocation into invaded rice cells and movement into uninvaded rice cells, from Khang et al. (2010).

The fungus also expressed BAS4:GFP (described in Chapter 2). PWL2:mRFP (red), but not BAS4:EGFP (green), was translocated to the cytoplasm of an invaded rice cell at 27 hpi. Also, mRFP fluorescence occurs in the cytoplasm of uninvaded neighbor cells. Images presented were acquired with long exposure times (10 sec for EGFP and 6 sec for mRFP) for visualization of faint fluorescence in the rice cytoplasm. From left to right merged differential interference contrast (DIC), EGFP, and mRFP channels, EGFP alone, and mRFP alone. Bar = 10 μ m.

Chapter 2 - *In Planta* Characterization of Candidate Blast Effector Proteins during Live Rice Cell Invasion by *Magnaporthe oryzae*

Abstract

The hemibiotrophic rice blast fungus *Magnaporthe oryzae* sequentially invades living rice cells using specialized biotrophic invasive hyphae (IH). The IH are tightly enclosed in a plant membrane, the extrainvasive hyphal membrane (EIHM), as they grow inside rice cells. To accomplish its biotrophic invasion, the fungus must secrete effector proteins across the EIHM inside the rice cells to turn down plant defense responses and to control plant processes and metabolism. Previous studies in the rice blast system have focused on the effector proteins encoded by avirulence (*AVR*) genes *AVR-Pita* and *PWL2*. Analysis of chimeric proteins produced by fusing *AVR-Pita* and *PWL2* to the green fluorescent protein (GFP) showed that they were secreted by IH and accumulated in novel structures, biotrophic interfacial complexes (BICs), located between the IH cell wall and the EIHM. We extend this analysis by examining secretion patterns for additional putative effectors; novel *in planta*-specific secreted proteins identified by microarray analysis. For four putative effectors, we generated fluorescent fusion proteins, enhanced yellow (EYFP) or monomeric red (mRFP) fluorescent proteins, at the C-terminus of the entire protein coding sequence and expressed them using the native promoter. We produced transformed fungal strains and assayed them for *in planta* protein secretion using the rice leaf sheath assay. Each of these four genes were specifically expressed and secreted during biotrophic invasion of rice cells. In the compatible interaction, they exhibit different localization patterns after secretion ranging from the BIC secretion pattern previously associated with avirulence proteins to intense uniform distribution within the EIHM around the entire IH. These BAS proteins are barely detected during an *AVR-Pita*-mediated hypersensitive resistance response. Ultimately, identification and characterization of rice blast effectors and understanding how they are delivered to the host cytoplasm will represent a major advance in molecular plant-pathogen interactions.

Introduction

Rice blast caused by the teleomorph fungus *M. oryzae*, also known as *Pyricularia oryzae* in its anamorph phase, represents a high risk for food security and sustainable agriculture

worldwide. Even with decades of effort toward disease control, this pathogen is still one of the main biotic causes of considerable yield losses, not just in rice but also in other world-staple cereal crops such as wheat, oat, rye, pearl millet and barley. Because of its high plasticity and effector instability, this pathogen is able to overcome deployed resistance (*R*) genes in the field within a couple of years (Correa-Victoria et al., 1994; Valent, 1997; Correll et al., 2000; Leach et al., 2001). Yield losses in rice fields can range from 100% in susceptible cultivars to 10 or 30% in cultivars containing some resistance genes (Talbot, 2003; Ebbole, 2007). Rice blast is a model pathosystem for difficult-to-study biotrophic fungi and fungal-plant interactions, due in part to the completed genome sequences for both the host and pathogen (Valent, 1990; Talbot, 2003; Dean et al., 2005; Ebbole, 2007).

Biotrophic fungi secrete and deliver specific proteins, called effectors, into the cytoplasm of living host cells to influence plant processes and promote disease in compatible interactions (Chisholm et al., 2006; Jones and Dangl, 2006; Kamoun, 2007; Valent and Khang, 2010). To date, mechanisms for secretion and delivery of effectors inside the host during disease establishment remain unknown. For a biotrophic plant pathogen, this is a critical step to ensure the successful infection. Most of the blast avirulence effector genes identified encode small-secreted proteins. The exception is ACE1, which encodes a secondary metabolite-related enzyme (Böhnert et al., 2004). All the other identified blast AVR gene products are known as cytoplasmic effector proteins that undergo recognition by the host resistance (*R*) gene product. During incompatible interactions, these proteins interact triggering cell death, also known as hypersensitive response (HR), which restricts fungal invasion. The currently known cytoplasmic AVR genes were identified by map-based cloning: *PWL1*, *PWL2*, *AVR-Pita1*, *AVR-CO39* and *AvrPiz-t* (Sweigard et al., 1995; Farman and Leong, 1998; Orbach et al., 2000; Li et al., 2009), by resequencing of a different *Magnaporthe* field isolate and association genetics: *AVR-Pii*, and *AVR-Pik/km/kp* (Yoshida et al., 2009), and by both approaches: *AVR-Pia* (Shinsuke et al., 2009; Yoshida et al., 2009). All known AVR proteins are unique small-secreted blast effector proteins, and the only commonality among them was their common accumulation during *in planta* invasion into a novel structure, called the biotrophic interfacial complex (BIC), which was discovered by live cell imaging of fluorescently-labeled *PWL1*, *PWL2* and *AVR-Pita* proteins (Khang et al., 2010). Identifying effectors and understanding how they function inside rice cells are important to attain long-lasting disease control. To address this challenge, I characterized

four candidate effector proteins that were highly expressed during the rice cell invasion (Mosquera, 2007; Mosquera et al., 2009). Using transgenic fungal strains that secrete fluorescently-labeled versions of each protein allowed me to follow them during invasion of plant cells by live cell imaging. This study revealed that these candidates are specifically secreted *in planta* during the compatible interaction, leading us to name them biotrophy-associated secreted (BAS) proteins. The fluorescent versions of these proteins were not observed in incompatible interactions. Gene knock-out (KO) experiments showed that individual BAS proteins are not required for infection of rice, suggesting functional redundancy. These BAS proteins displayed three distinctive localization patterns that range from a BIC-located protein, two putative cell-to-cell movement proteins, and a putative EIHM matrix protein. These distinct secretion patterns suggested a spatially-segregated mechanism for effector secretion.

Note that results of the characterization of BAS1-4 proteins included in this chapter are my contribution to the publication: Mosquera, G., Giraldo, M. C., Khang, C., Coughlan, S., and Valent, B. (2009). Interaction transcriptome analysis identifies *Magnaporthe oryzae* BAS1-4 as biotrophy-associated secreted proteins in rice blast disease. *The Plant Cell* 21, 1273-1290. (Rated F1000 Biology Factor 6, Must Read), with M. C. Giraldo as coequal first author.

Results of the BAS1:mRFP translocation presented in this chapter were published in Khang, C. H., Berruyer, R., Giraldo, M.C., Kankanala, P., Park, S.Y., Czymmek, K., Kang, S., and Valent, B. (2010). Translocation of *Magnaporthe oryzae* effectors into rice cells and their subsequent cell-to-cell movement. *The Plant Cell* 22, 1388-1403. (Rated F1000 Biology Factor 6, Must Read).

All the results included in this chapter are my contributions to these publications, Mosquera and Giraldo et al. (2009) and Khang et al. (2010), except for my unpublished results on BAS2:mRFP (Figure 2.5, A), which shows a strong and clear signal at the crossing points where the IH had moved from cell-to-cell, and on the *BAS4* gene knock-out (Figure 2.6, 2.7 and 2.8), which not showed a significant pathogenicity phenotype.

Results

Biotrophy-Associated Secreted Proteins in Rice Blast Disease

In the absence of clear bioinformatic signatures that lead the way to new blast effectors, localization of effector candidates *in planta* becomes a novel tool to confirm BIC localization, which so far is the main commonality among these small-secreted blast-effector proteins. To test for the BIC accumulation pattern observed in known blast effectors, four candidates were selected from the putative effector inventory generated by Mosquera (2007) and Mosquera et al. (2009) using microarray analysis. The criterion for selection was based on their highly-specific expression *in planta*, with >60 fold higher expression during biotrophic invasion relative to expression by hyphae *in vitro* (Table 2.1). The top three upregulated genes in Table 2.1 were validated as invasive hyphae-specific by qRT-PCR and RT-PCR, and also chosen for promoter expression, secretion and functional analysis (Mosquera, 2007; Mosquera et al., 2009). Characterization of the four selected candidates during invasion *in planta* was performed by live cell imaging of transgenic fungus that expresses chimeric proteins of each candidate fused to fluorescent-reporters (Figure 2.1, A). These candidates are specifically secreted during biotrophic invasion, thus named biotrophy-associated secreted (BAS) proteins (Figure 2.1, B).

Transformants of each candidate gene, with EYFP, EGFP or mRFP fusion fluorescent proteins, into different background strains (Table 2.2) were selected to test secretion and co-localization with fluorescently-labeled AVR-Pita. Selection of these transformants was based on hygromycin or geneticin resistance. Per candidate gene, 10 to 12 independent transformants were evaluated; variation of fluorescence intensities among them was observed but their localization patterns were consistent. In order to compare fluorescence intensities among different transformants, the exposure time during epifluorescence microscopy was standardized at 2 seconds. To test if fluorescence intensity variation is an effect of the number of copies of a gene integrated in the genome after *Agrobacterium tumefaciens*-mediated transformation (ATMT), southern hybridization was performed on the two transformants with the most contrasting fluorescence patterns (Figure 2.1, C-H). The EYFP coding sequence was used as a probe. The results for BAS1 and BAS2 suggested that fluorescence intensity might be related to number of copies (n). However, for BAS3, the weakest transformant (+) had 3 copies of the gene inserted, and the strongest (+++) had only 2. In addition, for BAS4, both the strongest and

the weakest transformants had a single copy insertion (Figure 2.1, C-H). All results together suggested that the intensity variation did not depend on the number of copies, and is more likely due to positional effect. That is, because *Agrobacterium*-mediated transformation is based on random insertion of the gene of interest in the genome, enhancers or silencers that regulate adjoining genes at the insertion site can determine variation of gene expression (Wilson et al., 1990).

Different localization patterns presented are based on microscopic visualization of >100 individual rice sheath infection sites per gene at each time point of the invasion.

A BAS Protein that Accumulates in BICs and is Translocated into the Rice Cytoplasm

BAS1 (MGG_04795.6)

BAS1 was 100-fold up-regulated in IH compared with negligible expression levels in mycelium growing on artificial medium (P-value 0), and it was confirmed to be specifically expressed in IH by quantitative RT-PCR (Mosquera, 2007; Mosquera et al., 2009). In genome version 6 (http://www.broad.mit.edu/annotation/genome/magnaporthe_grisea/MultiHome.html), BAS1 was located on chromosome IV. This gene encodes a secreted protein with 115 amino acids and no cysteine residues (Table 2.1). No paralogs were identified in *M. oryzae*, and no orthologs were identified in other organisms. Functional analysis by deletion of the entire BAS1 gene, reported by Mosquera (2007) and Mosquera et al. (2009), did not find any major pathogenicity phenotype, although 3 out of 6 independent whole-plant assays showed quantitative decreases in lesion numbers and lesion sizes in mutants relative to the wild type strain and ectopic transformants. Transformants expressing BAS1:EYFP fusion protein during invasion of susceptible rice sheath cells (compatible interaction) showed that this fusion protein was secreted in a classical BIC pattern (Figure 2.2, A). That is, BAS1:EYFP fluorescence was localized in primary BICs at hyphal tips, and then moved to the side of the first IH cell together with the BIC when the hyphae turns into a bulbous IH (Figure 2.2, B, 27 hpi). Fluorescence remained in the BIC as IH continued to grow in the cell (Figure 2.2, B, 32 hpi). Each biotrophic hypha that moved into a neighbor cell formed again the BIC, first at the filamentous IH tip and then beside the first bulbous IH cell (Figure 2.2, B 36 hpi). To confirm secretion into BICs, we

demonstrated that BAS1 fluorescent proteins failed to co-localize with a cytoplasmic cyan fluorescence reporter (CFP) in IH, but that it did co-localize with a fluorescent AVR-Pita1 reporter protein previously shown to localize to BICs (Figure 2.3,A,B). Therefore, BAS1 encodes a BAS protein that accumulates in BICs and is a strong blast effector candidate.

In the course of these studies, we noticed that fusion proteins containing mRFP produced brighter fluorescence when the fungus was growing inside rice cells than did fusion proteins containing EYFP. I therefore produced transformants with BAS1:mRFP for experiments to demonstrate protein translocation. To further facilitate visualization of translocation of fungal cytoplasmic-effector proteins, we used plasmolysis of inoculated leaf sheath epidermal cells to concentrate the faint signal in the intact, contracted plant protoplast. This avoided any overlap with auto-fluorescence signal from the cell wall as well as intensifying the signal from the translocated protein. Using BAS1:mRFP fusion protein and host cell plasmolysis allowed us to visualize its translocation into the rice cytoplasm (n=50). To verify translocation of BAS1:mRFP, BAS4:GFP was used as a EIHM-intactness marker in compatible interaction (Figure 2.4, A, B). Moreover, BAS1:mRFP was observed to move ahead into uninvaded neighbor cells (Figure 2.4, C).

BAS Proteins with a Potential Role in Cell-to-Cell Movement

BAS2 (MGG_09693.6)

This gene on chromosome V was 84-fold up-regulated in IH (P-value 0) and it was confirmed to be IH-specific by quantitative RT-PCR (Mosquera, 2007; Mosquera et al., 2009). It encodes a conserved hypothetical protein with 102 amino acids (Table 2.1). The encoded protein has similarity to proteins from two *M. oryzae* genes that are located ~800 kb apart on chromosome III. One of these, MGG_07969.6, encodes a potentially secreted, conserved hypothetical protein with 101 amino acids (E=2e-28). The other homolog, MGG_07749.6, encodes a larger, secreted protein, 198 amino acids, with homology at the N-terminus (E=4e-17). Both of these related genes have corresponding EST and SAGE sequences identified from mycelium grown *in vitro*, and they have fold-change levels between 1 and 2 in the microarray analysis presented by Mosquera (2007) and Mosquera et al. (2009), suggesting they are

expressed in fungal cell types other than IH. The BAS2 protein has homology to predicted proteins from other fungal pathogens with the highest level to a predicted protein from the wheat tan spot pathogen, *Pyrenophora tritici-repentis* ($E=4e-21$). BAS2 and all related polypeptides have 6 conserved cysteine residues. Gene replacement analysis failed to show phenotypes affecting pathogenicity, mycelial growth, sporulation, or appressorium formation and function (Mosquera, 2007; Mosquera et al., 2009). Therefore, BAS2 is a cysteine-rich BAS protein that localizes preferentially to BICs (Figure 2.2, C). After 36 hours post inoculation (hpi), BAS2:mRFP showed a strong and clear signal at the crossing points where the IH had moved from cell-to-cell (Figure 2.5, A). Unlike BAS1, BAS2 did not appear to move into surrounding cells preceding fungal infection.

BAS3 (MGG_11610.6)

This gene was 71-fold up-regulated in IH (P-value 0). It was confirmed to be IH-specific by quantitative RT-PCR (Mosquera, 2007; Mosquera et al., 2009) and placed on chromosome VI. The gene encodes a secreted protein with 113 amino acids including 10 cysteines (Table 2.1). BAS3 has two distant relatives in the blast genome. The closest of these, MGG_05895, which was deleted in genome version 6, has conserved cysteine residues ($E=2e-05$), and it was 25-fold up-regulated in IH.

Gene replacement functional analysis of BAS3 failed to identify an associated phenotype (Mosquera, 2007; Mosquera et al., 2009). Microscopy of the secreted BAS3:EYFP protein showed strong fluorescence at the appressorial penetration site and outlining the primary hypha (Figure 2.2, D). Low levels of fluorescence were observed in BICs in first-invaded cells (Figure 3D). After the IH had grown in the first invaded cell, approximately after 32 hpi, fluorescence faintly outlined the IH and formed focused fluorescent spots associated with individual IH cells near the cell wall (Figure 2.2, D, 32 hpi). Fluorescent BICs were not observed at the tips of IH that invaded neighbor cells. Instead, fluorescence accumulated at the point where each IH had crossed the cell wall, and sometimes surrounded the IH where they had crossed (Figure 2.2, D, 36 hpi). These results imply that BAS3 is a small cysteine-rich BAS protein with a localization pattern that suggested a function in cell-to-cell movement.

A BAS Protein that Outlines Invasive Hyphae Inside Rice Cells

BAS4 (MGG_10914.6)

This gene resides on chromosome VI (~200 kb from one end) and is 61-fold up-regulated in IH (P-value 0) (Mosquera, 2007; Mosquera et al., 2009). The gene encodes a secreted protein with 102 amino acids, including eight cysteine residues (Table 2.1). The BAS4 protein has homology to a conserved hypothetical *M. oryzae* protein, MGG_02154.6 ($E=1.9e-7$), which is also a small secreted protein with eight conserved cysteine residues. This latter gene is on chromosome II, ~1,139 kb from one end, and shows 3-fold higher expression in IH. The MGG_02154.6 protein has homology to proteins from other filamentous fungi, with the highest similarity to a small cysteine-rich protein from the wheat scab pathogen, *Gibberella zeae* ($E=9e-24$). Thus, the MGG_02154.6 protein is more diverged from its IH-specific paralog BAS4 than from its orthologs in other filamentous fungi.

BAS4:EYFP fusion proteins showed a secretion pattern that was clearly distinct from those of the other BAS proteins (Figure 2.2,E). Bright fluorescence uniformly outlined the IH from their initial penetration to invasion and growth in neighboring cells. Some fluorescence also occurred in the BICs, but not preferentially there, as seen for known AVR effectors and BAS1-3. Thus, the localization pattern of the cysteine-rich BAS4 protein is consistent with an interfacial matrix protein.

Further Functional Analysis of the Putative EIHM Matrix Protein BAS4

We evaluated the number of copies of the BAS4 gene in rice pathogens from different geographic regions and in a distantly-related *Digitaria* pathogen by southern blot hybridization. BAS4 occurred as a single copy gene in diverse rice pathogens: 70-15, the sequenced laboratory strain; O-137, a rice pathogenic field isolate from China; and Guy 11, a rice pathogenic field isolate from French Guiana. BAS4 homology was lacking in the non-rice pathogen G213, a Japanese field isolate pathogenic on *Digitaria smutsii* (Figure 2.6). Gene replacement mutants were obtained by targeted gene replacement using ATMT and the dual (positive and negative) selection (DS) system developed by Khang et al. (2005). From 304 hygromycin resistant putative transformants obtained in the first round of selection, I narrowed them down to 20 putative transformants using negative selection with 5-fluoro-2'-deoxyuridine (F2dU). Four of

these were selected as gene knock-out (KO) transformants by PCR amplification of hygromycin. However, just one true positive knock-out was confirmed by absence of PCR amplification of BAS4 coding sequence (Figure 2.7, A). Three independent transformants were evaluated by southern hybridization (Figure 2.7, B; 2.8) to confirm the KO and ectopic mutants. Different inoculation assays, leaf sheath, spray, mist and drop (Berruyer et al., 2006) inoculation were used to evaluate any pathogenicity effect of the KO and ectopic mutants (7 and 22). However, as with known effectors AVR-Pita, PWL2, and BAS proteins 1-3, no clear pathogenicity phenotype was found.

Although IH exhibited bright BAS4:EGFP fluorescence at most compatible infection sites, IH in some cells lacked uniform outlining (Figure 2.9, B). At these infection sites, the host cells appeared less healthy and many failed to plasmolyze. Additionally, fluorescent protein appeared to have leaked into the host cell (Figure 2.10). For example (Figure 2.9, C), an IH in a plasmolyzed host cell lacked uniform outlining, and EGFP fluorescence was observed in the host cytoplasm. Apparently, EGFP had leaked from the EIHM matrix. These results support our hypothesis that BAS4 is trapped inside the EIHM compartment instead of being bound to the IH cell wall. These results also indicated that not all IH in the compatible interaction were healthy and enclosed in an intact EIHM. We conclude that the fluorescently-labeled BAS4 provides a valuable indicator of EIHM integrity at individual infection sites during live cell imaging of biotrophic invasion.

Differential Expression of BAS Proteins in Compatible and Incompatible Interactions

Fungal transformants containing a native *AVR-Pita+* gene, were evaluated for secretion of the effector PWL2 and BAS1, BAS3 and BAS4 proteins in susceptible YT-16 (*pita-*) and in resistant Yashiro-mochi (*Pita+*) rice. In the compatible interaction with YT-16, high levels of PWL2 and BAS protein fluorescence occurred in 98% of infection sites, with >300 infection sites examined per protein. In contrast, in the incompatible interaction with Yashiro-mochi, fluorescence from PWL2 and BAS proteins was absent in 90% of ~50 infection sites per protein, or severely attenuated at 10%. Typical results are illustrated for a transformant expressing both PWL2 fused to mRFP and BAS4 fused to EGFP. Both fluorescent proteins were highly expressed at infection sites (>100 observed) in the compatible interaction (Figure 2.9, A, COM). However, in incompatible sites (>50 observed), the fungus generally stopped growing in the

first-invaded cell, and neither mRFP nor EGFP fluorescence was observed (Figure 2.9, A, INC). Occasionally in the incompatible interaction, faint PWL2:mRFP fluorescence occurred without BAS4:EGFP fluorescence. However BAS4:EGFP fluorescence alone was never observed. In one example, thin hyphae in damaged first-invaded Yashiro-mochi rice cells had spread to neighboring cells that also appeared damaged (Figure 2.9, B, INC). Only weak PWL2 fluorescence was observed. Thin hyphae in dying plant cells were never outlined with BAS4 reporter protein. Secretion of low levels of effector proteins in incompatible infection sites is consistent with the role of effectors in inducing R gene-mediated resistance. Clearly, BAS protein accumulation is characteristic of IH during compatible, but not during incompatible interactions.

Discussion

Biotrophy-Associated Secreted Proteins Distinctively Expressed during Compatible Interactions

Enrichment for secreted protein genes in the biotrophic interaction transcriptome is consistent with the recent report that mutation of the *M. oryzae* ER chaperone gene *LHS1* disproportionately affects biotrophic invasion in the compatible interaction, as well as induction of plant defenses in the incompatible interaction (Yi et al., 2009). The *M. oryzae* *LHS1* chaperone is required for proper processing and secretion of pathogen proteins. Mutants that lack *LHS1* grow normally in axenic culture and on the plant surface, but they are severely impaired in biotrophic colonization and sporulation. Consistent with the report of Yi et al. (2009) that proper secretion is required for the AVR-Pita1-mediated incompatible interaction, low levels of fluorescent effector/BAS proteins can be detected even in the incompatible interaction (Figure 2.9, B). These results highlight the importance of studying the proteins that IH secrete *in planta* as well as the secretion mechanisms involved.

This study has identified distinct secreted biotrophy-associated secreted (BAS) proteins for rice blast, and some of these are cysteine-rich. Secreted cysteine-rich polypeptides have been identified as effectors in other host-pathogen systems (Catanzariti et al., 2006; Kamoun, 2007). For rice blast, Dean et al. (2005) identified three cysteine-rich protein families in the *M. oryzae* genome. Although it was suggested that these might play a role as blast effectors, functional

analyses had not been performed. Among these, family 180, including ten cysteine-rich polypeptides (with ~150 amino acids and 6-10 cysteine residues) had five members that were up-regulated in biotrophic IH by 3-, 5-, 5-, 5-, and 25-fold in our analysis (Mosquera, 2007; Mosquera et al., 2009). The BAS2, BAS3 and BAS4 proteins belong in family 180, although they were not included among the original members (Dean et al., 2005). This is the first report of localization of some of these differentially expressed members of the 180 family of cysteine-rich proteins.

Although it is likely that BAS proteins play key roles during biotrophic invasion, targeted gene replacements of the four BAS proteins did not result in reproducible pathogenicity phenotypes. It remains possible that there are minor plant colonization phenotypes, especially with BAS1. Quantitative pathogenicity defects could be confirmed with improvements in blast pathogenicity assays, which are extremely sensitive to environmental and physiological conditions. However, the lack of phenotypes is consistent with the general lack of phenotypes associated with known *AVR* effector genes (Kamoun, 2007), and with the general failure to identify genes with IH-specific phenotypes through classical mutational analyses (Talbot, 2003; Ebbole, 2007). Together, these results suggest extensive functional redundancy associated with biotrophic invasion. Among these *BAS* genes (Table 2.1), BAS1 has no candidate for a functional paralog in the sequenced genome, *BAS2* has two candidates (although neither gene is up-regulated in IH), and *BAS3* had one candidate (subsequently deleted from genome version 6). Thus, in some cases, assaying double or triple mutants might provide clues to function. Additional insight to BAS protein function could come from determining if IH-specific proteins interact physically with induced rice proteins, or, as we demonstrate, from studying *in planta* secretion patterns.

The hypothesis that blast IH co-opt host plasmodesmata for cell-to-cell movement (Kankanala et al., 2007) could be confirmed by identification of fungal proteins involved in recognizing and manipulating plasmodesmata. Fluorescent BAS2 and BAS3 reporter proteins accumulate at rice cell-wall crossing points, suggesting that these proteins might play a role in cell-to-cell movement of IH. However, deletion of either the BAS2 or BAS3 genes produced no mutant phenotype to aid in discovery of functions. Identification of additional proteins with the cell wall-crossing localization pattern is a high priority. Deletion of two or more components participating in the same cellular process can produce a dramatic phenotype, even though the

fungus grows normally after mutation of each component individually (Tong et al., 2001). BAS2 and BAS3 preferentially localized in the two control points during compatible interactions appressorium penetration sites and cell-to-cell crossing points. This suggests the importance of co-localization studies with plasmodesmata components to test whether blast fungus moves through plasmodesmata or not. These BAS proteins could also be a good tool in complementation studies with viral movement proteins to prove whether these proteins function like viral cell-to-cell movement proteins or not.

BAS Proteins as Putative Effectors

The known AVR gene products AVR-Pita1, PWL1, and PWL2 are BAS proteins, suggesting that BAS proteins are a rich source for additional effectors. Identifying the entire set of rice blast effectors, including the subset of AVR effectors corresponding to rice blast resistance genes, remains an important challenge. Presently, the few known blast AVR effectors have not provided a bioinformatic handle for identifying effector candidates among secreted protein genes in the *M. oryzae* genome. Clues might have come from identification of large effector gene families, as seen with oomycetes (Kamoun, 2007), or from genome clusters of *in planta*-specific, secreted protein genes as seen for the corn smut pathogen *Ustilago maydis* (Kämper et al., 2006). Neither strategy has proven useful from our analysis. Additional blast cytoplasmic effectors could be identified through bioinformatics if they contained membrane translocation motifs such as the RXLR motif found in oomycete effectors (Kamoun, 2007). Oomycete pathogens deliver their cytoplasmic effectors across plant membrane by a mechanism that requires this amino acid motif following the classical signal peptide (Whisson et al., 2007; Dou et al., 2008). Searches for signature sequences for blast effectors and for potential amino acid translocation motifs in proven AVR or putative BAS proteins, have not succeeded.

Discovery of BICs represents a visual strategy for identifying effectors, based on the hypothesis that the specific BIC localization pattern is distinctive for blast effectors (Khang et al., 2010). Among the four analyzed BAS proteins, BAS1 shows the same BIC-specific localization pattern and host translocation as known effector PWL2. Therefore, BAS1 represented a candidate cytoplasmic effector that is translocated across the EIHM into the rice cells. Preliminary evidence suggests that, indeed, BICs are involved in translocation of known effectors into the cytoplasm of living rice cells (Khang et al., 2010). Because independent BAS

2 and BAS3 knockouts did not show any pathogenicity phenotype, these two BAS proteins might be used for functional analysis simultaneously to test the hypotheses that rice blast operates with functional redundancy and that both have a role in cell-to-cell movement (Kankanala et al., 2007; Mosquera, 2007; Mosquera et al., 2009). This analysis has identified potential players for continued investigation of roles for effectors and for BICs during biotrophic invasion.

EIHM Intactness Indicates Successful Blast Biotrophic Rice Cell Invasion at Individual Infection Sites in a Compatible Interaction

Results from Kankanala et al. (2007) revealed that the biotrophic IH remain enclosed by a plant-derived membrane, EIHM, through each subsequent cell invasion. FM4-64 shows how IH are enclosed by a plant membrane excluding fungal membranes and septa from staining (Kankanala et al., 2007). BAS4 provides additional evidence for the intactness of that coat membrane, which remains undamaged within sequentially invaded rice cells in the compatible interaction. Complete absence of BAS4:EGFP outlining of IH in the incompatible interaction (Figure 2.9, A, B) could be explained by repression of BAS4 expression resulting from recognition of AVR-Pita1, by expression of BAS4 but failure of the protein to concentrate inside the EIHM, or by both. This suggests that uniform outlining of IH as they grow in a living cell indicates that healthy IH inside an EIHM compartment have established a successful biotrophic interaction. Some infection sites in compatible interactions experience failure in biotrophic invasion, which is characterized by an irregular BAS4 pattern consistent with BAS4 leaking out from the EIHM and accumulating in the rice cell cytoplasm. This information is very important for cell biological studies of biotrophic invasion. Results from compatible interactions showed a few cases in which BAS4 appears to be leaking (Figure 2.9, C; 2.10) this raises an important caution to researchers studying translocation of blast effectors into the host cytoplasm. Breakage of the EIHM membrane enclosing the fungus would result in artifactual dispersal of EIHM matrix proteins to the surrounding rice cytoplasm. Because BAS4 is not translocated into the host cytoplasm, fluorescent BAS4 reporter protein is a good control for effector translocation studies in blast disease, which must account for EIHM integrity at individual infection sites. Further analysis of compatible interactions, following BAS4 as an EIHM marker inside rice

transformants expressing fluorescently-labeled plasma membrane and/or cellular components of the rice endocytic pathway will provide clues about the origin of the EIHM.

Analysis of these four BAS proteins revealed interesting aspects of the biology of *M. oryzae* biotrophic invasion. BAS1 is the case where a candidate that localized in BICs is also translocated into the rice cytoplasm, and even moves to cells ahead of fungal invasion (Khang et al., 2010). Based on this similarity to the known effector PWL2, BAS1 is a strong candidate blast effector protein. BAS2 and BAS3 bring new evidence to support the results presented by Kankanala et al. (2007), in which it was proposed that *M. oryzae* moves from cell-to-cell through plasmodesmata, which are accessible channels in the plant cell wall that provide direct cytoplasmic continuity between neighbor cells. Even though BAS2 and BAS3 showed a weak localization in BICs, they strongly localized in each crossing point at the cell wall for every subsequently new invaded cell. BAS2 and BAS3 are candidate movement-proteins involved in sensing or modifying the size exclusion limit (SEL) of the plasmodesmata. BAS4 represents a remarkable pattern; it clearly outlined the penetration peg as soon it is formed. BAS4 is secreted and highly expressed *in planta*, providing evidence of the intactness of the EIHM that enclose the IH in the biotrophic invasion (Kankanala et al., 2007). BAS 4 is a candidate EIHM matrix protein. Differential localization of secreted effector and BAS proteins suggests that rice blast might have a specialized secretion mechanism for effectors.

Material and Methods

Preparation of Infected Tissue and Live Cell Imaging

Fungal transformants were stored in dried filter papers, maintained in -20°C frozen storage, and cultured on oatmeal agar plates at 24°C under continuous light (Valent et al., 1991). Rice sheath inoculations were performed as described (Kankanala et al., 2007). Briefly, 5 cm-long sheath pieces from 3 week-old plants were placed in a glass container under high humidity conditions. Sheaths were placed on stable supports to avoid contact with the wet paper and to hold them horizontally flat for even inoculum distribution. A spore suspension, ~200 µl, (1×10^5 spores/ml in 0.25% gelatin, Cat. # G-6650, Sigma Aldrich) was injected in one end of the sheath using a 200 µl pipette. At 22 hours post inoculation (hpi), 0.5 cm pieces were removed from the incubated sheath ends to eliminate vegetative hyphae that grew into injured tissue.

Each segment was hand-trimmed and immediately observed using wide-field or confocal microscopy. The rice leaf sheath assay is documented in Supplemental Video 2.1.

Wide-field microscopy using differential interference contrast (DIC) and epifluorescence imaging was performed with a Zeiss Axioplan 2 IE MOT microscope. Fluorescence was observed with a 100 Watt FluoArc or an X-Cite®120 (EXFO Life Sciences) mercury lamp source. Filter sets used were: GFP (excitation 480 ± 10 nm, emission 510 ± 10 nm, filter set 41020, Chroma Tech. Corp., Rockingham, VT); YFP (excitation 500 ± 20 nm, emission 535 ± 30 nm, filter set 46); mRFP (excitation 535 ± 25 nm, emission $610 \pm 32 \frac{1}{2}$ nm); and ECFP (excitation 436 ± 10 nm, emission 480 ± 20 nm, filter set 47). The blast invasion was followed *in vivo* using C-Apochromat 40x/1.2 N.A (numerical aperture) and 63x/1.2 N.A water immersion objectives. Images were acquired with an AxioCam HRc camera and Axiovision® software version 4.8. Unless stated otherwise, microscopy components were obtained from Carl Zeiss (Oberkochen, Germany).

Confocal imaging was performed on a Zeiss Axiovert 200M microscope equipped with a Zeiss LSM 510 META system using water immersion objectives C-Apochromat 40X/1.2 N.A and 63X/1.2 N.A for bright field (BF). For EGFP excitation/emission wavelengths were 488 nm/505-550 nm and for mRFP, 543 nm/560-615 nm. Images were acquired and processed using LSM510 AIM version 4.2 SP1 software. This imaging was performed in the COBRE Confocal Microfluorometry and Microscopy Core in the KSU College of Veterinary Medicine.

Assays for Growth and Plant Infection

Fungal growth and sporulation was observed on oatmeal agar plates (Valent et al., 1991). Appressorium formation, penetration and biotrophic invasion were observed in the leaf sheath assay described in Supplementary Video 2.1. Drop inoculation, mist inoculation and whole-plant spray inoculation assays as has been described by Berruyer et al. (2006). For whole-plant assays, 3 week-old YT-16 rice plants were inoculated with spore suspensions (5×10^4 spores/ml in 0.25% gelatin), and evaluated 7 days later (Valent et al., 1991).

Vector Construction, Fungal Transformation and Southern Analysis.

Unless noted otherwise, transformation cassettes to observe secretion in rice cells were constructed containing the entire protein coding sequence (including the predicted signal peptide) with its native promoter (1 kb) in a translational fusion with EYFP, EGFP or mRFP and

a *N. crassa* beta-tubulin terminator sequence. The constructs used for AVR-Pita:EGFP in Figure 2.3, B and BAS4:EGFP in Figure 2.9 contained only the native promoter and signal peptide fused to EGFP. The EGFP expressed from both constructs behaved identically to EGFP expressed from constructs including the entire AVR-Pita and BAS4 coding sequences. The EGFP, EYFP and ECFP genes were obtained from Clontech, and the mRFP gene was from Campbell et al. (2002). Primers used for amplification of each gene are listed in Table 2.3. Each cassette was cloned into pBHt2 binary vector for transformation by *A. tumefaciens* (Khang et al., 2005), with selection for hygromycin resistance. Details of plasmid construction and corresponding fungal transformants used in this study are listed in Tables 2.4 and 2.5, respectively. *M. oryzae* field isolates O-137 (Orbach et al., 2000), Guy11 (Leung et al., 1988) and laboratory strain CP987 (Orbach et al., 2000) were used as recipients. Fungal transformants were purified by single spore isolation (Keitt, 1915; Rho et al., 2001) and 10 to 12 independent transformants were analyzed per gene.

For gene replacement transformation of the *BAS4* gene, cassettes were constructed by amplifying 1.5-kb each of 5'- and 3'-flanking regions for the predicted coding sequence. The final cassette contained 3 different fragments; a 5'-fragment flanked by *Pst*I and *Bam*HI, the hygromycin resistance gene (1.4 kb) flanked by *Bam*HI and *Kpn*I; and a 3'-fragment flanked by *Kpn*I and *Xba*I (Figure 2.8). The hygromycin phosphotransferase (*hyg*) gene from pCSN43 (Sweigard et al., 1995) was cloned between the two flanking regions using a restriction enzyme-ligation strategy (Khang et al., 2005). The three pieces together were cloned first into the pGEMT-T® vector (Promega), verified by sequence analysis, and later into binary vector pGKO2 (Khang et al., 2005) using a restriction-ligation strategy. Spores from strain 70-15 were transformed using *A. tumefaciens* (Khang et al., 2005). After two rounds of selection in TB3 media containing 250 ug/mL of hygromycin (positive selection), 304 independent fungal transformants were tested for sensitivity to F2dU as a negative selection against strains with ectopic integration events instead of gene replacement events. Twenty candidate positive mutants were evaluated for gene replacement events by PCR amplification of hygromycin and *BAS4* coding sequence. The true positive was selected by absence of the expected band with the *BAS4* coding sequence and presence of the expected band with the hygromycin resistance gene using *hyg*-specific primers (Figure 2.7, A). Gene replacement events were confirmed by Southern blot analysis using the AlkPhos Direct Labeling Kit for non-radioactive labeling of DNA. The

3' flanking coding sequence was used as the probe (Amersham RPN3690) (Figure 2.7, B; 2.8) in order to confirm predicted bands in both ectopic transformants and the replacement mutant.

Plasmolysis-Based Assay for Visualization of Translocated Cytoplasmic Effectors

Viability of infected cells was assessed by plasmolysis in 0.75 M sucrose. Rice cells were plasmolyzed before acquisition of the images in order to concentrate the cytoplasm and separate it from the cell walls. Plasmolysis was performed slowly, by sequential incubation of the rice tissue with 0.25 M, to 0.75 M sucrose (Khang et al., 2010). This steady step-wide plasmolysis minimizes damage to the host cells (Mellersh and Heath, 2001). Microscopy was performed on a Zeiss Axioplan 2 IE MOT microscope as described above. Fluorescence images were acquired using the Axiovision software module Multichannel Fluorescence with a series of incremental exposure times (1, 2, 3, and 4 s for EGFP, and 0.3, 1, 2, and 3 s for mRFP). Acquired images for each fluorescence channel were examined separately, or combined in single images to produce the maximum exposure images (10 s for EGFP and 6.3 s for mRFP) sometimes required for visualizing fluorescence in the rice cytoplasm. Images obtained at the reduced exposure times were valuable for assessing uniform outlining of IH by BAS4:FP and localized BIC secretion by BAS1:FP.

Accession Numbers

Sequence data from this article can be found in the GenBank database under the following accession numbers: AF207841.1 for AVR-Pita; U26313.1 for PWL2; U36923.1 for PWL1; FJ807764 for BAS1; FJ807765 for BAS2; FJ807766 for BAS3; and FJ807767 for BAS4. All *M. oryzae* genes can be accessed from the Broad Institute's Magnaporthe grisea Genome Database (http://www.broad.mit.edu/annotation/genome/magnaporthe_grisea/MultiHome.html) or the *Magnaporthe grisea Oryzae sativa* (MGOS) interaction database (<http://www.mgosdb.org/>; Soderlund et al., 2006).

Supplemental Data

Supplemental video 2.1. Describes the rice leaf sheath inoculation procedure. This video can be found with the item record for this thesis in the K-State Research Exchange (<http://krex.k-state.edu>).

The overall goal of this procedure is to assist microscopic imaging of rice blast invasion using rice leaf sheaths. This protocol is modified from Koga (2004) and Sakamoto (1949).

- Choose a 3-week-old rice plant.
- Select the portion of the rice plant with 3 fully expanded leaves and one developing leaf approximately half emerged.
- Cut the plant at the base, pull off the two external sheaths and pull out the developing leaf to obtain a sheath piece with a curved cavity.
- Then cut one section from the sheath, which is approximately 5 cm long.
- Place the sheath on a horizontal support such that the fungal spores will settle onto the inner epidermal cell layer over the thickest v-shaped portion of sheath. The edges of the sheath overlap at the top to form an enclosed cavity.
- The inoculum can be previously prepared from a 1-to 2 week old fungal culture.
- Use a spore suspension prepared at a concentration of 10^5 spores per milliliter in 0.25% gelatin solution.
- Using a pipette, inject approximately two hundred microliters of spore suspension per sheath into the hollow space enclosed by the sides of the sheath, until the suspension reaches the opposite end of the sheath.
- Make sure there is a drop at both or at least at one of the ends of the sheaths with the spore suspension.
- The inoculated sheaths are supported horizontally in a sealed container with a wet paper towel to make a humid chamber so the suspension will not dry out.
- After incubation and before imaging, cut approximately 0.5 cm piece from the incubated sheath ends to eliminate vegetative hyphae that grew into the injured tissue.
- Using a new razor blade, hand-trim the sheath to expose the inner epidermal layer.
- Then slice a long piece as thin as possible to get the epidermal cell layer with only two to three underlying cell layers.
- Next, trim both sides of the sheath to get a flat and clear strip of tissue.
- Finally, mount the strip of tissue on the microscope slide using sterile water. Remove air bubbles by flushing with water. Do not tap the cover slip.
- Now, use it for microscopic imaging of fungal invasion *in planta*.

Figures and Tables

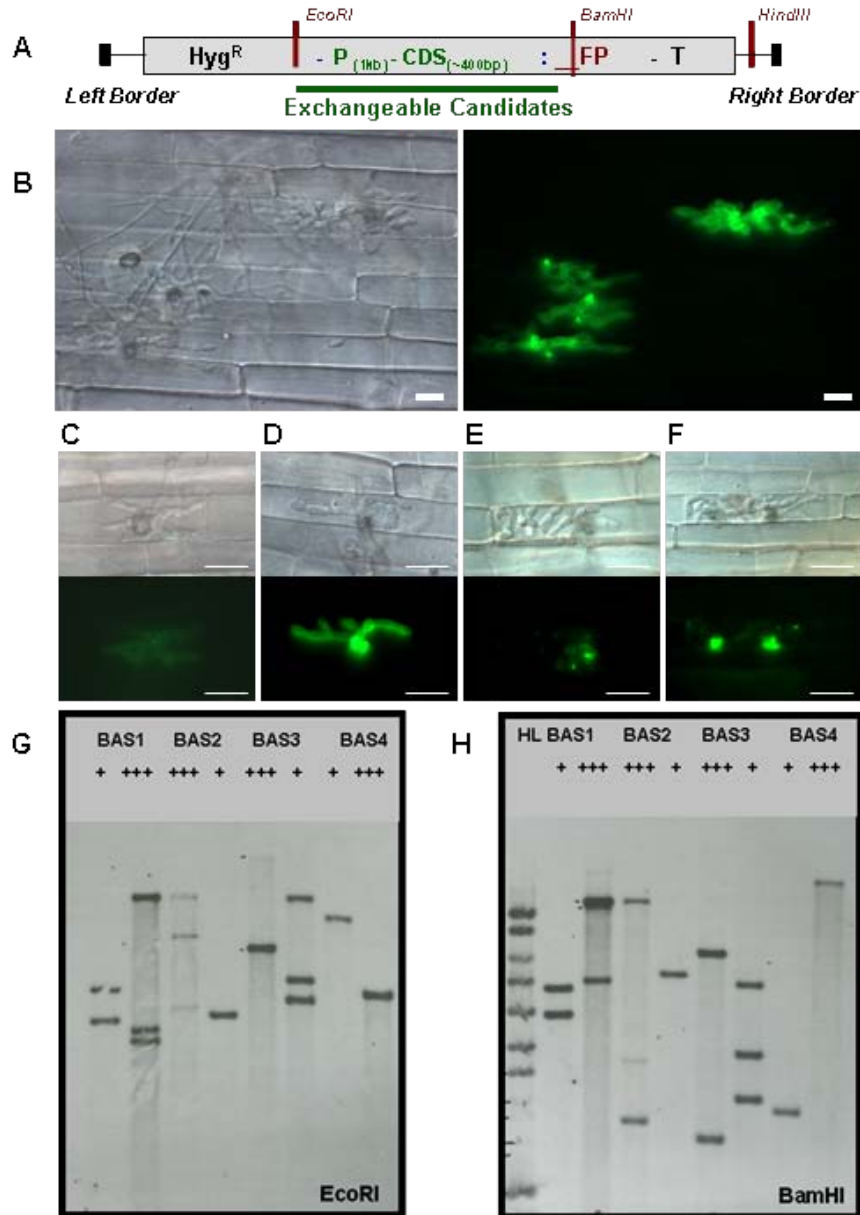


Figure 2.1. Constructs and expression of fluorescent chimeric proteins from *Agrobacterium*-mediated fungal transformation.

Fluorescence localization patterns are conserved for independent fungal transformants expressing putative effector with any fluorescent reporter proteins, although fluorescence intensities vary due to position effects. For each gene, 10 independent transformants were observed during invasion of rice leaf sheath epidermal cells. Images shown are DIC and EYFP.

In order to compare intensities of different transformants, the excitation exposure time was standardized at 2 seconds. (A) Different fluorescent proteins (enhanced yellow, EYFP; monomeric red, mRFP; or enhanced green, EGFP) were expressed in translational fusions with BAS native promoter and the entire BAS coding sequence. These cassettes were cloned into pBHt2 binary vector (T-DNA region) for *A. tumefaciens*-mediated fungal transformation by restriction enzyme digestion-ligation. (B) *In planta* specific expression using BAS4 as an example. Notice the strong expression at infection sites inside rice epidermal cells, but no expression in aerial mycelia on the surface of the sheath piece, observed in the DIC image. Wide-field images, left to right: DIC and EGFP. (C-F) Wide-field images, top to bottom: DIC and EGFP. (C) and (D) Variation between two independent fungal transformants of BAS4, MGG_10914.6, showing the lowest (+) and the strongest (+++) expression, respectively. (E) and (F) Variation between two independent fungal transformants of BAS3, MGG_11610.6, showing the lowest (+) and the strongest (+++) expression, respectively. (G) and (H) Southern hybridization analysis was performed with the least (+) and the strongest (+++) fluorescent transformants of BAS1 (MGG_04795.6), BAS2 (MGG_9693.6), BAS3 (MGG_11610.6) and BAS4 (MGG_10914.6). The Southern hybridization analysis used EYFP as a probe and restriction enzymes (G) *EcoRI* and (H) *BamHI*. This analysis suggested that the intensity did not depend on copy number, but most likely on position effect. Since fluorescence patterns were consistent for each gene, we evaluated the strongest expressed transformants. Bars = 20 μm .

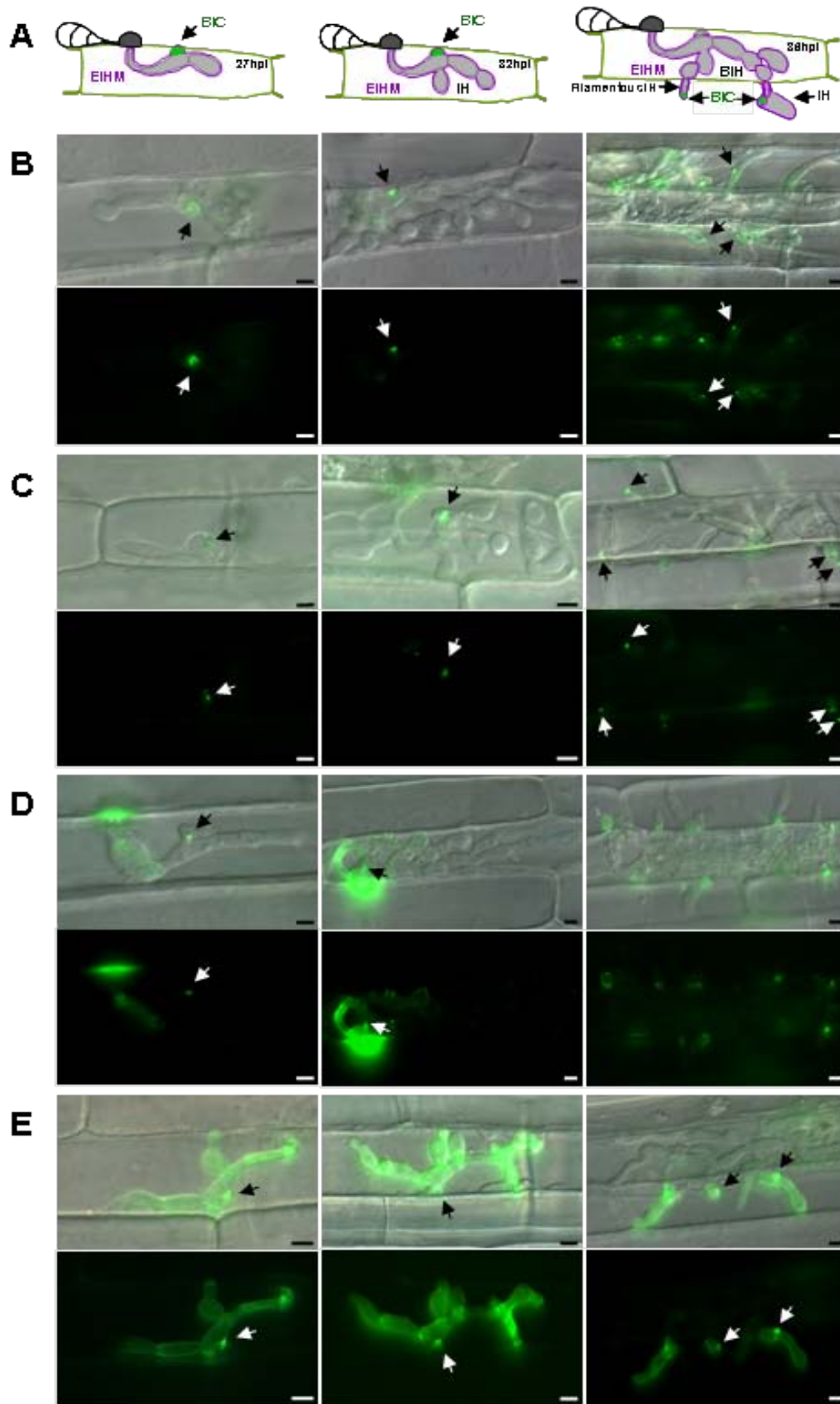


Figure 2.2. Distinct localization patterns of *M. oryzae* BAS proteins *in planta*.

(A) Cartoons showing the BIC development and localization pattern characteristic of AVR effectors at 27, 32, and 36 hpi. The first stage of BIC development, secretion into the extrainvasive hyphal membrane (EIHM) membraneous cap at the tip of primary hypha is not represented. Bulbous invasive hyphae (IH). (B), (C), (D) and (E) For secretion analysis, the promoter and coding sequence for each gene was cloned with EYFP as a C-terminal translational fusion. Fungal transformants expressing BAS:EYFP fusions were observed as they invaded susceptible rice cells of the cultivar YT-16. Shown for each, merged DIC and EYFP images (top) and EYFP fluorescence images alone (bottom). Time points shown are: 27 hpi (left), 32 hpi (middle), and 36 hpi (right). BICs are indicated by arrows. (B) Secretion of BAS1:EYFP fusion protein into BICs. Only representative BICs are labeled with arrows at 36 hpi. (C) Secretion of BAS2:EYFP fusion protein into BICs. Representative BICs are labeled with arrows at 36 hpi. (D) Secretion of the BAS3:EYFP fusion protein. At 27 hpi, note fluorescence at the penetration site and outlining the primary hypha, in addition to a faint BIC. At 32 hpi, multiple fluorescent spots were dispersed around the IH. At 36 hpi, fluorescence is near the cell wall crossing points and not in BICs. (E) Secretion of BAS4:EYFP fusion protein. Fluorescence uniformly outlined the IH. Some fluorescence was also seen in BICs. Bars = 5 μ m.

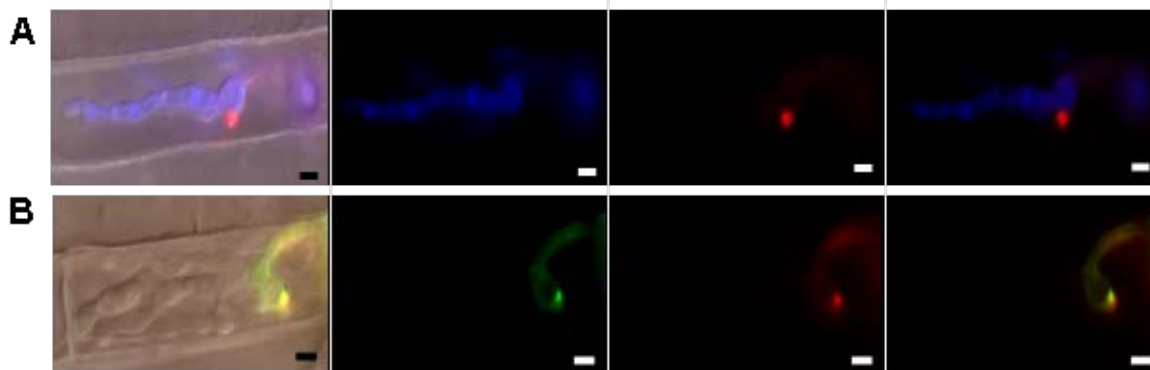


Figure 2.3. BAS1:mRFP secretion and co-localization with AVR-Pita:GFP proteins.

(A) Secretion of BAS1:mRFP by a fungal strain expressing cytoplasmic ECFP at 24 hpi during a compatible interaction. Exposure time for mRFP was 1 sec and for ECFP was 0.2 sec. Wide-field images, left to right: merged DIC, ECFP and mRFP channels; ECFP alone; mRFP alone; Merged ECFP and mRFP. (B) BAS1:mRFP colocalizes with AVR-Pita:EGFP in BICs and around the BIC associated hyphal cells in YT-16 rice at 32 hpi (2 sec exposures). Wide-field images, left to right: Merged DIC, EGFP and mRFP channels; EGFP alone; mRFP alone; merged EGFP and mRFP. Bars = 5 μ m.

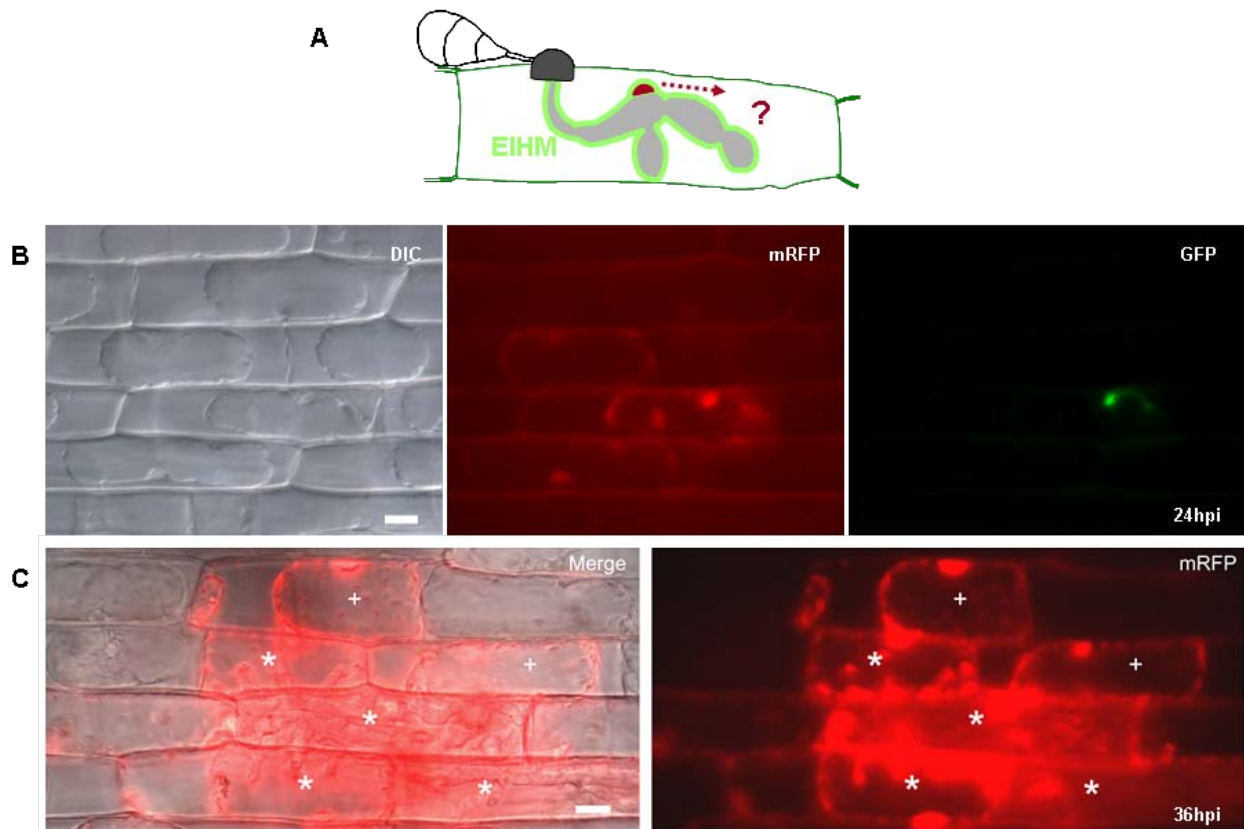


Figure 2.4. BAS1:mRFP, but not BAS4:GFP, is translocated inside rice cytoplasm of invaded cells and moves into uninvaded neighbor cells.

(A) Cartoon showing BAS4:EYFP as EIHM-marker to prove translocation of cytoplasmic effector proteins across an intact EIHM. (B) Fungal transformant KV99 expresses BAS1:mRFP (red) and BAS4:EYFP (green). BAS1:mRFP was observed in the cytoplasm of invaded cells as well as in surrounding cells, in contrast to BAS4 that outlined the primary hyphae at 22 hpi. Wide-field images of individual channels: from left to right: DIC, mRFP, and EGFP. (C) BAS1:mRFP imaged at 36-hpi as described in (B) is translocated into the rice cytoplasm of invaded cells and moves ahead in the neighboring uninvaded cells. Asterisks indicate rice cells with IH and pluses indicate rice cells without IH. Exposure time for mRFP was 1.5 seconds. Wide-field images from left to right: merged DIC and mRFP channels, and mRFP alone. Bars = 10 μ m

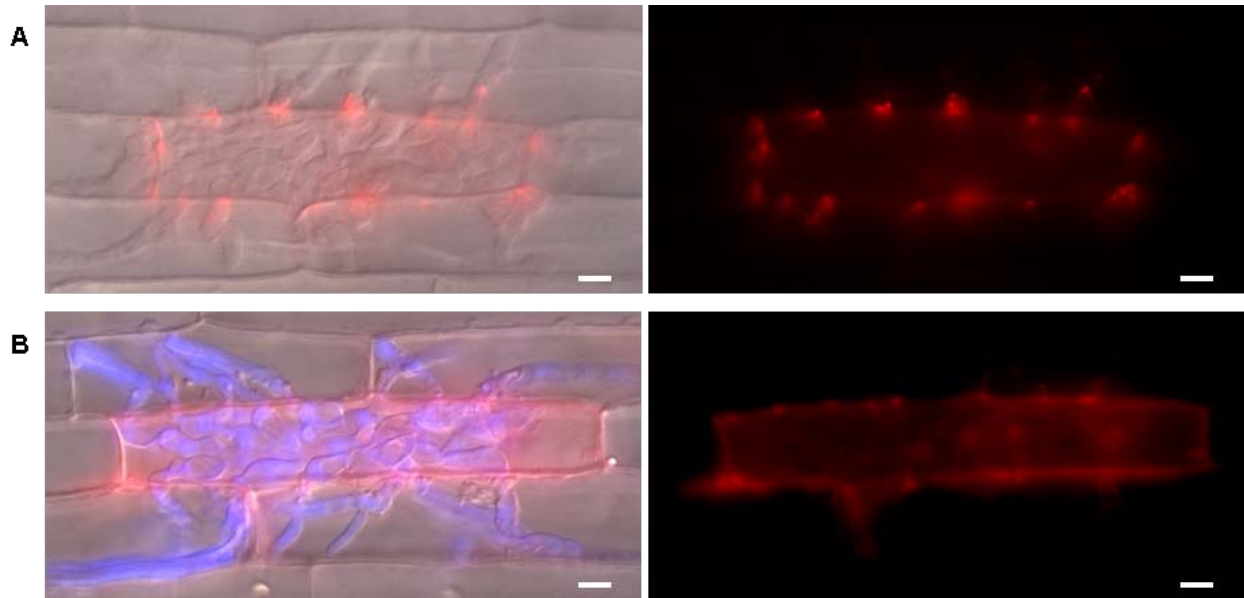


Figure 2.5. BAS2:mRFP and BAS3:mRFP accumulate at the cell wall crossing points where the fungus moves to neighbor cells.

(A) Transformant expressing BAS2:mRFP, wide-field images, left to right: merged DIC, and mRFP channels; mRFP alone. (B) Transformant expressing BAS3:mRFP and cytoplasmic ECFP, wide-field images left to right: merge DIC, ECFP and mRFP channels, and mRFP channel alone. Bars = 5 μm .

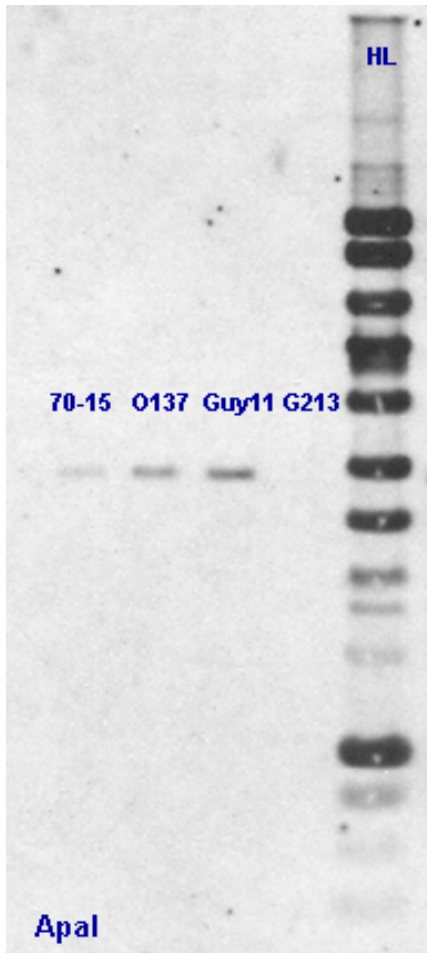


Figure 2.6. Southern blot hybridization of *BAS4* in different *M. oryzae* strains.

Genomic DNAs of strains 70-15, O-137, Guy 11 and G213 were digested with restriction enzyme *ApaI*. Hybridization was performed using *BAS4* coding sequence as a probe. (HL) Hyper ladder I from Bioline. Note that G213, the only strain that is not a rice pathogen, does not have a copy of *BAS4*.

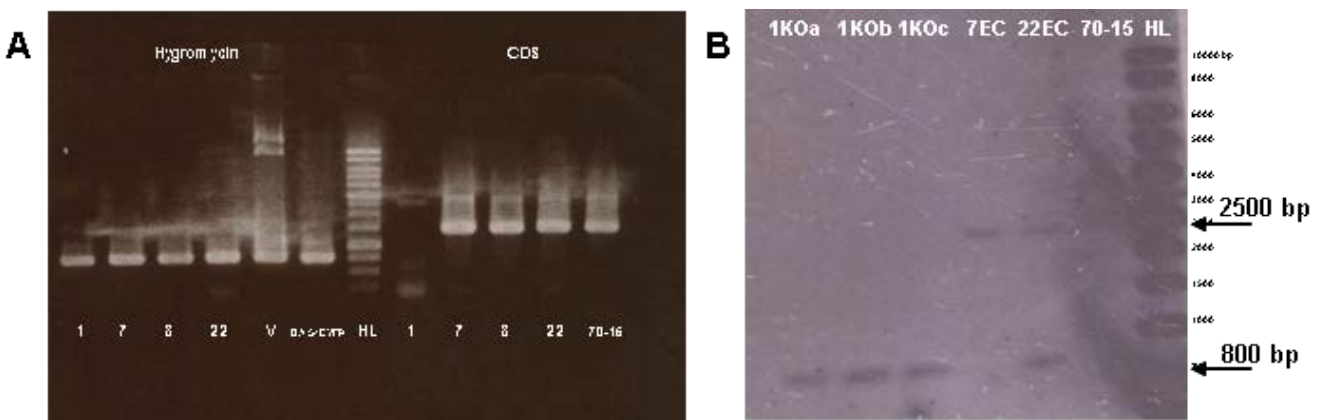


Figure 2.7. Evidence for the *BAS4* gene knock-out (KO) mutant.

(A) From left to right, PCR amplification of the hygromycin resistance gene (*Hyg*; ~750bp) from transformants 1, 7, 8, 22, the vector control, and previously obtained *BAS4*:EYFP transformant containing the *Hyg* gene. The next lane contains Hyper ladder I, followed by samples from a different PCR amplification using specific primers for *BAS4* coding sequence (~1300 bp) of transformants 1, 7, 8, 22, and wild type 70-15. Note that the *Hyg* resistance gene was amplified from transformant 1, but not the *BAS4* fragment suggesting transformant 1 is a KO mutant. (B) Southern hybridization using the 3' fragment between *XhoI*-*HindIII* from the KO cassette as a probe (Figure 2.8). For a true positive KO mutant the expected size is ~800 bp and for an ectopic mutant, ~2500 bp. Samples from left to right, 3 independent monoconidial cultures of mutant 1, the unique KO candidate (~800bp), and 2 different ectopic mutants 7, 22, wild type 70-15 (~2500 bp), and Hyper ladder I, with bands from bottom to top, 750, 1000, 1500, 2000, 2500, 3000, 4000, 5000, 6000, 8000 and 10000 base pairs.

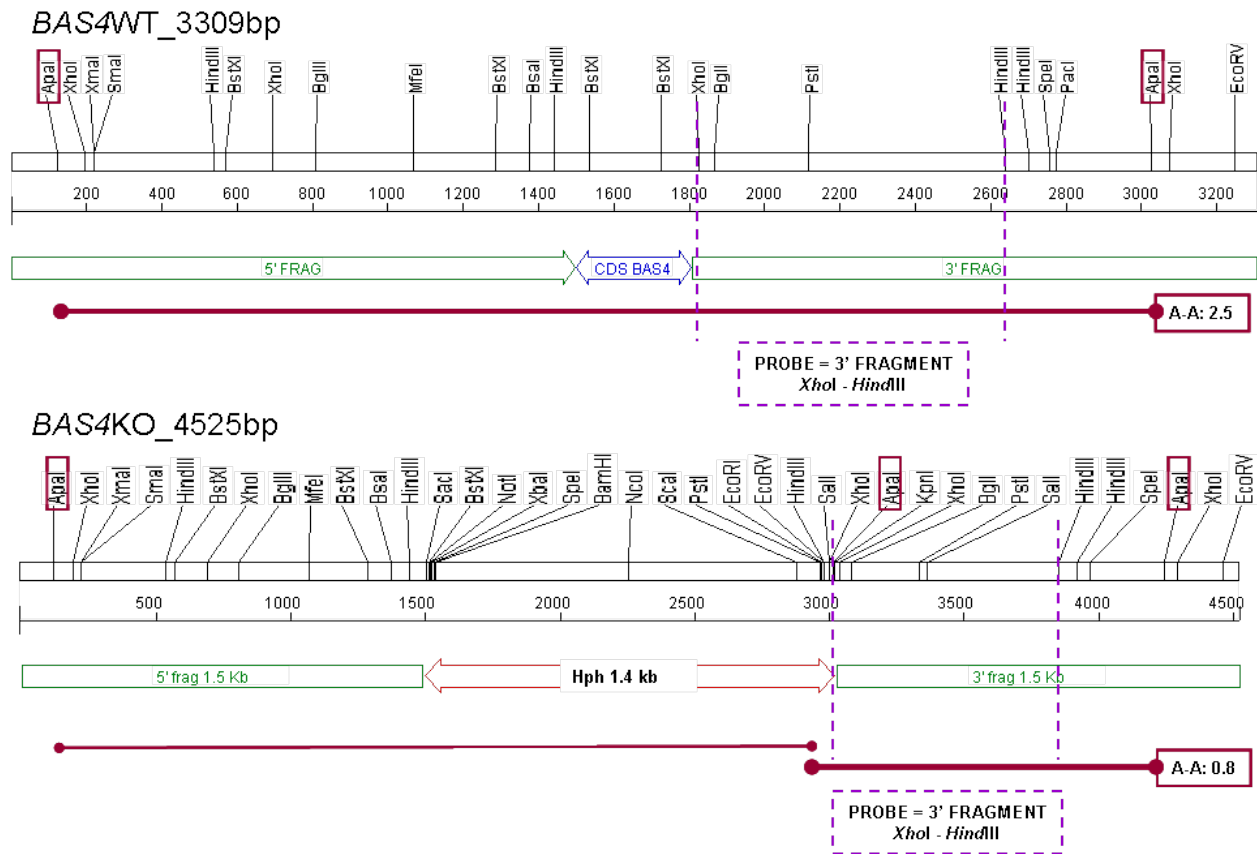


Figure 2.8. Restriction Enzyme Map of *BAS4* and the *BAS4* KO allele.

Both maps show the fragments expected from genomic DNA of *BAS4* wild type and *BAS4* KO mutant after digestion with *ApaI* restriction enzyme and hybridized using the 3' *XhoI* – *HindIII* fragment as a probe.

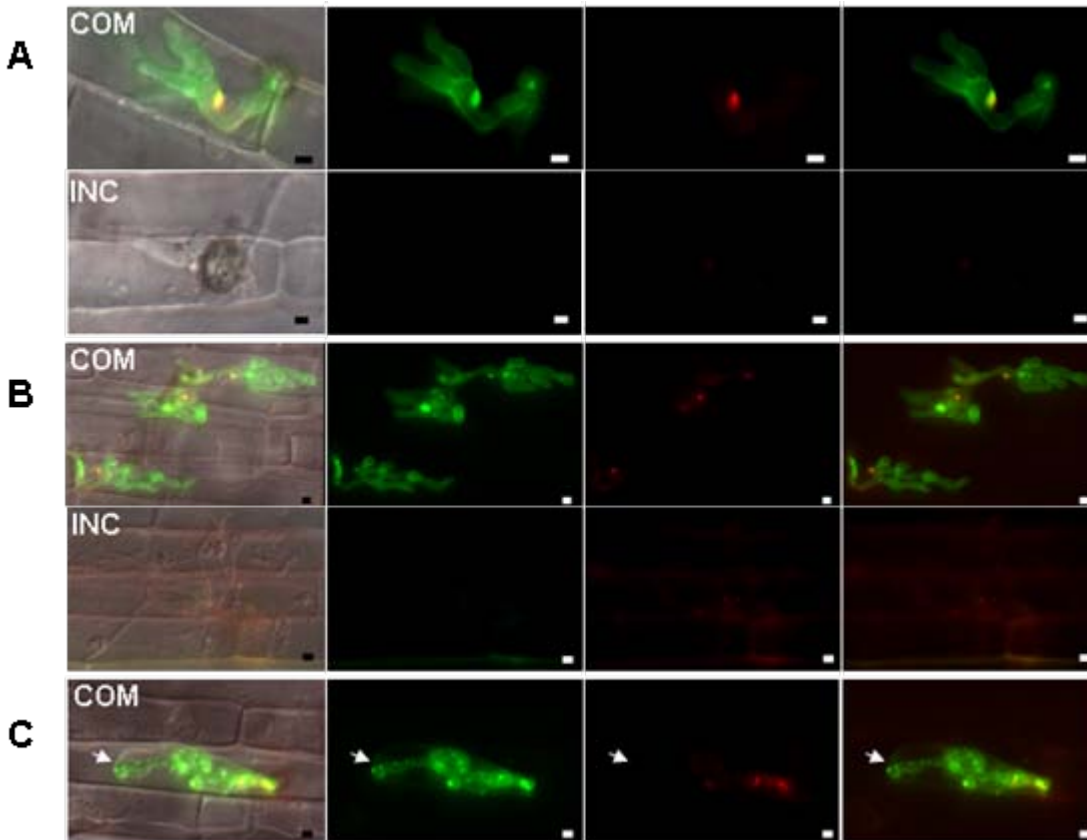


Figure 2.9. BAS proteins accumulate together with the effector PWL2 in susceptible, YT-16, but not in resistant, Yashiro-mochi, rice cells.

(A, B, C) Inoculations on YT-16 rice plants without *Pita* (*Pita*⁻) for compatible (COM) and on Yashiro-mochi containing *Pita* (*Pita*⁺) for incompatible (INC) interactions using fungal strain O-137 (*AVR-Pita*⁺) co-expressing PWL2:mRFP and BAS4:EGFP. (A) Infection at 24 hpi. (B-C) Infection at 33 to 34 hpi, the rice cells are plasmolyzed in 0.75 M sucrose. (B) COM showed normal expression and secretion of both PWL2:mRFP and BAS4:EGFP. INC showed thin hyphae from the first invaded cell had moved to the next cells. The rice cytoplasm appears severely disrupted, and faint fluorescence from PWL2:mRFP was observed, but not BAS4:EGFP. (C) COM infection site at 33 to 34 hpi, the IH on a plasmolyzed rice cell showed non uniform BAS4:EGFP outlining of the IH, which seems to have spilled into the surrounding plasmolyzed rice cytoplasm. This infection site also showed faint mRFP signal in the BIC. Exposure times were 1 sec for mRFP; and 500 ms for GFP. Wide-field images, left to right: merged DIC, EGFP and mRFP channels; EGFP alone; mRFP alone; merged EGFP and mRFP. Bars = 5 μ m.

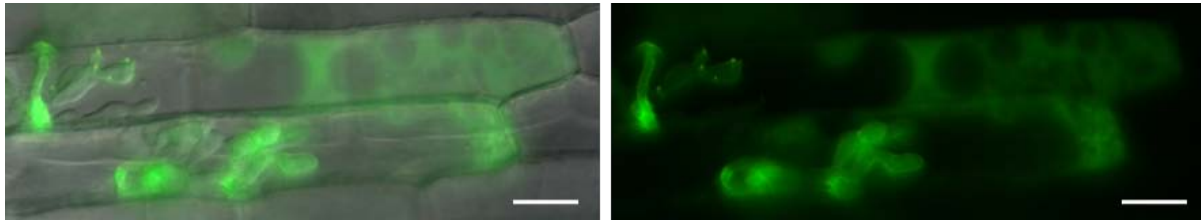


Figure 2.10. BAS4:EYFP failed to outline IH and appeared in the host cell, indicating unsuccessful infection sites during compatible interactions.

Inoculations on YT-16 rice plants without *Pita* (*pita*-) for compatible interaction with fungal strain O-137 (*AVR-Pita*+) expressing BAS4:EYFP at 27 hpi. EYFP exposure time was 500ms. Wide-field images, left to right: merged DIC and EYFP channels, and EYFP alone. Bars = 20 μ m.

Table 2.1. List of gene candidates characterized and *AVR* genes, *PWL2* and *AVR-Pita1*.

Probe (Fold-change) ^a	Gene Name ^b	AA (cys)	<i>M.o.</i> hits (E-value)	Other fungal hits (Organism; E-value) ^d	Chr. Location / Comments ^e
AMG08261 (100)	MGG_04795.6 <i>BAS1</i>	115 (0)	None	none	IV: 1,216,801-
AMG08541 (84)	MGG_09693.6 <i>BAS2</i>	102 (6)	MGG_07969.6 (E=2e-28); MGG_07749.6 (E=4e-17)	<i>P. tritici</i> (E=4e-21); and 5 other fungi	V: 5,545,247+
AMG12560 (71)	MGG_11610.6 <i>BAS3</i>	113 (10)	none	none	IV: 3,454,688+
AMG15980 (61)	MGG_10914.6 <i>BAS4</i>	102 (8)	E=2e-7	none	VI: 236,698+
AMG11184 (63)	MGG_04301.6 <i>PWL2</i>	145 (2)	MGG_13863.6 (E=0); MGG_07398.6 (E=8e-16)	none	IV: 1,480,013-
Same as above	MGG_13863.6 <i>PWL2</i>	145 (2)	MGG_04301.6 (E=0); MGG_07398.6 (E=8e-16)	none	III: 5,594,534-
RMG00001 (3)	MGG_15370.6 <i>AVR_Pita1</i>	224 (9)	E=0; E=2e-19plus others	<i>A.capsulatus</i> E=8E-12	VII: 232,500- Located next to MGG_15371.6

Table 2.2. Testing candidate genes with different fluorescent proteins in different background strains.

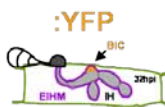
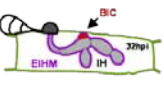

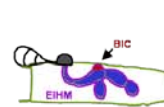
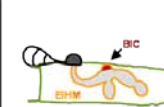
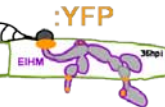
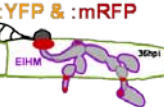
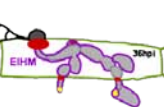
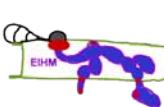
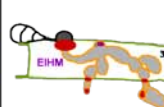

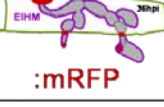
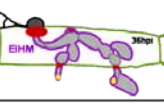

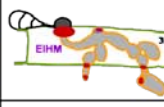

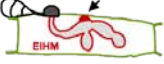

Strain \ Gene	avrPita ⁻	AVRPita ⁺	avrPita:GFP BIC Pattern	CONSTITUTIVE GFP	BAS4:YFP SECRETED
			Colocalization	Secretion	EIHM – Intactness
BAS1 (MGG_04795.6)					
BAS2 (MGG_09693.6)					
BAS3 (MGG_11610.6)					
BAS4 (MGG_10914.6)					

Table 2.3. Primers used for KO and expression constructs of BAS proteins.

Primer Name	Sequence 5'-3'	Description
Fungal primers for gene knock-out cassette		
MGG_10914.6-5'F	CTGCAG TTG GTA GAT GGA ACA TTT C	1.5-kb-5'-flanking region of
MGG_10914.6-5'R	GGATCC TGT GAA AAG ATT CGT TGT G	MGG_10914.6
MGG_10914.6-3'F	GGTACC GAGGGTTCTTTCACCTCGA	1.5-kb-3'-flanking region of
MGG_10914.6-3'R	TCTAGA CCAAAGCGGCCCAAG C	MGG_10914.6
HYG-1F	GGCTTGGCTGGAGCTAGTGGAGG	1.4-kb hygromycin gene
HYG-2R	AACCCGCGGTCGGCATCTACTCTA	1.4-kb hygromycin gene
Primers for fluorescent protein fusion		
MGG_04795.6		1.3-kb promoter plus entire coding
BAS1-F	ACAGAATAAGACACGGCAAGATTTA	sequence
MGG_04795.6		
BAS1-R	CGGGTAATAATTCTCCACCCGTCTA	
MGG_09693.6		1.4-kb promoter plus entire coding
BAS2-F	GGAAAGCTCGACTCCCAGAGAGCTG	sequence
MGG_09693.6		
BAS2-R	GAAACCCTGCTTCTTGACCTGCTCC	
MGG_11610.6		1.5-kb promoter plus entire coding
BAS3-F	GCAGAGTGTCCATCCGATAATCACAT	sequence
MGG_11610.6		
BAS3-R	GTGGGCACTGTTGGCAGCGCCGTTC	
MGG_11610.6		1.0-kb MGG_11610.6
BAS3-R2	GGTAGCTTCTACGGATGCGTCCGAT	
MGG_10914.6		1.5-kb promoter plus entire coding
BAS4-F	AGCAGGGGGGATAGACGAGCCAGTA	sequence
MGG_10914.6		
BAS4-R	ACAGAATAAGACACGGCAAGATTTA	
<i>FBam</i> YFP	CGCGGATCCGCGATGGTGAGCAAGGGCG AGGAGCTGT	1.0-kb EYFP and <i>Neurospora crassa</i> β -tubulin terminator
<i>RHind3</i> T	CCCAAGCTTGGGATCATCATGCAACATGC ATGTACTG	
MGG_04795.6	GGATCCTTTAGGAATAATTGGTAAAGAT	1.0-kb MGG_04795.6 promoter
BAS1-R2		sequence; used with the primer MGG_04795.6_BAS1-F

Primers for fluorescent protein fusion, continued

MGG_11610.6 BAS3-R2	GGATCCCTTGATGGTTGGGTTTTGG	1.0-kb MGG_11610.6 promoter sequence; used with the primer MGG_11610.6_BAS3-F
CKP110_SP5P-F	GAATTCGGTAGCTTCTACGGATGC	1.0-kb MGG_10914.6, BAS4,
CKP111_SP5P-R	GGATCCTGTGAAAAGATTCGTTGTG	promoter sequence
CKP104_SP5SP-F	GGATCCATGCAGCTCTCATTCTC	MGG_10914.6, BAS4, signal
CKP105_SP5SP-R	CTGCAGGGTGCGAGTCGGCCGTAG	peptide sequence
CKP35_mRFP-Bam	GGATCCGCCTCCTCCGAGGACGTC	mRFP reporter gene
CKP36_mRFP-Sph	GCATGCTTAGGCGCCGGTGGAGTG	

Table 2.4 Plasmids used for fungal transformation.

Clone	Description
pBV14	EYFP expression vector derived from pSM324 (Bourett et al., 2002)
pBV176	EGFP expression binary vector derived from pBHt2 (Mullins et al., 2001), containing <i>M. oryzae</i> ribosomal protein 27 promoter (RP27) <i>EcoRI-PstI</i> fragment, EGFP <i>PstI-SphI</i> fragment, and <i>Neurospora crassa</i> β -tubulin terminator <i>SphI-HindIII</i> fragment. Cloned in <i>EcoRI-HindIII</i> sites of pBHt2. P27 was amplified by PCR from pBV11 (=pSM565; Bourett et al., 2002), and EGFP: <i>N. crassa</i> β -tubulin terminator from pSK1810 (Seogchan Kang, unpublished results).
pBV181	1.0-kb PCR product of EYFP and <i>Neurospora crassa</i> β -tubulin terminator from pBV13 (Berruyer et al., 2006) was digested with <i>BamHI</i> and <i>HindIII</i> , and subsequently cloned in <i>BamHI</i> and <i>HindIII</i> sites of binary vector pBHt2. Kanamycin and hygromycin resistance
pBV192	0.7-kb PCR product of mRFP reporter gene (monomeric red fluorescence protein; (Campbell et al., 2002) cloned in pGEM-T vector (Promega)
pBV197	1.0-kb <i>EcoRI-BamHI</i> fragment of BAS1, MGG_04795.6 promoter cloned in <i>EcoRI-BamHI</i> sites of pBV176
pBV227	1-kb <i>EcoRI-BamHI</i> fragment of MGG_11610.6 promoter cloned in <i>EcoRI-BamHI</i> sites of pBV176
pBV231	1.2-kb PCR product of BAS1, MGG_04795.6 promoter plus entire coding sequence was digested with <i>EcoRI</i> and <i>BamHI</i> , and subsequently cloned in <i>EcoRI-BamHI</i> sites of pBV181. Kanamycin and hygromycin resistance
pBV232	1.4kb PCR product of BAS3, MGG_11610.6 promoter plus entire coding sequence was digested with <i>EcoRI</i> and <i>BamHI</i> , and subsequently cloned in <i>EcoRI-BamHI</i> sites of pBV181. Kanamycin and hygromycin resistance
pBV233	1.3kb PCR product of BAS4, MGG_10914.6 promoter plus entire coding sequence was digested with <i>EcoRI</i> and <i>BamHI</i> , and subsequently cloned in <i>EcoRI-BamHI</i> sites of pBV181. Kanamycin and hygromycin resistance
pBV234	1.3kb PCR product of BAS2, MGG_09693.6 promoter plus entire coding sequence was digested with <i>EcoRI</i> and <i>BamHI</i> , and subsequently cloned in <i>EcoRI-BamHI</i> sites of pBV181. Kanamycin and hygromycin resistance
pBV261	SK2645 MgAPT2 knock out construct, pGKO2 (Khang et al., 2005)
pBV324	1.0-kb <i>EcoRI-BamHI</i> fragment of MGG_10914.6, BAS4 promoter and 72-bp <i>BamHI-PstI</i> fragment of MGG_10914.6 signal peptide cloned in <i>EcoRI-PstI</i> sites of pBV176. C-terminal translational fusion of BAS4 promoter sequence and signal peptide to the EGFP reporter gene
pBV367	mRFP expression binary vector derived from pBGt (Seogchan Kang, unpublished results), consisting of three modules of P27 (<i>EcoRI-BamHI</i> fragment), mRFP (<i>BamHI-SphI</i> fragment

Clone	Description
	of pBV192), and <i>N. crassa</i> β -tubulin terminator (<i>SphI-HindIII</i> fragment) that were cloned in <i>EcoRI-HindIII</i> sites of pBGt. Kanamycin and G418 resistance
pBV440	1.2-kb <i>EcoRI-BamHI</i> fragment from pBV231 cloned in <i>EcoRI-BamHI</i> sites of pBV367. C-terminal translational fusion of BAS1 entire coding sequence to the mRFP reporter gene. Kanamycin and G418 resistance
pBV441	1.4-kb <i>EcoRI-BamHI</i> fragment from pBV232 cloned in <i>EcoRI-BamHI</i> sites of pBV367. C-terminal translational fusion of BAS3 entire coding sequence to the mRFP reporter gene. Kanamycin and G418 resistance
pBV442	1.3-kb <i>EcoRI-BamHI</i> fragment from pBV234 cloned in <i>EcoRI-BamHI</i> sites of pBV367. C-terminal translational fusion of BAS2 entire coding sequence to the mRFP reporter gene. Kanamycin and G418 resistance
pBV443	1.3-kb <i>EcoRI-BamHI</i> fragment from pBV233 cloned in <i>EcoRI-BamHI</i> sites of pBV367. C-terminal translational fusion of BAS4 entire coding sequence to the mRFP reporter gene. Kanamycin and G418 resistance
pBV566	4.4-kb BAS4 KO, <i>PstI-XbaI</i> fragment into pBV261. Kanamycin and hygromycin resistance

Table 2.5. Fungal transformant strains.

Name	Description [background strain; plasmid used]
KV9	Transformant containing a constitutive, cytoplasmic ECFP reporter gene
KV89	Transformant with promoter (P) _{MGG_04795} :MGG_04795 coding sequence (CDS):EYFP:Ter [CP987; pBV231], BAS1:EYFP
KV90	Transformant with P _{MGG_11610} :MGG_11610CDS:EYFP:Ter [CP987; pBV232], BAS3:EYFP
KV91	Transformant with P _{MGG_10914} :MGG_10914CDS:EYFP:Ter [O-137; pBV233], BAS4:EYFP
KV92	Transformant with P _{MGG_09693} :MGG_09693CDS:EYFP:Ter [O-137; pBV234], BAS2:EYFP
KV93	Transformant with P _{MGG_04795} :EGFP:Ter [Guy11; pBV197], BAS1:EGFP
KV94	Transformant with P _{MGG_11610} :EGFP:Ter [Guy11; pBV227], BAS3:EGFP
KV95	Transformant containing both a fusion of <i>AVR-Pital</i> promoter and sequence for signal peptide with EGFP reporter gene, and a fusion of MGG_04795, BAS1 promoter and entire coding sequence with mRFP reporter gene [Ft080; pBV440]
KV96	Transformant containing a constitutive, cytoplasmic ECFP reporter gene, and a fusion of MGG_04795, BAS1 promoter and entire coding sequence with mRFP reporter gene [KV9; pBV440]
KV97	Transformant with P-SP _{MGG_10914} :EGFP:Ter [O-137; pBV324], BAS4promSP:EYFP
KV98	Transformant with P-SP _{MGG_10914} :EGFP:Ter [KV97; pBV 377], BAS4promSP:EYFP and PWL2 promoter and entire coding sequence fused with mRFP reporter gene
KV99	Transformant containing BAS4:EYFP and a fusion of MGG_04795, BAS1 promoter and entire coding sequence with mRFP reporter gene [KV91; pBV440]
KV100	Transformant containing both a fusion of <i>AVR-Pital</i> promoter and sequence for signal peptide with EGFP reporter gene, and a fusion of MGG_11610, BAS3 promoter and entire coding sequence with mRFP reporter gene [Ft080; pBV441]
KV101	Transformant containing a constitutive, cytoplasmic ECFP reporter gene, and a fusion of MGG_11610, BAS3 promoter and entire coding sequence with mRFP reporter gene [KV9; pBV441]
KV102	Transformant containing BAS4:EYFP and a fusion of MGG_11610, BAS3 promoter and entire coding sequence with mRFP reporter gene [KV91; pBV440]
KV109	MGG_10914.6, BAS4 knock-out transformant #1 [70-15; pBV261]
KV110	MGG_10914.6 BAS4 ectopic transformant # 22 [70-15; pBV261]
KV111	MGG_10914.6 BAS4 ectopic transformant # 7 [70-15; pBV261]
KV112	Transformant containing BAS1 with mRFP reporter gene [O-137; pBV367]
KV113	Transformant containing both a fusion of <i>AVR-Pital</i> promoter and sequence for signal

Name	Description [background strain; plasmid used]
	peptide with EGFP reporter gene, and a fusion of BAS1 promoter and entire coding sequence with mRFP reporter gene [Ft080 (CP987); pBV367]
KV114	Transformant containing BAS2 with mRFP reporter gene [O-137; pBV367]
KV115	Transformant containing both a fusion of <i>AVR-Pital</i> promoter and sequence for signal peptide with EGFP reporter gene, and a fusion of BAS2 promoter and entire coding sequence with mRFP reporter gene [CP987; pBV367]
KV116	Transformant containing BAS4 with mRFP reporter gene [O-137; pBV367]
KV117	Transformant containing both a fusion of <i>AVR-Pital</i> promoter and sequence for signal peptide with EGFP reporter gene, and a fusion of BAS4 promoter and entire coding sequence with mRFP reporter gene [CP987; pBV367]
KV119	Transformant containing BAS4:EYFP and a fusion of BAS2 promoter and entire coding sequence with mRFP reporter gene [O-137; pBV367]
KV120	Transformant containing a constitutive, cytoplasmic ECFP reporter gene, and a fusion of BAS2 promoter and entire coding sequence with mRFP reporter gene [KV9; pBV367]
Ft080	Transformant containing a fusion of <i>AVR-Pital</i> promoter and sequence for signal peptide with EGFP reporter gene [CP987; pSK1880]

Chapter 3 - Identification of the Spitzenkörper and Polarisome in *Magnaporthe oryzae* during Biotrophic Rice Invasion.

Abstract

In the rice blast fungus, *Magnaporthe oryzae*, the unique commonality found among all known effector proteins is their accumulation in the novel *in planta* BIC (biotrophic interfacial complex) structure, which stays beside the first bulbous IH cell as the fungus continues to grow in the rice cell. BIC accumulation of effectors suggests either a specialized mechanism for effector secretion from the BIC-associated cells behind the growing hyphal cells or a mechanism for movement to BICs after secretion at the hyphal growth points. Understanding the mechanism of secretion of blast effector proteins into BICs may help in identification of new blast effectors, provide evidence that supports the hypothesis that the BIC is a site of blast effector translocation inside rice cells, and validate the hypothesis that *M. oryzae* undergoes differential secretion mechanisms for proteins involved in hyphal growth, extracellular enzymes, and effectors. Availability of a wide range of fluorophores and of an extensive list of markers for the secretion apparatus in filamentous fungi, provide an opportunity to dissect cellular trafficking with ideal spatiotemporal resolution *in vivo*. The ability to tag cellular components of the secretion machinery in *M. oryzae* provides a tool for understanding the mechanism of protein secretion into BICs, and analyzing the cellular trafficking with respect to BICs. Our research objective was to visualize the main fungal secretion components in order to identify which of these components might be involved in blast-effector secretion into BICs. We generated fungal transformants that contained fluorescently-labeled components of the Spitzenkörper, polarisome, early endosomes, β -tubulin and actin cables. Visualization of secretion-associated sites and machinery relative to BICs, by live cell imaging during the invasion *in planta*, suggested that most likely the secretion of effectors to BICs involves early endosome-coupled exocytosis. We found that the Spitzenkörper, the secretory vesicle supply center typically observed at the apex of the filamentous hyphae *in vitro*, is also localized at the apex of the filamentous primary hyphae *in planta*. However, after the IH had differentiated to bulbous IH *in planta*, a vesicle supply center-like structure fluorescently-labeled by Mlc1p and Snc1p was still present in the BIC-associated cells, usually as an intense spot close to the BICs. We suggest naming this putative

vesicle supply center inside the first bulbous IH cell as the “Seitenkörper”, since it is not at a hyphal apex. In addition, localization of the polarisome marker Spa2p is spatially distinct from the localization of Mlc1p and Snc1p *in planta*, after the fungus switches growth from the filamentous primary hypha to bulbous IH. These findings support the hypothesis that there is a spatially-segregated mechanism for secretion of effectors into BICs. Continuous active secretion in the BIC-associated cells supports the importance of the BICs in the efficient translocation of critical effector proteins inside the host cytoplasm during biotrophic invasion. Additionally, these results show that the switch of growth from polarized to bulbous IH is accompanied by a modification of the filamentous hyphal secretion mechanism.

Introduction

Filamentous fungi are differentiated from yeast cells by highly polarized growth at the hyphal apex. The mechanism involved in this distinct growth requires a transfer of secretory vesicles from the trans-Golgi apparatus to the plasma membrane at the tip by way of an apical vesicle supply center named the Spitzenkörper (apex body, Spk) (Bartnicki-Garcia et al., 1989; Bartnicki-Garcia et al., 1995). The contents of these vesicles are important for membrane and cell wall synthesis and in some cases for secretion of enzymes or other proteins that are essentials for pathogenicity. After the secretory vesicles are fissioned from the trans-Golgi, they are moved along actin cables towards the sites of polarized growth. Actin cables are nucleated by a formin, Bin1, assisted by the polarisome, a three-protein complex of Spa2p, Pea2p and Bud6p (Originally named in *Saccharomyces cerevisiae*). The formation and activity of the polarisome are controlled by the Cdc42p as part of a complex with Bem1. This fission and fusion of secretory vesicles to the plasma membrane is directed by the SNAREs (soluble N-ethylmaleimide-sensitive factor attachment protein receptors), the v-SNAREs Snc1p, Snc2p on the vesicle, and the t-SNAREs Sec9p, Sso1p, and Sso2p on the membrane (Knop et al., 2005). The exocyst is an octameric-protein complex comprised of Sec3p, Sec5p, Sec6p, Sec8p, Sec10p, Sec15p, Exo70p and Exo84p. Sec4p, an essential Rab GTPase, determines the linear movement that directs the secretory vesicles to the exocytosis subunit Sec15p. The transport of secretory vesicles along actin cables is mediated by Myo2p, a class V Myosin, and by its essential regulatory light chain 1, Mlc1p. Myo2p and Mlc1p are localized at sites of growth, generally at hyphal tips (Crampin et al., 2005; Sudbery and Court, 2007; Shoji et al., 2008)

Two essential pathways in vesicular trafficking are conserved in eukaryotic cells. The first is the exocytosis pathway where the traffic moves from the endoplasmic reticulum (ER), through the Golgi cisternae-cis, medial, and trans-to the plasma membrane (PM). The second is the endocytosis pathway, where internalization occurs in the opposite direction from the PM via a set of vesicles called endosomes. Early endosomes (EE) have a bidirectional movement, and can be targeted to move from the plasma membrane and back for recycling; and late endosomes (LE) are targeted to the lysosome for degradation. Both pathways depend on membrane-bound vesicles to transfer cargo proteins between compartments, and regulation of this secretory pathway depends on the Ypt/Rab GTPase family (Segev, 2001; Samaj et al., 2004; Lodish et al., 2008; Shoji et al., 2008). In yeast, 11 genes encoding Ypts have been identified and, in humans, 60 Rab family members have been identified. Specific domains in the Rab proteins are key for the interaction of Ypt/Rabs with their regulators and downstream effectors. In these pathways, vesicle and compartment transport occurs via molecular motors that bind to membranes mediated by SNAREs and move along the cytoskeleton. In the cytoskeleton, microtubule-based motors, kinesins and dynein, mediate the long-range movement and actin motors, myosins, mediate the short-range movement (Valkonen, 2003; Valkonen et al., 2007).

SNAREs have been classified in relation to their localization. v-SNAREs are anchored in the vesicular membrane, and are referred to as vesicle-associated membrane protein (VAMP). v-SNAREs supply an arginine (R) residue in the assembled core SNARE complex containing a specific synaptobrevin domain, and are also known as R-SNAREs because of their composition. t-SNAREs are located at the cell membrane and contain a glutamine (Q) residue in the SNARE complex, and because of their composition, are also known as a Q-SNAREs. The binding specificity is directed by their structural domains, typically from 60-70 amino acids (Kuratsu et al., 2007; Valkonen et al., 2007).

In *Saccharomyces cerevisiae*, Mlc1p is required for vesicle delivery at the mother-bud neck during cytokinesis (Wagner et al., 2002). Mlc1p, has a EF-hand motif, found in a large family of calcium binding proteins, located in both the N- and C-terminal ends of the protein, connected via a linker region. Mlc1p also interacts with the IQ motifs (basic and hydrophobic residues that bind Calmodulin) of other proteins, such as a class V myosin essential for vesicle polarization in *S. cerevisiae* (Bielli et al., 2006). Class V myosins, which are highly conserved among eukaryotes, act as actin motors that bind to organelles and secretory vesicles by their C-

terminal EF-hand domains to allow movement along actin filaments. Direct protein-protein interaction required for polarized secretion has been demonstrated between Mlc1p, Myosin V motor proteins and the Rab GTPases Ypt31/32 (proteins that function by switching from GTP- to GDP-bound state). Mlc1p has an essential role in the regulation of the timing and specificity of vesicle attachment and docking in vesicular trafficking (Wagner et al., 2002; Casavola et al., 2008; Lipatova et al., 2008). Most recently, Casavola et al (2008) demonstrated direct protein-protein interactions between both Ypt32p and Mlc1p and the Myo2p C-terminal globular tail domain (GTD) by using the yeast two-hybrid system, *in vitro* pull down assays and site directed mutagenesis. Thus, Mlc1p interact at the Myo2p GTD region, overlapping with Ypt32p, (Rab/Ypt protein), forming a membrane-bound complex that is essential for regulation of Sec2p and Sec4p (exocyst subunit) in vesicle-motor interactions (Wagner et al., 2002).

Discovery of fluorescent proteins and their application in cell biology increased our capability to follow the behavior of critical proteins in living cells (Chiu et al., 1996; Chalfie and Kain, 1998; Cutler et al., 2000; Campbell et al., 2002; Czymmek et al., 2002). Riedl et al (2008) (Riedl et al., 2008) developed and verified an F-actin general marker in eukaryotes called Lifeact. Lifeact has been successful for F-actin labeling *in vitro* studies in *Neurospora crassa* (Berepiki et al., 2010) and in *M. oryzae* (Patkar et al., 2010). Lifeact is a 17 amino acid peptide derived from Abp140, a nonessential yeast actin-binding protein.

Recent advances in genomics and proteomics also bring new tools for analysis of critical cellular mechanisms like secretion. In *S. cerevisiae*, Zhang et al (2009) presented a computational and experimental methodology for high-throughput screening of protein-protein interactions, to uncover coiled-coil interactions implicated in vesicular trafficking. This computational methodology is based on structural annotations of domains that bring a map of protein-protein interactions, providing a number of relations that can be key for functional studies in vesicular trafficking.

Study of key components of polarized growth in filamentous fungi is essential to understand the strong association between morphogenesis, secretion and pathogenicity. Sudbery and Court (2007) presented a review of polarized growth in fungi, in a comprehensive view of the main cellular components and their roles from budding yeast to highly polarized filamentous fungi. The genome sequence of *M. oryzae* (Dean et al., 2005), a hemibiotrophic plant fungal pathogen, revealed an enrichment for G-protein coupled receptors, which supported the high

levels of flexibility displayed by this pathogen to respond to diverse environmental signals (Dean et al., 2005; Kulkarni et al., 2005). In *Candida albicans* and *Ustilago maydis*, that flexibility has been associated with dramatic changes in growth required for virulence (Wedlich-Soldner et al., 2000; Gow et al., 2002; Crampin et al., 2005). For *M. oryzae* the lack of pathogenicity phenotypes from functional studies of blast effectors dramatically contrasts results from mutational studies on GTP-binding proteins, Rho3 and Cdc42, and on polarity factor, Tea4. Deletions of these genes showed significant virulence phenotypes (Zheng et al., 2007; Zheng et al., 2009; Patkar et al., 2010).

Results from this study suggested that most likely the secretion of effectors to BICs involves early endosome-mediated recycling and regulated exocytosis. We present results from evaluation *in planta* of *M. oryzae* MoMlc1p, MoSnc1p, MoYup1p and MoSpa2p that support the hypotheses that active secretion occurs from the BIC-associated cells into BICs. These results also suggest that BICs play a role in efficient and regulated translocation of blast effector inside the rice cell during biotrophic invasion, and that the switch of growth from polarized to bulbous IH is accompanied by a modification of the secretion mechanism critical for the biotrophic invasion. We suggest naming the putative secretory vesicle supply center localized in the BIC cells as the “Seitenkörper” (side body), since it is not located at the hyphal apex, where the Spk is typically localized. Fluorescent labeling of critical components for the secretion machinery in *M. oryzae* IH cells should begin to uncover mechanisms of BIC accumulation, by defining the location and mechanism of secretion of effector proteins relative to non-BIC localized proteins like BAS4 and fungal cell wall components.

Results

Candidate M. oryzae Orthologs of Widely Conserved Key Secretion and Cell Polarity Components

We selected and identified the corresponding *M. oryzae* orthologs of 11 highly conserved cellular components of the secretion machinery in eukaryotes. These key cellular components were selected from different exhaustive reviews presented by Drees et al (2001) on cell polarity; by Sudbery and Court (2007) on polarized growth in fungi; by Shoji et al (2008) on components of the secretory pathway in filamentous fungi; and by Steinberg (2007a) on hyphal growth. The

criterion for selection was based on previous work on filamentous fungi that clearly showed their cellular localization using fluorescently-labeled versions in hyphae *in vitro* (Figure 3.1). The putative *M. oryzae* orthologs were identified in the genome sequence by blast searches with the corresponding yeast genes from the *Saccharomyces* genome database (SGD) (<http://www.yeastgenome.org/sitemap.html>). After the selection of the *M. oryzae* genes that best represented components of the Spitzenkörper, polarisome, and SNAREs, each protein sequence and accession identification was analyzed and verified from SGD, NCBI-GeneBank, BROAD Institute's *M. grisea* genome and *Magnaporthe grisea/oryza* community annotation MGOS databases (Table 3.1).

We analyzed the distinctive conserved domains found for each protein sequence, and aligned them using BLASTP, BlastWU, and ClustalW2 against various fungal genomic databases, such as *M. oryzae*, *S. cerevisiae*, *N. crassa*, *A. nidulans*, *C. albicans*, and for Yup1p, *U. maydis*. To confirm the conservation between the corresponding fungal proteins and the putative *M. oryzae* orthologs, we visualized the protein sequence alignment from CLUSTALW2 using Jalview, and phylogenetic trees were constructed using Neighbour Joining tree _BLOSUM62. Phylogenetic trees are represented (Figure 3.2) for the first four genes in Table 3.1, which were successfully expressed.

In summary, the selected genes were: (1) Mlc1, the essential light chain for Myo1 and Myo2, (2) Snc1, a vesicle membrane receptor protein (v-SNARE) involved in the fusion between Golgi-derived secretory vesicles and the plasma membrane, (3) Yup1, a t-SNARE endosomal target, (4) Spa2, a component of the polarisome, which functions in actin cytoskeletal organization during polarized growth, (5) Tub1 or alpha-tubulin, the most highly expressed microtubule component, (6) Sec2, a guanyl-nucleotide exchange factor (GEF) that is transported by actin cables to the tip and accumulated in the Spk along with Sec4 and Mlc1, (7) Sec15, an exocyst subunit that docks secretory vesicles to the plasma membrane, (8) Myosin-5, a molecular motor component that mediates secretory vesicle delivery, (9) PIP5K, phosphatidylinositol-4-phosphate-5-kinase associated with the plasma membrane and/or exocytotic vesicles, (10) Cdc42, a small Rho-like GTPase associated with the polarisome, and (11) Exo70, a subunit of the exocyst complex.

Each of the *M. oryzae* orthologs was labeled with fluorescent-reporter proteins to visualize them *in vitro* and *in planta*. From the 11 initially selected genes, not all were

successfully cloned and expressed. The genes that it was not possible to clone were PIP5K, Sec15 and Myosin-5. The putative *M. oryzae* orthologs of Cdc42, Tub1, Exo70 and Spa2 were cloned and fungal transformants were produced and purified by single spore isolation. After screening them *in vitro* and *in planta*, none of the ten independent transformants showed the expected localization. Their encoded proteins exhibited cytoplasmic fluorescence patterns with very low expression.

The successfully-labeled components with interesting results were named with the prefix Mo for *M. oryzae*. These are MoMlc1p and MoYup1p from our laboratory and MoSnc1p and MoSpa2p from Dr. Nicholas Talbot's laboratory (Exeter University, UK). Each of these candidates was labeled by a C-terminal fusion with enhanced green fluorescent protein (EGFP) to evaluate their expression and localization *in vitro* and *in planta*. The *in vitro* assay was needed to confirm that these proteins behave as the typical secretion-related component in vegetative hyphae and the *in planta* assay was used to follow their localization during biotrophic blast colonization with respect to BICs in compatible interactions. The presentation of preliminary results from this objective initiate collaborative research work with Dr. Nicholas Talbot's laboratory (Exeter University, U.K). We will prepare a joint publication on cellular components in *M. oryzae* expressed *in vitro* and *in planta*, which will be the first report of any secretion cellular component for *M. oryzae in planta*.

Localizing the Spitzenkörper (Spk) in M. oryzae Hyphae

Endocytosis of FM4-64, Differences *In Vitro* and *In Planta*

Previous studies identified the *M. oryzae* Spk using FM4-64 staining of vegetative hyphae *in vitro* (Fischer-Parton et al., 2000; Atkinson et al., 2002). FM4-64 is an endocytotic dye, which has been used to follow the endocytosis pathway in eukaryotic cells. One minute after addition of FM4-64, it is quickly internalized in living cells, labeling the plasma membrane, small organelles and finally vacuoles, in a sequential manner (Fischer-Parton et al., 2000; Atkinson et al., 2002; Bolte et al., 2004).

We used this endocytotic dye to follow the internalization through plasma membrane, septa and Spk of vegetative hyphae cells growing on the surface of water agar slides (Figure 3.3, A). In these *in vitro* studies, FM4-64 identified the Spk at vegetative hyphal tips as expected.

However, blast IH inside rice cells failed to internalize FM4-64 even after longer dye exposure times of up to 6 hours (Figure 3.3, B). This confirms the original report of Kankanala et al. (2007). Because FM4-64 is not internalized in blast bulbous-IH during biotrophic invasion, it is not a useful marker for labeling fungal membranes or Spk of *M. oryzae* IH *in planta*. The presented results reflect observations from four independent assays, *in vitro* observations of 40 vegetative hyphal cells, and *in planta* observations of 12 infection sites.

Labeling the *M. oryzae* Spitzenkörper using MoMlc1:GFP

In yeast, Mlc1p (YGL106W) is the essential light chain for Myo1p and Myo2p; and stabilizes Myo2p by binding to the bud neck region. Mlc1p interacts directly with the Myo2 GTD domain and the Ypt32p in yeast (Casavola et al., 2008) or the Sec4p in *C. albicans* with a typical localization at the Spk (Jones and Sudbery, 2010). The putative *M. oryzae* MoMlc1p (MGG_09470.6), which contains the expected EF-hand-conserved domain, was compared with EF-hand containing proteins from yeast and other fungi by sequence protein alignment and their phylogenetic tree was obtained (Figure 3.2, A). MoMlc1p is most similar to the EF-hand containing protein from *N. crassa*.

This protein was expressed *in vitro*, as in *C. albicans* (Crampin et al., 2005). In *M. oryzae* germinated spores and vegetative hyphae, co-localization of MoMlc1:GFP with FM4-64 (Figure 3.4), demonstrated that MoMlc1p labels the *M. oryzae* Spk and it is a suitable Spk marker for *M. oryzae in planta*. MoMlc1:GFP and FM4-64 showed co-localization at septa in germinated spores and at the tips of the germination tubes (Figure 3.4, A). Observations of MoMlc1:GFP in vegetative hypha (Figure 3.4, B) present MoMlc1:GFP as a bright spot at the hyphal tip during continuous growth under starvation conditions (on water agar slides), with a hyphal extension rate from 5 to 10 μm per minute (Supplemental video 3.1). During biotrophic invasion, MoMlc1:GFP localized to a discrete spot at the growing primary hyphal tip next to the tip BICs after fungal penetration at 22 hpi (Figure 3.5, A). After the first differentiated cell is formed, from 24 to 27hpi, MoMlc1:GFP localized to smaller but bright spots near to the BICs and to septa (Figure 3.5, B and C). These observations were consistent in independent transformants co-labeled with MoMlc1:GFP and PwL2:mRFP. Using this strain, MoMlc1:GFP was observed as a spot at the primary hyphal tip beside the red fluorescent BIC resembling the Spk shown in vegetative hyphal tips (Figure 3.6, A). However in bulbous IH cells after 27 hpi,

MoMlc1:GFP localizes to a distinct spot next to the BICs (Figure 3.6, B). It is also present at the septation or branching sites. As in *C. albicans* pseudohyphae, which lack Spk, MoMlc1:GFP was not present at the tips of bulbous IH. This *in planta* analysis allowed us to visualize Spk during rice blast biotrophic invasion and localize it with respect to BICs, as a bright spot at the tip of the primary hyphae. After the IH lose polarization and switch to bulbous growth, the vesicle supply center still appeared to be localized in the BIC-associated cells, usually close to the BICs. MoMlc1p also localized at the septa and branching points, as a small bright spots, and it is absent at the tip of the bulbous IH (Figure 3.6; B). We hypothesize that the Spk-like structure in the BIC-associated bulbous IH cell is a Spk that has remained behind to become the “Seitenkörper”, a secretory vesicle supply center that most likely supports and regulates secretion to BICs during biotrophic invasion in compatible interactions (Giraldo and Valent, Unpublished).

To test the dynamics of the Spk at the tip, we used fluorescence recovery after photobleaching (FRAP) analysis. With this analysis, we also compared the recovery of MoMlc1p in vegetative hyphae *in vitro* with the primary hyphae *in planta*, which shows similar polarized filamentous growth. The recovery of the MoMlc1:GFP in vegetative hyphae *in vitro* (Figure 3.7, Supplemental movie 3.2 and Table 3.5) occurs faster and stronger than in the primary hyphae *in planta* (Figure 3.8, Supplemental movie 3.3 and Table 3.5). However, in both cases the MoMlc1 was able to reach near complete recovery. Results from this study support the idea that filamentous vegetative hyphae have high secretion activity at the tip to allow the building of cell walls and polarization, which is required for their extension (supplemental video 3.1). In contrast, IH *in planta* could undergo lower secretion activity associated with a slower growth. These results reflect observations from six independent assays, *in vitro* observations of 50 vegetative hyphal cells, and *in planta* observations of 30 infection sites.

Localizing Secretory Vesicles during Blast Biotrophic Invasion using MoSnc1:GFP

The v-SNARE, Snc1p, is a vesicle membrane receptor protein involved in the fusion between Golgi-derived secretory vesicles and the plasma membrane. Snc1 is member of the Synaptobrevin VAMP family of R-SNAREs, which are involved in anterograde and retrograde trafficking between the Golgi and the plasma membrane in yeast (Gurunathan et al., 2000).

Putative MoSnc1p (MGG_12614.6) contains the Synaptobrevin domain highly conserved among the VAMP family members. The MoSnc1p sequence contained the synaptobrevin domain as a core sequence in the protein as shown by the high conservation level in the sequence alignment (Figure 3.2, B).

MoSnc1:GFP, was observed as a bright cluster of multiple vesicles accumulated at the hyphal tips in vegetative hyphae (Figure 3.9, A) and also at the tips of the polarized primary hyphae *in planta* (Figure 3.9, B). However, after the primary hyphae switched to bulbous IH, MoSnc1:GFP was also observed as a cluster of multiple vesicles and a distinct brighter spot next the BICs in the first bulbous IH cell, as well as in sites of active growth like branching sites, observed at 24 and 28 hpi (Figure 3.10, A and B). Time-lapse series acquired from confocal imaging showed the dynamic nature of the vesicles in Figure 3.10, A, in the supplemental movie 3.4 (image every 3 sec per 15 frames). Results presented reflect observations from three independent assays, *in vitro* observations of 30 vegetative hyphal cells and *in planta* observations of 10 infection sites.

Putative Endocytic Pathway Visualized by MoYup1:GFP

By isolation of a temperature sensitive mutant (ts) in *Ustilago maydis*, Wedlich-Soldner et al (2000) (Wedlich-Soldner et al., 2000), found and presented the characterization of a candidate endosomal t-SNARE, Yup1, UM05406.1, which contained a highly conserved PX SNARE domain; the phosphoinositide binding Phox homology domain typical of t-SNAREs, and of other proteins involved in membrane trafficking in fungi. The *U. maydis* yup1 defective mutant was affected in fungal morphogenesis and virulence.

Protein sequence analysis of the *M. oryzae* hypothetical MoYup1p (MGG_05428. 6) revealed the highest levels of homology to the *C. albicans* yup1-like protein that belong to the subgroup Vam7p, the same subgroup as *S. cerevisiae* Vam7p that had the highest homology with *U. maydis* Yup1p (Wedlich-Soldner et al. 2000) (Figure 3.2, C). The multiple protein sequence alignment reveals the high conservation among all the candidate t-SNAREs at the C-terminal PX domain.

To test if MoYup1:GFP labels endocytic vesicles in IH during biotrophic invasion, we first tested if the expression in filamentous hyphae *in vitro* corresponded to endocytic vesicles by co-localization with FM4-64 staining (Figure 3.11). MoYup1:GFP and FM4-64 presented

partial co-localization in vegetative hypha and spores. In spores, germination tubes and vegetative hyphae, MoYup1:GFP localizes to multiple small spots with a fast bidirectional movement close to the hyphal tips, and also labels vacuolar membranes as was shown for *U. maydis* Yup1p.

MoYup1p was fluorescently-labeled and transformed into a background strain that contains PwL2:mRFP to label the BICs during biotrophic invasion. Thus, co-labeling of MoYup1:GFP with PwL2mRFP *in planta* showed highly active small vesicles next to the primary hyphal tip at 24 hpi (Figure 3.12, A). MoYup1:GFP labels multiple-highly dynamic spots that fuse and separate from the membrane of the large vacuole present in the BIC-associated cells, and the plasma membrane next to BICs, during biotrophic invasion in compatible interaction at 24 hpi (Supplemental movie 3.5).

The model for Yup1p function based on *U. maydis* reported that early endosomes cluster in regions of growth, where membrane recycling is needed after secretion of cell wall components. Live cell imaging of MoYup1p labeled potential endosomes as small vesicles that are highly active in a bidirectional movement along the IH as expected. MoYup1p also labels vacuolar membranes as in *U. maydis*. Interestingly, at 27 hpi MoYup1p also labeled structures that were highly dynamic and concentrated beside BICs (Figure 3.12, B and Supplemental video 3.6). Around 36 hpi, when the bulbous IH completely pack the first invaded rice cell, MoYup1:GFP showed small and dynamic vesicles that were still active next to the BIC and around the large vacuole that forms in the first differentiated bulbous IH cell associated with the BIC (Figure 3.12, C). Results from this analysis suggest that the secretion of effectors into BICs involves MoYup1p-mediated endocytosis, which mediates recycling in a regulated secretion mechanism. The results presented reflect observations from ten independent assays, *in vitro* observations of 40 vegetative hyphal cells and *in planta* observations of 50 infections sites.

Labeling the M. oryzae Polarisome

Spa2p is one of the polarisome components identified in yeast and in model filamentous fungal systems such as *N. crassa*. Previous results in *Aspergillus niger* (Meyer et al., 2008) and in *N. crassa* (Araujo-Palomares et al., 2009) showed localization of Spa2, the polarisome, as a distinct spot at the growing hyphal apex similar to the Spk (Meyer et al., 2008). However, in *C. albicans* (Crampin et al., 2005) and in *U. maydis* (Carbó and Pérez-Martín, 2008) differential

localization of Spk and polarisome in relation to the type of growth (yeast, hyphae or pseudohyphae) has been shown.

MoSpa2p, MGG_03703.6, was selected and aligned using the Spa2 ID protein sequences reported in previous work from Meyer et al (2008), which characterizes all the polarisome components in *A. niger*, including Spa2p as SpaA (Meyer et al., 2008). The conserved domains for Spa2p were identified and the protein alignment (Figure 3.2, D) supported the phylogenetic tree presented by Meyer et al (2008), in which *M. oryzae* and *N. crassa* are grouped as the most closely related proteins. Although, the sequences from different fungi are on different branches of the tree, they follow the phylogenetic relationships of these fungi, and the high conservation in their signature domains is clear.

For *M. oryzae* vegetative hyphae *in vitro*, MoSpa2:GFP was clearly localized at the tips of each hyphae as a distinct spot (Figure 3.13, A), and its fluorescence was easily bleached in less than a minute. A time lapse series assay shows the bleach of MoSpa2:GFP at the hyphal tips of two vegetative hyphae during image acquisition using confocal microscopy (Supplemental video 3.7).

In planta, MoSpa2:GFP, was observed as a distinct spot at the apex of the polarized primary hyphae (Figure 3.13, B). Notice that at 22 hpi, when the first bulbous IH begins to differentiate, the bright spot seems to move and accumulate towards the direction of hyphal enlargement instead of directly behind the BIC (Supplemental video 3.8). At 24 hpi (Figure 3.14, A) when the primary hyphae begins to differentiate, MoSpa2:GFP is observed at the growing hyphal tip. But at 27 hpi, (Figure 3.14, B) MoSpa2:GFP is not observed next to BICs or in any BIC-associated cells, but at the tip of each new branch. Results presented reflect observations from three independent assays, with *in vitro* observations of 20 vegetative hyphal cells and *in planta* observations of 15 infections sites. Results from this chapter are summarized in Figure 3.15, using a cartoon to describe the differences between filamentous-polarized and bulbous invasive hyphal growth during compatible interactions, as identified by localization of these candidate *M. oryzae* secretion components *in planta*.

Discussion

Recent advances in *M. oryzae* detailed the secretion and cell-to-cell movement of effector proteins inside rice cells and revealed a novel structure where most of the biotrophy-associated secreted (BAS) proteins and blast avirulence effector proteins accumulated during biotrophic invasion. This structure is called the biotrophic interfacial complex, BICs (Khang et al., 2010). The main objective of this study was to test if effectors are secreted directly into BICs, which are hypothesized to play a role in effector translocation during compatible interactions, by labeling *M. oryzae* ortholog protein-markers of the secretion mechanism in filamentous fungi. Due to the high level of conservation among these orthologous proteins in eukaryotic cells, candidate *M. oryzae* orthologs were identified and shown to localize as was reported for other fungi in vegetative hyphae. For filamentous fungi, constitutive secretion is known to involve the Spitzenkörper at the apex of the hyphae. However, a previous report with Snc1p in *Trichoderma reesei* demonstrated spatially regulated SNARE interactions found on the plasma membrane (Valkonen et al., 2007), which differ depending on if it is at a growing hyphal tip or in a non-growing hyphae. In *C. albicans*, Crampin et al (2005) confirmed the presence of Spk in hyphae by localization of Mlc1p and FM4-64 to a distinct spot at the growing hyphal tip. However, they showed that Mlc1p:YFP labeled Spk, observed as a distinct spot at the hyphal tip, is no longer observed in yeast or pseudohyphae. For *C. albicans*, Crampin et al (2005) proved that after disruption of actin cables, which deliver cargo to the hyphal tips, the Spk completely disappeared because of the isotropic deposition of new cell wall material. Thus, they concluded that the Spk is not present in yeast and pseudohyphae, but a polarisome is present in these fungal cell types.

Dimorphism in M. oryzae during Biotrophic Invasion Labeled by Spk Markers

In *M. oryzae*, co-localization of MoMlc1p with the FM4-64 *in vitro* demonstrates that MoMlc1p is a good Spitzenkörper marker for rice blast IH *in planta*. MoMlc1:GFP *in planta* showed a clear Spk at the tip of the primary hyphae, but after the primary IH turns into a bulbous IH, the MoMlc1:GFP is not observed at the tips of each branching bulbous IH. Instead, a putative Spk-like structure is present in the BIC-associated bulbous IH cell, and also at septa. This result could suggest a change of localization of the vesicle supply center or disintegration and reformation of it when hyphae are not polarized.

Under the assumption that the *M. oryzae* ortholog of the exocytotic SNARE protein Snc1p, MoSnc1p, also localized at the hyphal apex within the Spk, as was previously demonstrated for *T. reesei in vitro* hyphae (Valkonen et al., 2007), MoSnc1p could be useful to support and complement observations with MoMlc1p in bulbous IH *in planta*. MoSnc1:GFP *in planta* was observed as a cluster of secretory vesicles, containing an especially bright spot next to the primary hyphal tips. After the primary hyphae differentiated into bulbous IH, a brighter spot was located next to BICs and next to each growing branching bulbous IH. This result supports our hypothesis that secretory vesicles are delivering special cargo at the BICs, shown by the accumulation of avirulence effector proteins into BICs, and also supports the idea that a different mechanism of secretion could be turned on when the newly bulbous IH cell forms during the blast biotrophic invasion.

The Spitzenkörper (apex body), which is distinctively located at the apex of the fungal hyphae, no longer appears at the bulbous IH tip but instead may be located near the BICs in that first bulbous IH cell. Therefore, we suggested that the spot labeled by MoMlc1p:GFP and MoSnc1p:GFP *in planta* could be called the “Seitenkörper” (a side body). The differential localization of these secretory vesicles after the switch of hyphal growth form could occur either because the Spk disappeared when the bulbous IH forms or because a new vesicle supply center is reformed for the regulated secretion of avirulence effectors into BICs, an event that is required for the biotrophic colonization.

In filamentous fungi, few genes encoding SNARE proteins have been cloned. In *U. maydis*, the putative t-SNARE Yup1p was cloned and characterized. Yup1p is believed to couple exocytosis and endocytosis by mediating membrane recycling processes (Wedlich-Soldner et al., 2000). The putative *M. oryzae* Yup1 protein contains the N-terminal PX domain that is highly conserved in proteins involved in membrane trafficking.

In vitro partial co-localization of MoYup1:GFP with FM4-64 in *M. oryzae* suggests that the labeled vesicles might be part of the endocytic pathway. As FM4-64 can not reveal the endocytic pathway for *M. oryzae* invasive hyphae *in planta*, MoYup1:GFP can be an alternative marker for potential endocytotic vesicles as well as for vacuolar membranes. After demonstrating the co-localization of MoYup1:GFP and FM4-64 in hyphae *in vitro*, we presumed that MoYup1:GFP localization *in planta* will represent sites of active endocytosis during blast biotrophic invasion. As was shown in *U. maydis* by Wedlich-Soldner et al (2000),

MoYup1:GFP during blast live rice cell invasion identified fluorescent, highly expressed small, dynamic vesicles next to BICs as well as vacuolar membranes. Specially intense spots fused to and detached from the membrane of the vacuole next to BICs. It is known that blast avirulence-effector proteins are secreted and accumulate into the BICs, and known that the endocytotic vesicles play a role in the secretion pathway. Therefore, it is likely that MoYup1:GFP was labeling early endosomes located close to places where regulated secretion occurs. These results support the hypothesis that secretion of effectors to BICs involves the endocytosis pathway, which is coupled to exocytosis for recycling in a regulated secretion mechanism.

In Figure 3.15, our model of *M. oryzae* secretion components in the cartoon represents the switch of hyphal growth form from filamentous-polarized growth (Figure 3.15, A) to bulbous invasive hyphal growth (Figure 3.15, B). This developmental switch is accompanied by a modification of the filamentous hyphal secretion mechanism. The differences in localization of the candidate *M. oryzae* secretion components suggests that there is a spatially-segregated mechanism for secretion of effectors into BICs.

Differential Localization of the Spk and Polarisome in Bulbous IH

The polarisome has been visualized using fluorescently-labeled Spa2p in *N. crassa* (Araujo-Palomares et al., 2009) and *C. albicans* (Crampin et al., 2005). The polarisome localized at the apical region of *in vitro* hyphae closer to the tip than the Spk, and was described as a crescent shaped zone at the tip that partially colocalizes with the Spk. In *C. albicans*, Crampin et al (2005) demonstrated by deletion analysis of polarisome components that Spa2p and Bud6 are required for Spk formation and hyphal growth. As Spa2 is present in areas of active growth or constitutive secretion, I expected that during rice blast invasion, MoSpa2:GFP would show the switching of growth from primary hyphae to bulbous IH. As in *C. albicans*, MoSpa2:GFP was present at the apex of the primary hyphae, and also at the tip of each bulbous IH after the BIC cell differentiates. MoSpa2:GFP in contrast to the Spk components, MoMlc1p and MoSnc1p, was not observed either next to BICs or in the BIC-associated bulbous IH cell. The distinct localization pattern for Spk and polarisome components in bulbous IH, represented in Figure 3.15, could support our hypothesis of spatially-segregated secretion mechanisms in *M. oryzae* during live rice cell invasion.

These results support the polarisome function in the cytoskeleton organization during polarization, directing the hyphal growth. Because the first differentiated cell, where the BIC is located, does not undergo active polarized growth, we would not expect to see localization of the polarisome in these cells. That first differentiated bulbous cell does present the consistent localization of the novel structure, BIC, where we know the effectors and some BAS proteins accumulate in compatible interactions during biotrophic invasion.

Potential Mechanism of Blast Effector Secretion to BICs

Localization of MoMlc1:GFP and MoSnc1:GFP *in planta* during live rice cell invasion, demonstrated that *M. oryzae* primary hyphae contain a Spitzenkörper-like structure, as a distinct spot behind the growing primary hyphae (Figures 3.5, A; 3.6, A; 3.9, B). It remains to be proven if, after the switch of growth into a bulbous IH, the distinct Spk-like structure maintains its position close to BICs or if the Spk disappears and a new structure forms. Since Snc1p is a vesicle membrane receptor protein (v-SNARE) involved in the fusion between Golgi-derived secretory vesicles and the plasma membrane, the localization of MoSnc1:GFP contiguous to BICs in the first differentiated bulbous IH cell suggests a dynamic activity of these secretory vesicles in that site as well as at other places of active bulbous IH growth (Figure 3.10). Valkonen et al (2007) demonstrated *in vitro* for *T. reesei*, the presence of multiple exocytic SNAREs functionally and spatially segregated. That is, the SNARE complex formed by Snc1 and Sso1 at the subapical hyphal locations along the plasma membrane and was not detected at the growing tips, considered the major location of exocytosis.

The specific localization of MoSpa2p at the branching points or at the tip of each bulbous IH and not next to BICs also supports the hypothesis that *M. oryzae* has a differentiated mechanism for secretion of avirulence effectors into BICs.

Blast Bulbous IH are Important for Live Rice Cell Invasion

For *U. maydis* (Wedlich-Soldner et al., 2000) and *C. albicans* (Crampin et al., 2005) hyphal dimorphism is critical in virulence. During the compatible interaction, *M. oryzae* showed a dimorphic switch to a distinctive bulbous IH, which correlated with the full invasion of the first invaded rice cell. Bulbous IH were not observed during incompatible interactions, which is characterized by a filamentous IH that stops growing or that crosses from one cell to the other without spending so much time in the first invaded cell (Heath et al., 1990b; Kankanala et al.,

2007; Mosquera et al., 2009; Khang et al., 2010) This dimorphic switch is always accompanied by the formation of the BICs, which are associated with the hyphal cells that undergo the switch. The BIC that forms at the tip of the primary hypha remains beside that first bulbous IH during the entire invasion of the first invaded rice cell. That dimorphism is also correlated with the change of localization of the secretory vesicle clusters fluorescently-labeled by MoMlc1p and MoSnc1p (Figures 3.5, B, C; 3.6, B; 3.10, A, B). Also, MoSpa2:GFP labeling the polarisome, revealed specific localization at the tips of bulbous IH and not at the BIC-associated bulbous IH cell (Figures 3.14, A, B). These results are represented in Figure 3.15, as it is presented in the cartoon, their localization could suggest that there is a spatially segregated mechanism for secretion of effectors into BICs. These results also support the importance of the BICs in the efficient translocation of critical effector proteins into the host cell for the successful biotrophic rice blast colonization.

Lessons from Localization of Fungal Secretion Components

The failure of expression in the transformants with Cdc42, Tub1 and Exo70, can be due to a dosage or positional effect, since deletion mutants of those genes have proven that they are critical for development. Visualization *in vitro* is required as a confirmation that these cellular components of the secretion pathway are performing as expected before localization *in planta* is attempted. *In planta* localization of cellular components is difficult because these components might not show the normal *in vitro* pattern, as was observed in this study.

In planta as well as *in vitro*, visualization of fluorescently-labeled secretion components is challenging because their expression depends on the active growth of the fungus. If the fungus stops growing, these components are known to quickly disappear. Also, *in planta* fluorescently-labeled secretion components bleached faster than those in the *in vitro* vegetative hyphae, making the time-lapse series assays more challenging. Confocal imaging using our best 63x objective caused immediate photobleaching of the relatively faint fluorescence in these studies. Therefore, all the images in this study were acquired using 40x objective to reduce the photobleaching effect. This of course resulted in decreased resolution in the imaging. The differences in the intensity of expression of the secretion components observed *in vitro* versus *in planta* could suggest that the secretion activity in vegetative hyphae is higher and more continuous, with a faster rate growth, than the secretion in invasive hyphae.

Material and Methods

Assays for M. oryzae Live Cell Imaging In Vitro and In Planta

Fungal transformants were stored in dried filter papers, maintained in -20°C frozen storage, and cultured on oatmeal agar plates at 24°C under continuous light (Valent et al., 1991). From fresh fungal cultures, a small piece from the edge of the hyphal growth was cut out to inoculate the border of a sterile water agar slide, which was incubated in a humid chamber for 16 to 18 hours. Vegetative hyphae continued to grow on the water agar surface allowing observation of flat filamentous vegetative hyphae during active growth.

First, new fungal transformants were evaluated at 16 to 18 hpi using vegetative hyphae to confirm fluorescence expression and evaluate active growth by time-lapse series using AxioVisionLE program version 4.8 software. Selection of the best independent transformants was based on intensity of the expression of the fluorescent marker. These transformants were evaluated during infection *in planta* by rice sheath inoculations. Rice sheath inoculations were performed as described by Kankanala et al (2007) using the susceptible rice line YT-16. Briefly, five cm-long sheath pieces from 3 week-old plants were placed in a glass container under high humidity conditions. Sheaths were placed on stable supports to avoid contact with the wet paper and to hold them horizontally flat for even inoculum distribution. A spore suspension, ~200 µl, (1×10^5 spores/mL in 0.25% gelatin, Cat. # G-6650, Sigma Aldrich) was injected in one end of the sheath using a 200 µl pipette. At 22 hours post inoculation (hpi), 0.5 cm pieces were removed from the incubated sheath ends to eliminate fungus that grew vegetatively into injured tissue. Each segment was trimmed and immediately observed using wide-field microscopy with differential interface contrast (DIC) and epifluorescence or with bright field (BF) confocal microscopy. The leaf sheath assay can be observed in supplemental video 2.1.

Wide-field microscopic imaging was performed with a Zeiss Axioplan 2 IE MOT microscope. Fungal transformants were observed with a 63X/1.2 NA (numerical aperture) C-Apochromat water immersion objective lens. Images were acquired using a Zeiss AxioCam HRc camera and analyzed with Zeiss Axiovision digital image-processing software, version 4.8. Fluorescence was observed with a 100 Watt FluoArc or an X-Cite®120 (EXFO Life Sciences) mercury lamp source. Filter sets used were: GFP (excitation 480 ± 10 nm, emission 510 ± 10

nm, filter set 41020, Chroma Tech. Corp., Rockingham, VT); and mRFP or FM4-64 (excitation 535 ± 25 nm, emission $610 \pm 32 \frac{1}{2}$ nm).

Confocal microscopy imaging was performed on a Zeiss Axiovert 200M microscope equipped with a Zeiss LSM 510 META system using two water immersion objectives, 40X/1.2 NA and 63X/1.2 NA C-Apochromat. For EGFP excitation/emission wavelengths were 488 nm/505-550 nm, and for mRFP or FM4-64, 543 nm/560-615 nm. Images were acquired and processed using LSM510 AIM version 4.2 SP1 software.

Fluorescence Recovery After Photobleaching – FRAP

Experiments were performed using a Zeiss LSM 510 confocal microscope with a 488nm argon laser and a C-Apochromat 40x/1.2 NA water immersion objective at 2x optical zoom. The region at the hyphal tip containing a fluorescent spot of MoMlc1:GFP was identified in vegetative hypha growing on the top of water agar slides and also in primary hyphae in a YT-16 rice sheath epidermal cell at 24 hpi. For FRAP analyses, the specific region of interest (ROI) was selected for bleaching. Ten to 12 bleaching iterations were required at a reduced laser power, 80% for *in vitro* and 50% for the *in planta* hyphae. Image scans were taken with the acousto-optic tunable filter attenuated to 5% laser power immediately before and after bleaching. Data from FRAP *in planta* hyphae include the image scan 30 minutes after bleaching in which the ROI almost reached a complete recovery. The interval time after bleaching from 10.4 seconds to 30 minutes is represented in the graph as a gap-line. For quantitative analyses, the MoMlc1:GFP fluorescence recovery curves were measured as the mean intensity of ROI pixels using the LSM software (version 4.2 SP1), normalized, and plotted by Microsoft Excel.

Sequence analysis

Analysis of the predicted protein sequences was performed using BLASTP (Altschul et al., 1997) from NCBI GeneBank (<http://www.ncbi.nlm.nih.gov/genbank/>), Broad Institute's *Magnaporthe grisea* Genome Database (http://www.broadinstitute.org/annotation/genome/magnaporthe_grisea/MultiHome.html), MGOS (<http://www.mgosdb.org/>), SGD (<http://www.yeastgenome.org/sitemap.html>), and the Biological General Repository for Interaction Datasets (BioGRID) database (<http://www.thebiogrid.org>) that was developed to house and distribute collections of protein and genetic interactions from major model organism species. Multiple protein sequence alignments

were used to find diagnostic patterns to characterize protein families and to detect homology between *M. oryzae* ortholog sequences and existing families of sequences. These protein sequence alignments were performed using CLUSTALW2 from EMBL-EBI (<http://www.ebi.ac.uk/Tools/clustalw2/index.html>), a sensitive multiple sequence alignment program that refines the progressive alignment through sequence weighting, position-specific gap penalties and weight matrix choice. In ClustalW2, the guide trees, used to guide the multiple alignment, were calculated by a distance matrix method using the Neighbour Joining tree _BLOSUM62 (Saitou and Nei, 1987). This method is more robust against the effects of unequal evolutionary rates in different lineages, giving better estimates of individual branch lengths that are used to obtain the sequence weights. ClustalW2 provides the workbench, Jalview, for multiple alignment visualization, interactive editing, and analysis tool. Jalview is a multiple alignment editor written in Java.

FM4-64 staining in vitro and in planta

Fungal transformants were stained with FM4-64 (4 µg/ml in water). An aqueous 17 mM stock solution of FM4-64 (Cat # 13320, Invitrogen, Carlsbad, CA) was made and stored at minus 20°C as describe Bolte et al (2004) (Bolte et al., 2004). Vegetative hyphae at ~16 to 18 hpi on the complete water agar slide were incubated in 10 µM aqueous solution of FM4-64 for uniform staining after 5 to 30 min. *In planta*, inoculated trimmed leaf sheaths, ~24 hpi, were incubated in a 10 µM aqueous working solution for 1 to 5 hours.

Vector Construction and Agro-mediated Fungal Transformation

Unless noted otherwise, transformation cassettes to observe *M. oryzae* fluorescently-labeled cellular components were constructed containing the entire protein coding sequence with its native promoter (1 kb) in a translational fusion with EGFP. Second constructs for Spa2p and Tub1 contained a strong constitutive promoter RP27 (from ribosomal protein 27), with the coding sequence fused to EGFP and mRFP. However, the only expression construct that works for Spa2p was produced in Dr. Nicholas Talbot's laboratory (Exeter, U.K). The EGFP gene was obtained from Clontech, and the mRFP gene was from Campbell et al. (2002). Primers used for amplification of each gene are listed in Table 3.2. Each cassette was cloned into the pBHt2 binary vector for transformation by *A. tumefaciens* (Khang et al., 2005) and for selection of positive transformants using hygromycin or G418 resistance. Details of plasmid construction

and corresponding fungal transformants used in this study are listed in Tables 3.3 and 3.4, respectively. *M. oryzae* field isolates O-137 (Orbach et al., 2000), Guy11 (Leung et al., 1988) and laboratory strain CP987 (Orbach et al., 2000) were used as recipients. Fungal transformants were purified by single spore isolation (Keitt, 1915; Rho et al., 2001) and 7 to 10 independent transformants were analyzed per gene.

Accession Numbers

Sequence data from this chapter can be found in the *Saccharomyces* genome database (SGD) (<http://www.yeastgenome.org/sitemap.html>) under the following accession numbers MLC1/YGL106W, SNC1/YAL030W, SPA2/YLL021W, TUB1/YML085C, SEC2/YNL272C, SEC15/YGL233W, MYO5/YMR109W, CDC42/YLR229C, EXO70/YJL085W.

M. oryzae orthologous genes, MGG_, can be accessed from the Broad Institute's *Magnaporthe grisea* Genome Database (http://www.broad.mit.edu/annotation/genome/magnaporthe_grisea/MultiHome.html) or from the MGOS Database (<http://www.mgosdb.org/>; (Soderlund, 2006). In GenBank, the sequence data for PWL2 and Yup1 are found under the accession numbers U26313.1 and UM05406.1 respectively.

Supplemental Data

Supplemental videos can be found with the item record for this thesis in the K-State Research Exchange (<http://krex.k-state.edu>). The general setting for capturing time lapse series was acquisition every 3 seconds per 15 to 20 cycles.

- Supplemental Video 3.1. *In vitro*, MoMlc1:GFP labeling the Spk in *M. oryzae*.
- Supplemental Video 3.2. *In vitro*, FRAP of MoMlc1:GFP at the Spk *M. oryzae*.
- Supplemental Video 3.3. *In planta*, FRAP of MoMlc1:GFP at the Spk *M. oryzae*.
- Supplemental Video 3.4. *In planta*, MoSnc1:GFP localized in *M. oryzae* vegetative hyphae.
- Supplemental Video 3.5. *In planta*, MoYup1:GFP co-localized with PWL2:mRFP at 24 hpi..
- Supplemental Video 3.6. *In planta*, MoYup1:GFP co-localized with PWL2:mRFP at 27 hpi..
- Supplemental Video 3.7. *In vitro*, MoSpa2:GFP.
- Supplemental Video 3.8. *In planta*, MoSpa2:GFP at 22 hpi..

Figures and Tables

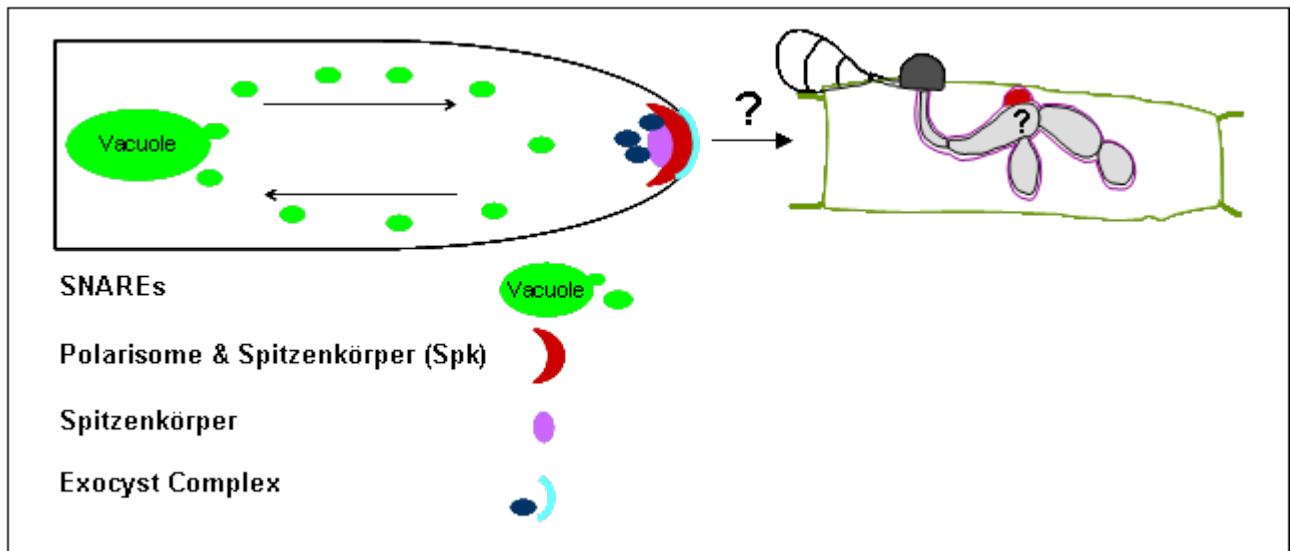


Figure 3.1. Cartoon showing the criterion for selection of cellular secretion components based in their localization patterns in filamentous fungi.

A. MoMlc1 (MGG_09470.6): tree distances

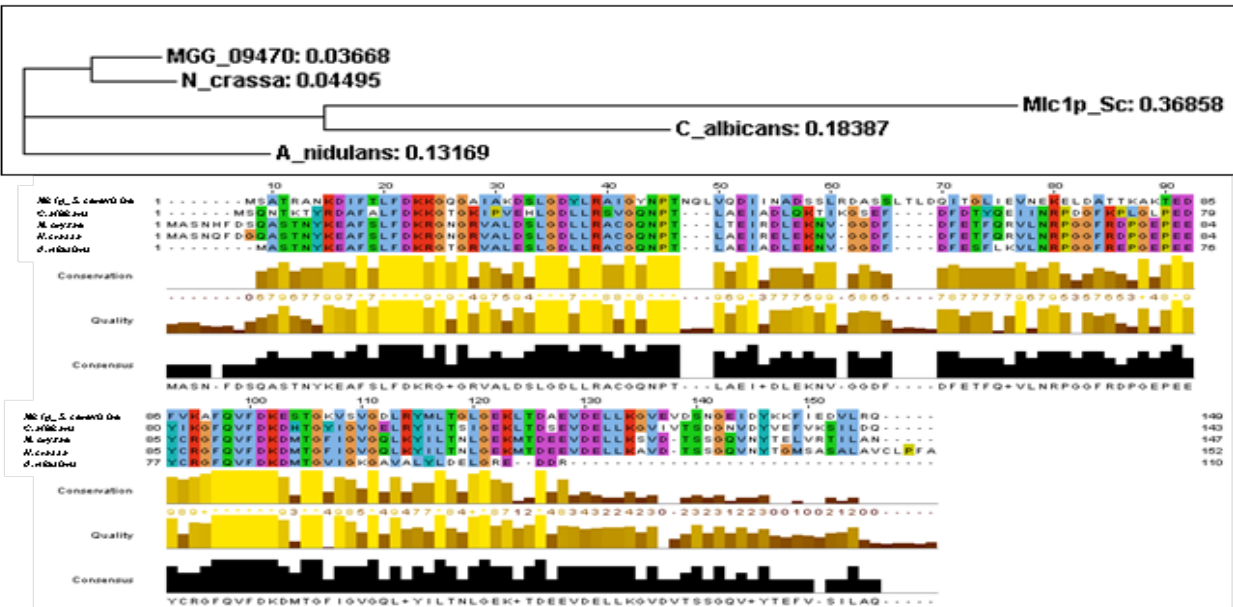


Figure 3.2. Phylogenetic trees of selected fungal proteins involved in secretion and the *M. oryzae* orthologs.

Top: Trees were obtained using Phylip from CLUSTALW2

(<http://www.ebi.ac.uk/Tools/clustalw2/index.html>). Each branch is labeled with the accession number and its tree distance (ID:Distance). Guide trees were used to lead the multiple alignments, calculated by a distance matrix method using Neighbour Joining tree _BLOSUM62, which give estimates of individual branch lengths that are used to obtain the sequence weights and avoids effects of unequal evolutionary rates in different lineages. The distance is scaled in units of the expected fraction of amino acids changed.

Bottom: Jalview output, indicating the conservation level, from high to low with lighter to darker brown respectively, and the consensus row at the bottom of the alignment showing the most frequent residue at each column or a '+' if two or more residues are equally abundant.

Figure 3.2, A. Phylogenetic tree of the putative MoMlc1p and orthologs from other fungi including the reference Mlc1p sequence from *S. cerevisiae*. Multiple protein sequence alignment presents in the phylogenetic tree the sequences from *M. oryzae* (Mo) and *N. crassa* (Nc) as the closest orthologs, follow by the sequences from *A. nidulans* (An), *C. albicans* (Ca). The sequence from *S. cerevisiae* (Sc) is presented as the most distant, with more amino acid sequence changes. Jalview showed that all proteins shared conserved domains, visualized by the high consensus alignment, from top to bottom: Sc, Ca, Mo, Nc and An.

B. MoSnc1 (MGG_12614.6): tree distances

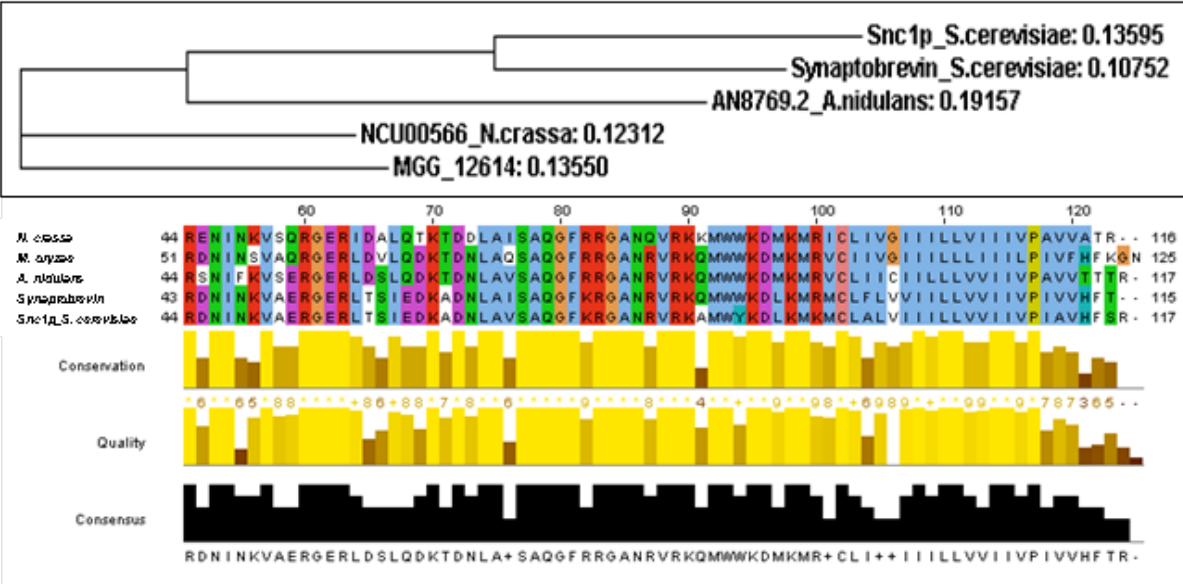


Figure 3.2, B. Phylogenetic tree of the putative MoSnc1p and orthologs from other fungi including the reference Snc1p sequence from *S. cerevisiae* and the Synaptobrevin sequence domain typical of v-SNARE proteins. Multiple protein sequence alignment presents in the phylogenetic tree the sequences from Snc1p_ *S. cerevisiae* (Snc1p) and Synaptobrevin (Syn) as the most similar, followed by the sequences from *N. crassa* (Nc) and *M. oryzae* (Mo), and the sequence from *A. nidulans* (An) as the most distant with the most amino acid changes. Jalview represented the high conservation levels among them, visualized by the high consensus alignment, from top to bottom: Nc, Mo, An, Syn and Snc1p.

C. MoYup1 (MGG_05428.6): tree distances

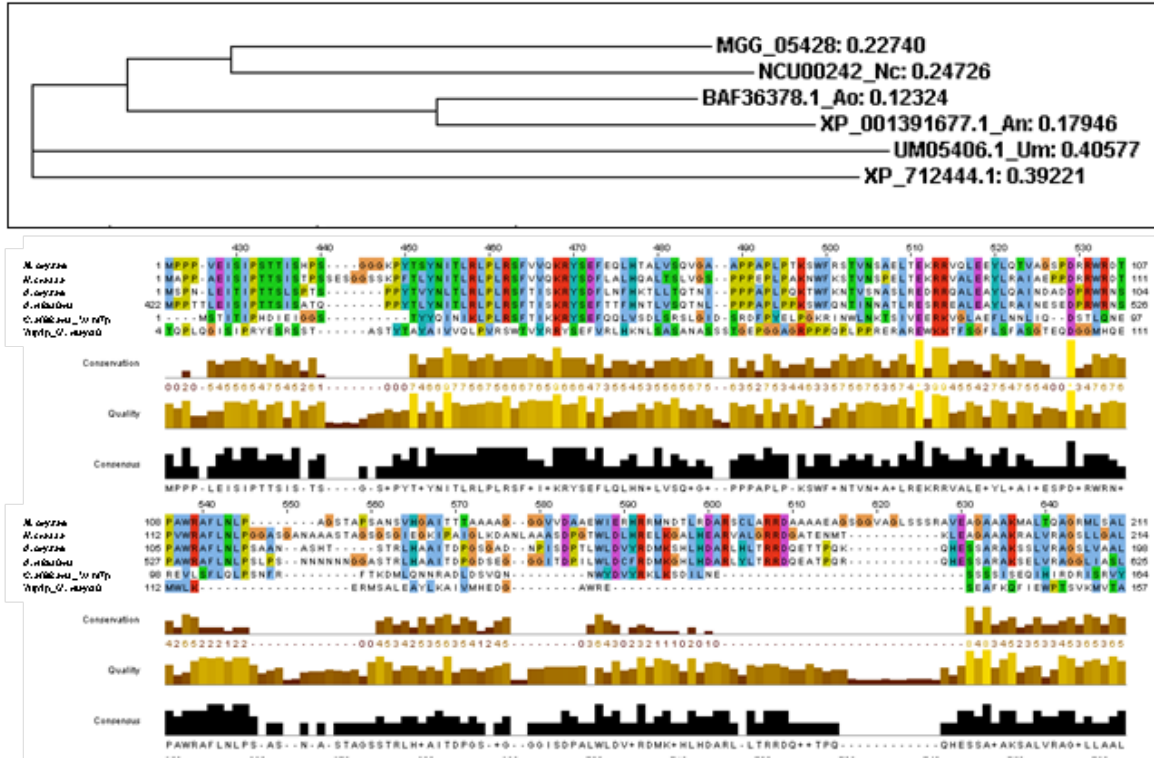


Figure 3.2, C. Phylogenetic tree of the putative MoYup1p and orthologs from other fungi including the reference Yup1p sequence from *U. maydis*. Multiple protein sequence alignment presents the sequences from *A. nidulans* (An) and *A. oryzae* (Ao) as the most similar protein sequences followed closely by the sequences from *M. oryzae* (Mo) and *N. crassa* (Nc), and by the sequences from *U. maydis* (Um) and from *C. albicans* (Ca) that is a Vam7-like protein (a typical v-SNARE). Jalview represents the high levels of conservation among them, visualized by the high consensus alignment, from top to bottom: Mo, Nc, Ao, An, Ca and Um.

D. MoSpa2 (MGG_03703.6): tree distances

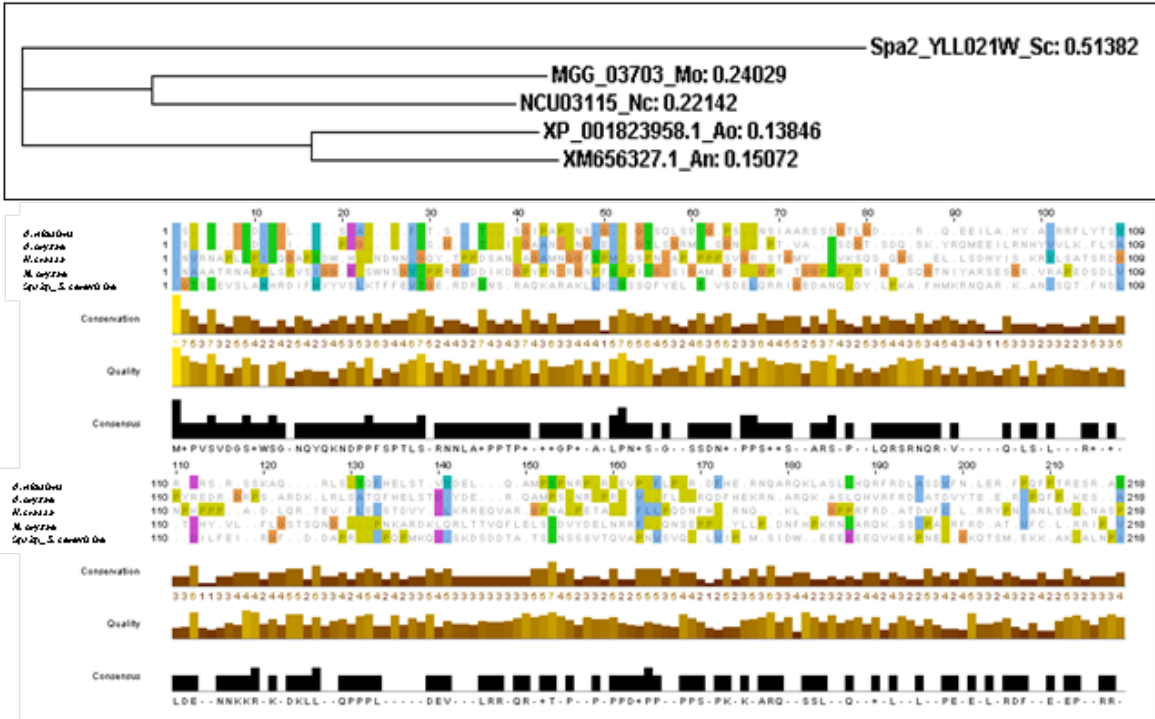


Figure 3.2, D. Phylogenetic tree of the putative MoSpa2p and orthologs from other fungi including the reference Spa2p sequence from *S. cerevisiae*. Multiple protein sequence alignment presents the sequences from *A. nidulans* (An) and *A. oryzae* (Ao) as strongly related followed closely by the sequences from *N. crassa* (Nc) and *M. oryzae* (Mo). The Spa2 protein sequence from *S. cerevisiae* is represented as the most distantly related sequence. Jalview represented the high conservation levels among all proteins, visualized by the high consensus alignment, from top to bottom: An, Ao, Nc, Mo and Sc.

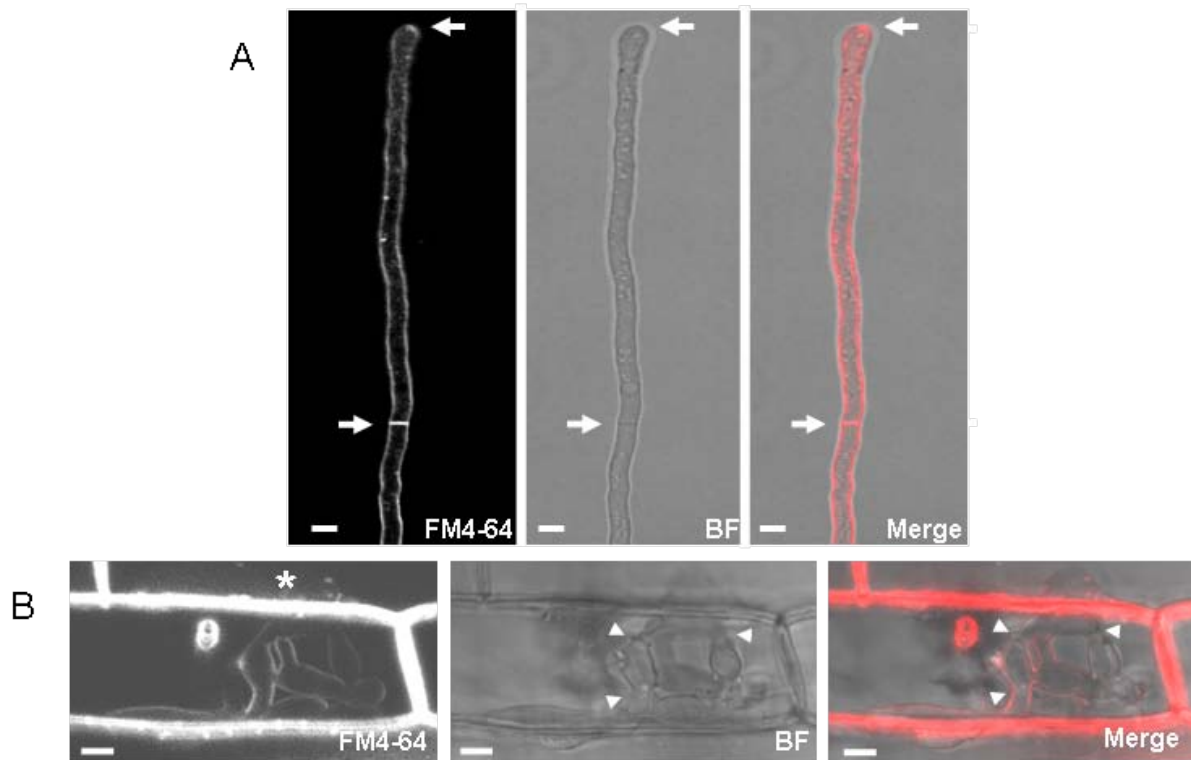


Figure 3.3 FM4-64 staining of rice and *M. oryzae* membranes *in vitro* and *in planta*.

(A) *M. oryzae* vegetative hyphal cells *in vitro* stained with FM4-64. The dye is internalized by the hypha through lateral membrane diffusion and the endocytotic pathway, and shows clear staining of the Spk and septum (arrows). This confocal image was obtained 10 minutes after dye addition. Bars=5 μ m. (B) Rice blast invasion *in planta*, stained by FM4-64. The dye is internalized by the rice cells (*), but septa (arrows) and fungal organelles, including vacuolar membranes in IH are not stained. In contrast, the dye clearly stains the BIC and the plant derived membrane (EIHM) that encloses the IH during biotrophic invasion. The penetration pore is also labeled. Imaged 4 hours after dye addition. Confocal images, left to right: FM4-64 fluorescence (red shown as white), bright field (BF) and merged BF and FM4-64 (red). Bars=5 μ m.

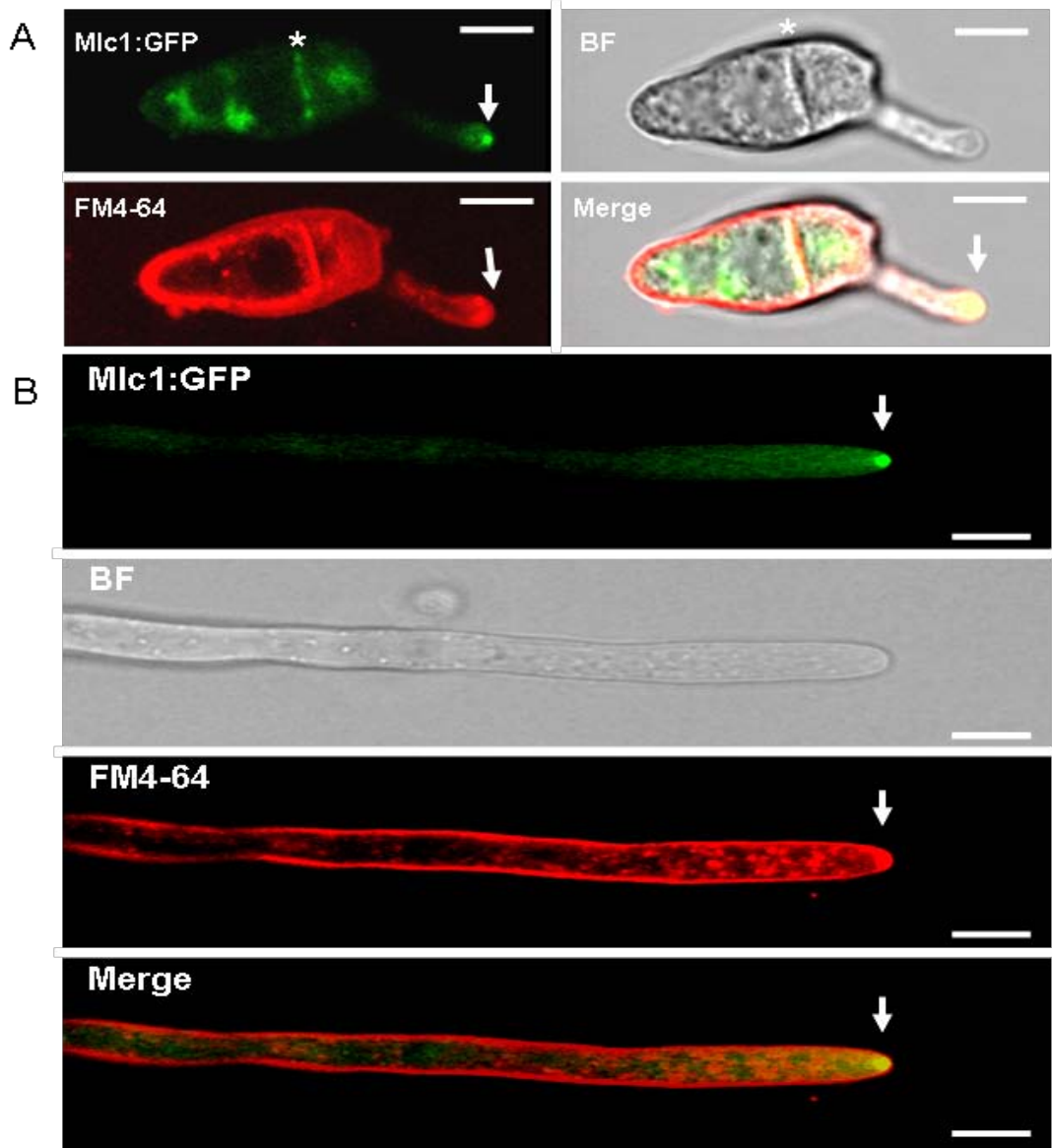


Figure 3.4. Co-labeling of *M. oryzae* hyphae *in vitro* with MoMlc1:GFP and FM4-64

An *M. oryzae* transformant expressing MoMlc1:GFP (green) was stained with FM4-64 (red). Co-localization (yellow) of the two markers identified the Spk as a discrete spot at the growing hyphal tip (arrow), as well as at septa (*). This discrete spot at the tip resembles *C. albicans* Mlc1p localization defining the Spk in true hyphae. Confocal images were acquired 10 minutes after dye addition. (A) Germinated spore imaged by GFP, BF, FM4-64, and merged BF, GFP and FM4-64 channels. (B) Vegetative hyphae growing *in vitro*. Images from top to bottom are GFP, BF, FM4-64, and merged GFP and FM4-64 channels. Bars=5 μ m.

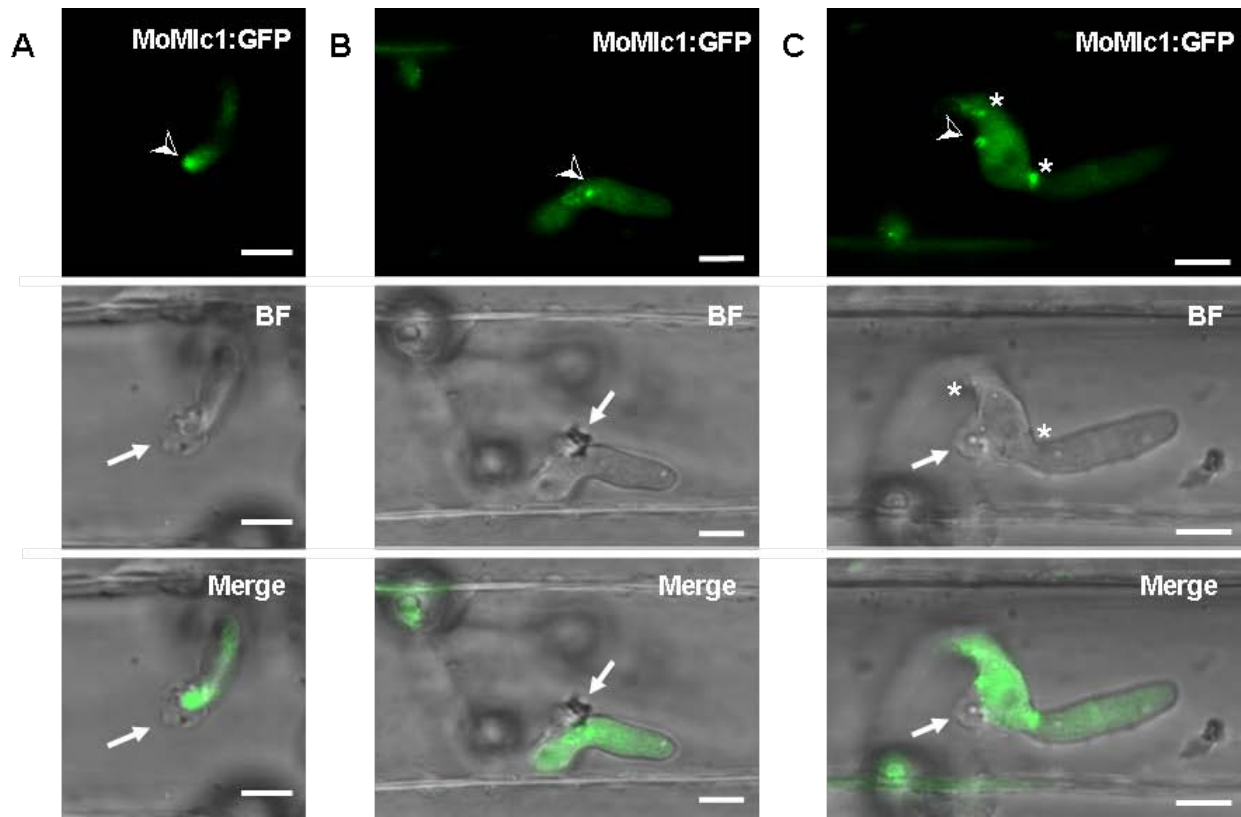


Figure 3.5. MoMlc1:GFP identified the Spitzenkörper during rice blast invasion.

(A) During biotrophic invasion, MoMlc1:GFP localizes to a discrete spot (➤) at the growing primary hyphal tip directly adjacent to the BIC (22 hpi). (B) and (C) IH cells at 27 hpi, MoMlc1:GFP localizes to a distinct spot (➤) in the first differentiated bulbous IH cell that is associated with the BIC. (C) In an independent infection site, it is again present in the BIC-associated bulbous IH cell (➤) as well as near septa or branching sites (*). BICs are indicated by arrows. (A), (B) and (C) Confocal images from top to bottom are GFP, BF and merged BF and GFP channels. Bars = 5 μm.

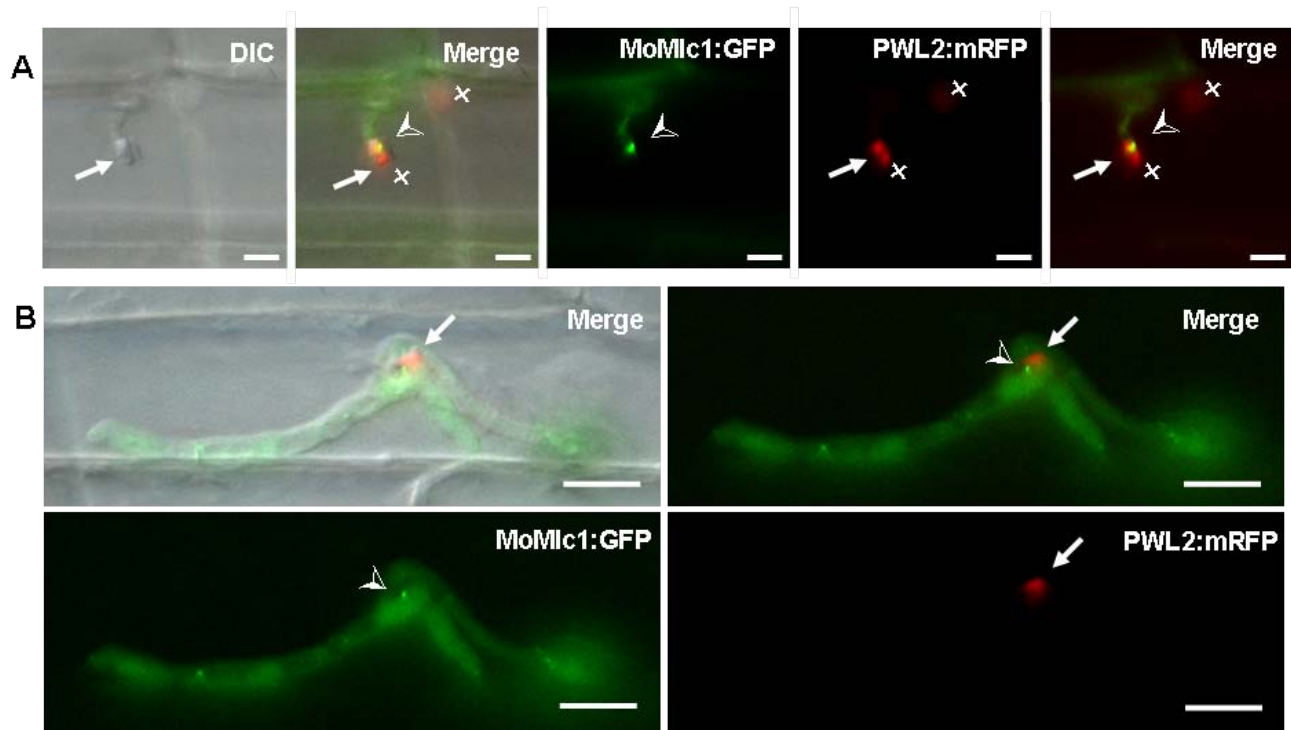


Figure 3.6. Co-labeling MoMlc1:GFP and PWL2:mRFP localized the putative Spk with respect to the BIC during blast biotrophic invasion *in planta*.

(A) Co-labeling of MoMlc1:GFP with PWL2:mRFP, which is secreted into the primary BIC and translocated inside rice cells as a red fluorescence (x). Wide-field images from left to right are DIC alone, merged DIC, GFP and mRFP channels, GFP alone, mRFP alone, and merged GFP and mRFP channels. At 24 hpi, MoMlc1:GFP localizes to a discrete spot (➤) at the tip of the filamentous primary hyphae right behind the BIC. Bars=5 μ m. Wide-field images from left to right are DIC, merged DIC, GFP and mRFP, GFP, mRFP and merged GFP and mRFP.

(B) At 27 hpi, MoMlc1:GFP (➤) localizes to a smaller but distinct spot next to the BIC, labeled by PWL2:mRFP (red), and also next to septa. The BIC is indicated by arrows. Wide-field images left to right: (top) merged DIC, GFP, and mRFP channels, merged GFP and mRFP channels, (bottom) GFP alone and mRFP alone. Bars = 10 μ m.

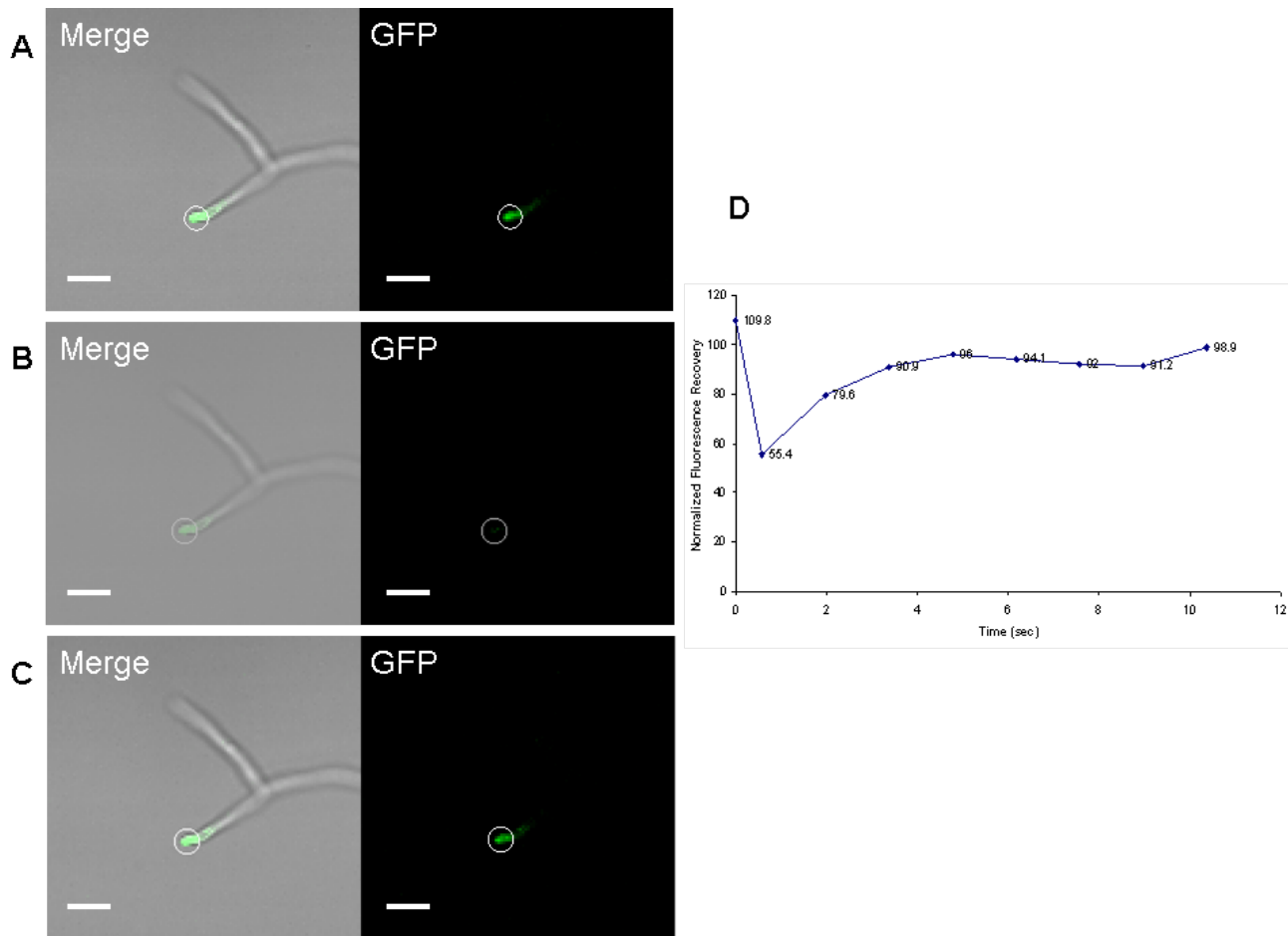


Figure 3.7. The Fluorescence Recovery After Photobleaching assay (FRAP) demonstrated continuous, stronger and faster dynamic activity of MoMlc1:GFP in the Spk of vegetative hyphae *in vitro*.

(A) Confocal images of a fungal strain expressing MoMlc1:GFP in vegetative hypha after 18 hpi of *in vitro* growth on the water agar slide. The polarized vegetative hyphae present faster growth than *in planta* IH, showing MoMlc1:GFP as a brighter spot at the hyphal tip. (A) Pre-bleach, fluorescence in a hyphal tip. (B) Bleach. (C) Allowed to recover. The final FRAP image at 11.8 seconds showed almost complete recovery. Confocal images with merged BF and GFP channels, and GFP alone (Supplemental video 3.2). (D) Fluorescence recoveries were measured as the mean intensity of a specific region of interest (ROI) pixels, represented as a white circle. The values are listed in Table 3.5, and recovery is visualized in an 11.8 seconds (Supplemental movie 3.1). Bars = 10 μ m.

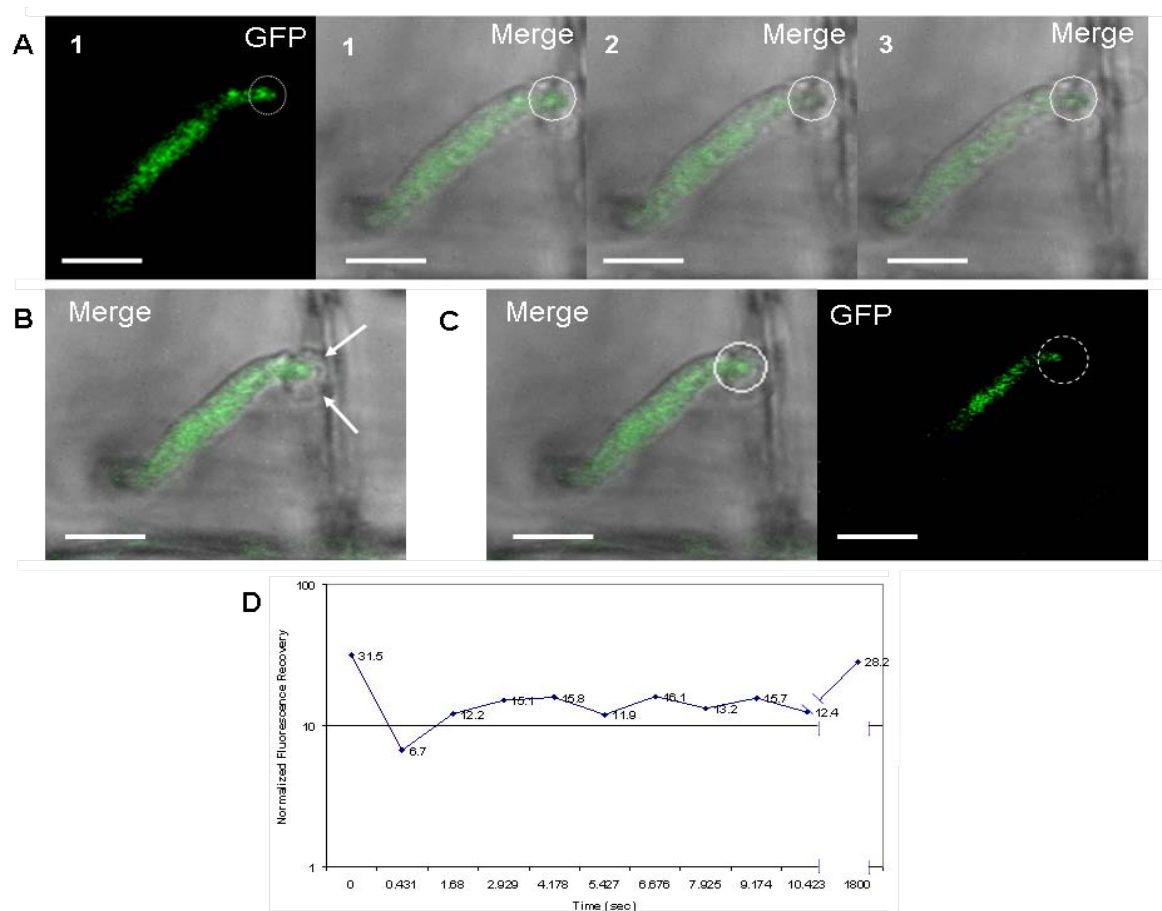


Figure 3.8. Fluorescence Recovery After Photobleaching assay (FRAP) demonstrated continuous activity of MoMlc1:GFP at the Spitzenkörper of primary hyphae, *in planta*.

(A) Confocal images of a fungal strain expressing MoMlc1:GFP during biotrophic invasion of a rice epidermal cell at 22hpi. The filamentous primary hyphae have a polarized growth style and they show MoMlc1:GFP as a brighter spot at the tip next to the BIC. (A, 1) Pre-bleach, fluorescence in a hyphal tip at 22hpi. (A, 2) Bleach. (A, 3) Allowed to recover for 10.4 sec. (B) The BIC is observed as a membrane cap beside the tip labeled by MoMlc1:GFP, which is indicated by arrows. (C) Almost complete recovery had occurred by 30 min after the final FRAP image at 10.4 seconds (Supplemental video 3.3). (D) Fluorescence recoveries were measured as the mean intensity of a specific region of interest (ROI) pixels, represented as a white circle. The values are listed in Table 3.5, and the assay is documented in a 10.4 seconds video (Supplemental movie 3.2). The time between 10.4 sec to 30 min is represented as a gap on the x-axis. Confocal images, GFP alone and merged GFP and BF. Bars = 5 μ m.

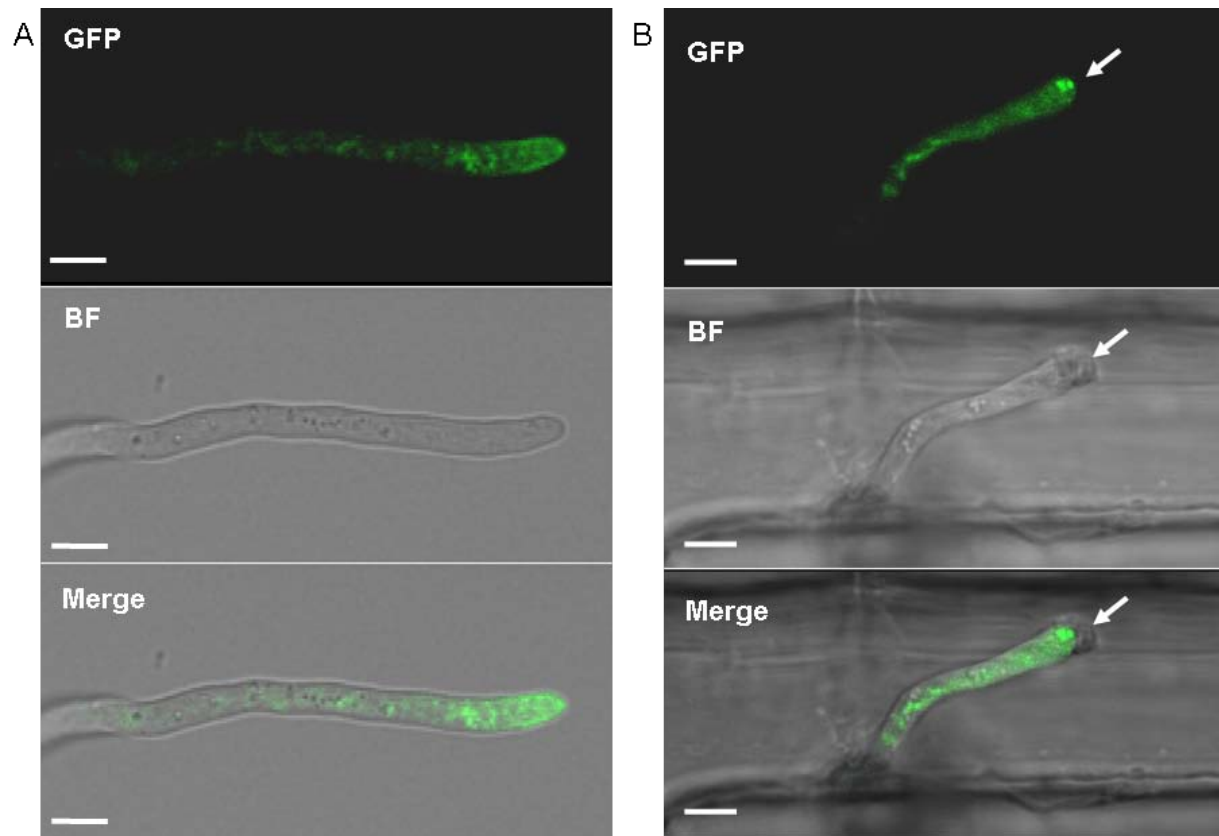


Figure 3.9. MoSnc1p:GFP defines the Spitzenkörper *in vitro* and *in planta* at the growing hyphal tip

(A) Confocal imaging of MoSnc1p:GFP in an *M. oryzae* vegetative hypha at 18 hpi showed the typical Spk-like accumulation at the hyphal tip. (B) MoSnc1p:GFP *in planta* during a compatible interaction at 24 hpi. Notice the BIC as an accumulation of membrane, a cap at the hyphal tip, and the bright spot of MoSnc1p:GFP as a concentrated dot next to the tip of the primary hyphae. Arrow shows the tip-BIC. Images top to bottom: GFP, BF, and merged BF and GFP. Bars = 10 μm .

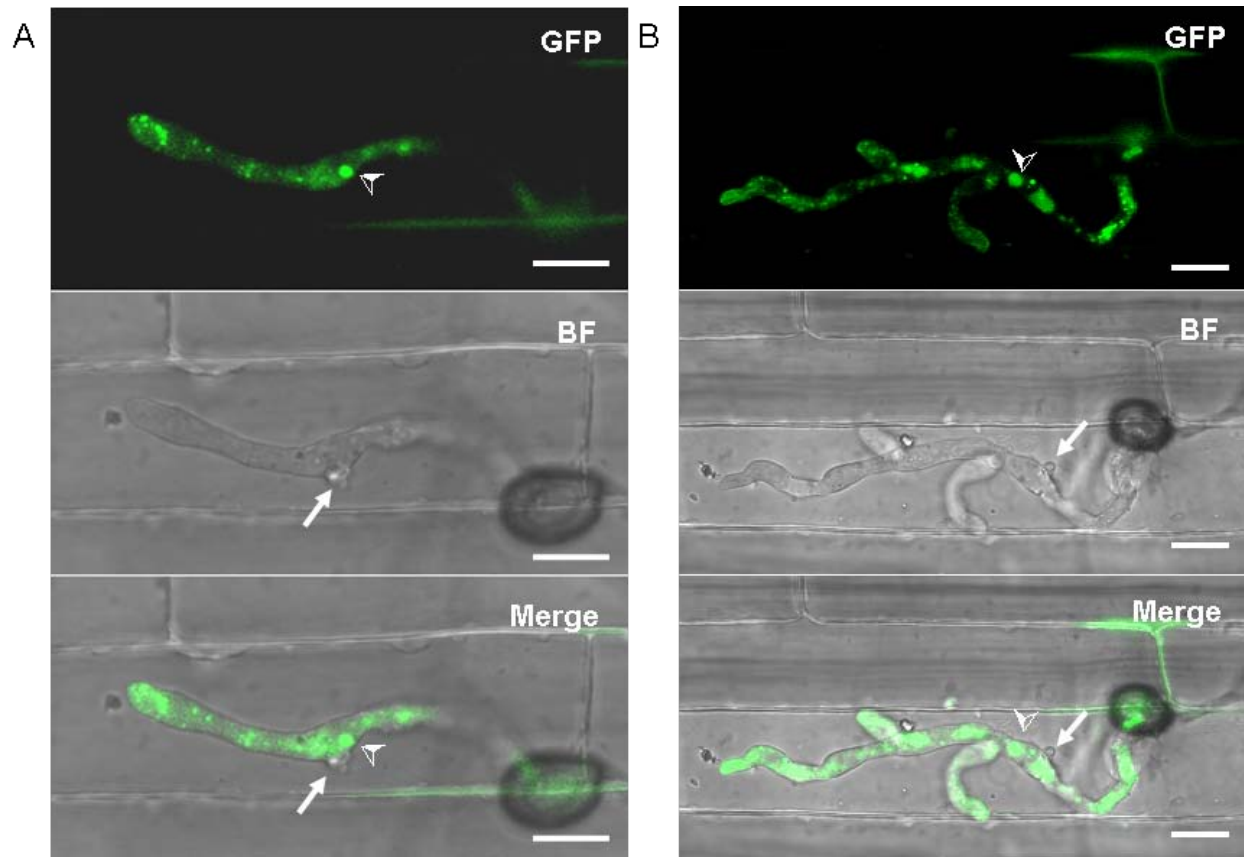


Figure 3.10. MoSnc1p:GFP in the first bulbous IH cell next to the BIC supports the hypothesis of active secretion in this cell.

Biotrophic differentiated bulbous IH are shown. (A) At 24 hpi, MoSnc1:GFP localizes to a brighter and bigger spot next to the BIC (➤) and shows a concentration of small vesicles next to the growing bulbous IH tip. This is documented in supplemental video 3.4. (B) At 28 hpi, MoSnc1:GFP localizes to a brightest and bigger spot next to the BIC (➤) and as brightest small vesicles next to branching sites and bulbous IH tips. Arrow shows the BICs. Images top to bottom: GFP alone, BF alone, and merged BF and GFP channels. Bars = 10 μ m.

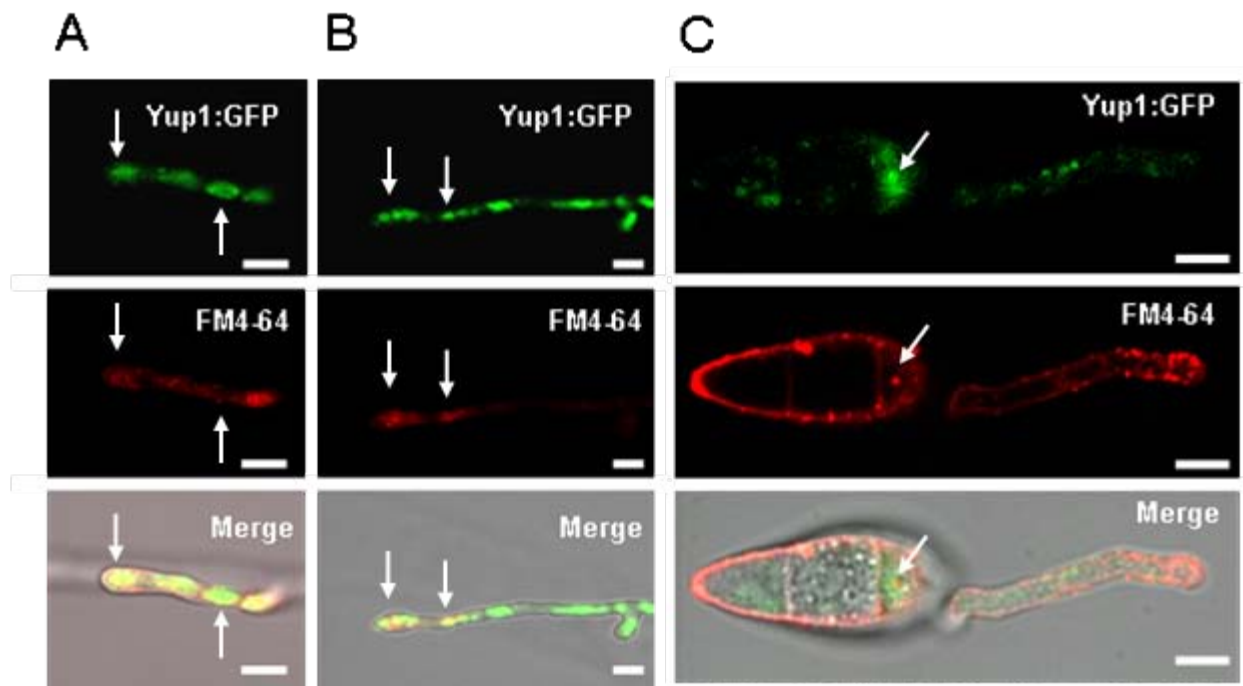


Figure 3.11. MoYup1:GFP co-localization with FM4-64 identified endocytic vesicles *in vitro*

(A) Yup1:GFP and FM4-64 present partial co-localization in vegetative hypha. (B) In the MoYup1:GFP transformant, GFP localizes to multiple small spots with a fast bidirectional movement close to the hyphal tips, and labels vacuolar membranes as in *U. maydis*. (C) Spores also show partial co-localization, especially in the cell from which the germination tube is growing. Imaged 15 minutes after dye addition. Co-localization is indicated by arrows.

Confocal images top to bottom: GFP, FM4-64, and merged BF, GFP and FM4-64. Bars=5 μ m.

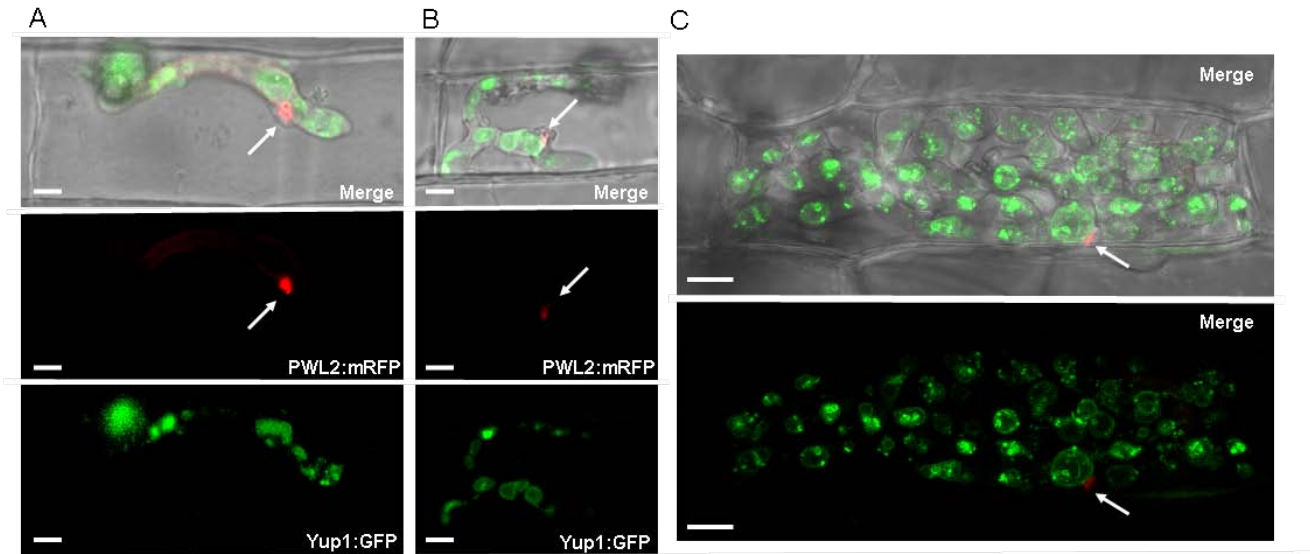


Figure 3.12. *In planta*, a fungal strain expressing MoYup1:GFP and PWL2:mRFP showed localization of putative early endosomes and vacuoles with respect to BICs.

Yup1:GFP in bulbous IH, BIC is indicated by arrow (A) at 24 hpi and (B) at 27 hpi, showed multiple-active small spots that fuse and separate from the membrane of a big vacuole that appears characteristic of the BIC-associated cell, as is observed in time lapse series assays added as supplemental videos 3.5 and 3.6, respectively. Confocal images from top to bottom: merged BF, GFP and mRFP channels, mRFP alone and GFP alone. (C) MoYup1:GFP still labels active vesicles along with vacuolar membranes in biotrophic IH at 36 hpi, after IH have completely packed the first invaded rice cell. PWL2:mRFP still labels the BIC (arrow). Confocal images from top to bottom: merged BF, GFP and mRFP channels, merged mRFP and GFP channels. Bars = 5 μ m.

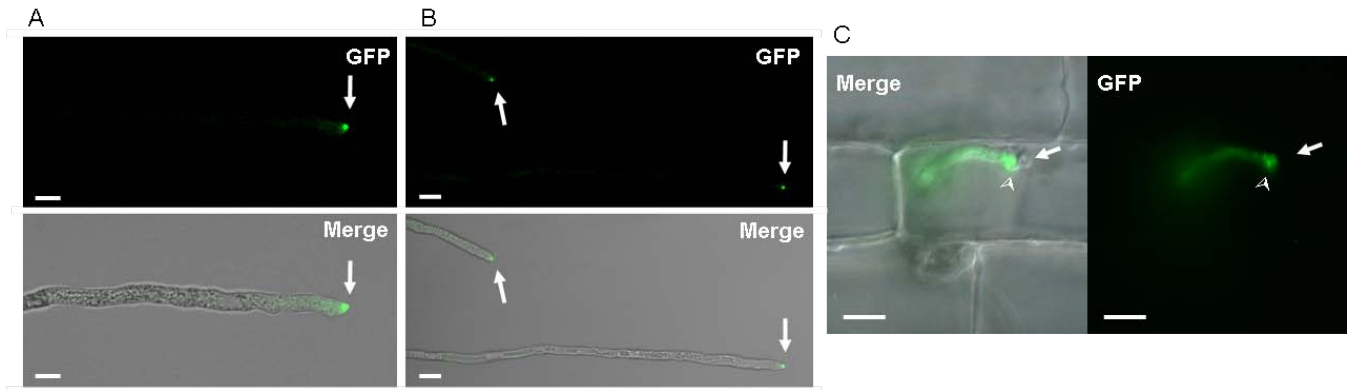


Figure 3.13 MoSpa2p:GFP revealed the *M. oryzae* Polarisome *in vitro* and *in planta*.

(A) *In vitro*, MoSpa2p:GFP localized as a distinct spot specifically at the vegetative hyphal tip. Bars= 5 μ m. (B) *In vitro*, MoSpa2p:GFP localized as a distinct spot specifically at the tip of each vegetative hypha. Confocal images were GFP alone, and merged BF and GFP. Bars= 10 μ m. See the time lapse series assay in supplemental video 3.7, which shows how fast MoSpa2p:GFP bleached in vegetative hyphae. The arrow indicates the polarisome.

(C) *In planta* at 22 hpi, the MoSpa2p:GFP is concentrated at the tip of the primary hyphae, behind the primary BIC before the growth switches to bulbous IH. Arrow shows BIC and ➤ indicates the polarisome. Wide-field images merged DIC and GFP, and GFP alone. Bars = 10 μ m. See in the time lapse series assay in supplemental video 3.8, which indicates how the MoSpa2p:GFP bright spot next to the BIC changes its orientation when the first bulbous IH begins to differentiate. The bright spot seems to move and accumulate towards the direction of hyphal enlargement instead of directly behind the BIC.

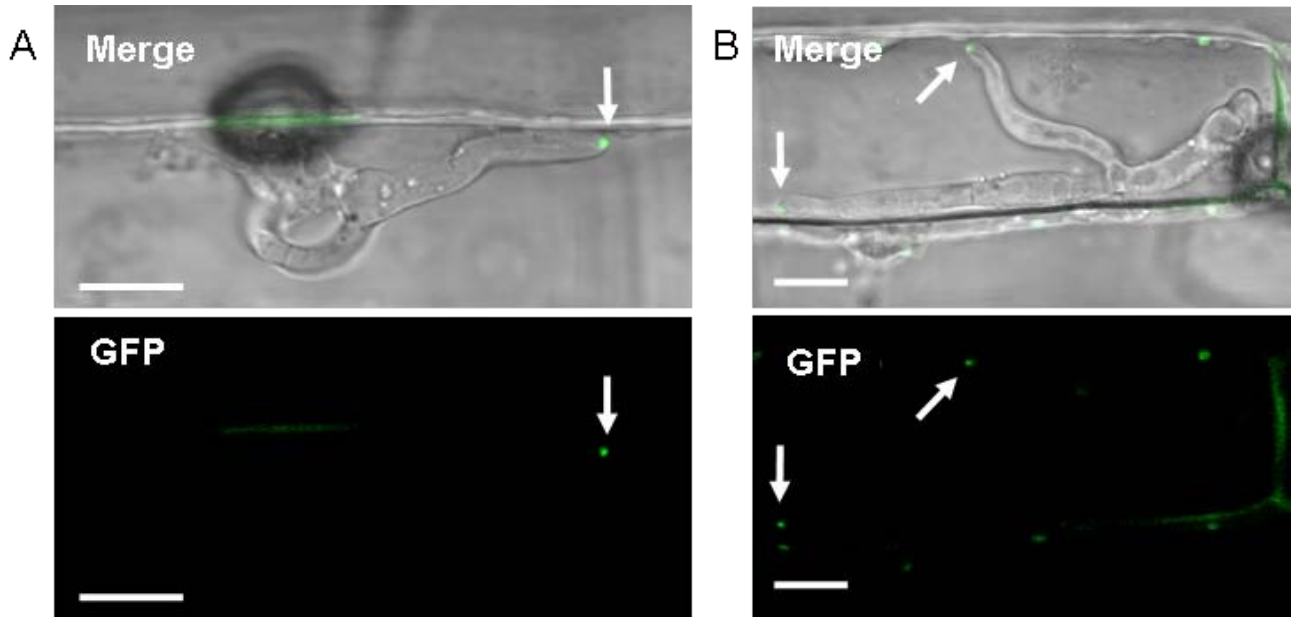


Figure 3.14. MoSpa2:GFP revealed *M. oryzae* Polarisome *in planta*.

(A) *In planta* at 24 hpi, MoSpa2p:GFP localized as a distinct spot specifically at the tip of the first branch from the differentiated BIC-associated bulbous IH cell. No polarisome was observed in the BIC-associated cells. The arrow shows the polarisome. Confocal images were merged BF and GFP channels, and GFP alone. Bars = 10 μ m.

(B) *In planta* at 27 hpi, the MoSpa2p:GFP is concentrated at the tip of each branch of the bulbous IH. The fluorescence is not observed in the BIC-associated bulbous IH cell. Arrows show the polarisome at each hyphal tip. Confocal images showed merged BF and GFP channels, and GFP alone. Bars = 10 μ m.

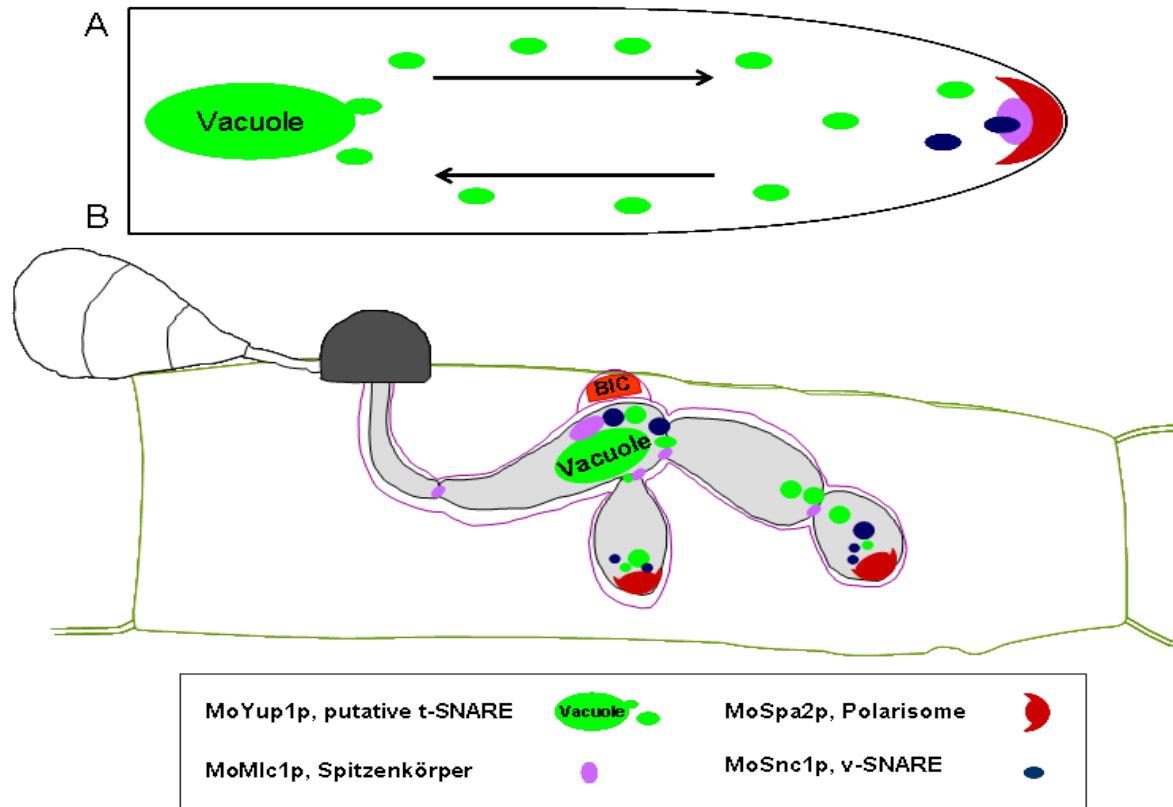


Figure 3.15. Localization of *M. oryzae* secretion components showed *in planta* differences between filamentous-polarized hyphae and bulbous invasive hyphae during compatible interactions.

This cartoon is based on live cell imaging *in planta* of four fluorescently-labeled candidate *M. oryzae* secretion components. MoYup1:GFP labels vacuolar membranes and small spots that have a fast bidirectional movement along the hyphae. MoMlc1:GFP, as a Spitzenkörper (Spk) marker, labels the secretory vesicle supply center during rice blast biotrophic invasion including putative Spk-like structures near the BIC and at septa in bulbous IH. MoSpa2:GFP labels the polarisome at each growing invasive hyphal tip. MoSnc1:GFP labels active spots as putative secretory vesicles where secretion actively occurs. (A) Represents the similarity in localization of these cellular components between vegetative hyphae *in vitro*, and filamentous-polarized primary invasive hyphae *in planta*. (B) Represents the invasive hyphal dimorphic switch that is always accompanied by the association of the BICs with the hyphal cells that undergo the switch *in planta*. MoMlc1p and MoSnc1p are present in the BIC-associated cells as an intense spot close to the BICs; we suggest naming this putative vesicle

supply center beside the first bulbous IH cell as the “Seitenkörper” (side body), since it is not at a hyphal apex. The polarisome marker MoSpa2p, showed spatially distinct localization from the MoMlc1p and MoSnc1p, which suggested that there is a spatially-segregated mechanism for secretion of effectors into BICs.

Table 3.1. Cellular markers for protein secretion components in filamentous fungi.

Name	SGD or GeneBankID	MGG_ Broad Inst Version 6	Size nt (aa)	Cellular Marker_localization	Conserved Domain	Blastp % e-value
Yup1	UM05406.1	MGG_05428.6	1128 (375)	Early endosomes and vacuolar membranes	5' PX_SNARE-3'	72% 3e-10
Mlc1	YGL106W	MGG_09470.6	1018 (147)	Spitzenkörper, Targeted membrane deposition	Core: EF-hand	60% 3.1e-24
Snc1	YAL030W	MGG_12614	1295 (125)	v-SNARE fusion between Golgi-derived secretory vesicles and the plasma membrane	Core: Synaptobrevin	68% 3.6e-25
Spa2	YLL021W	MGG_03703.6	3006 (951)	Polarisome	Core: SHD of GIT	55% 3.5e-22
Tub1	YML085C	MGG_06650.6	2330 (450)	Microtubules	Core: Tubulin /FtsZ family -GTPase and FtsZ C-terminal	81% 3.0e-177
Sec15	YGL233W	MGG_00471.6	2833 (755)	Exocyst subunit that docks secretory vesicles to the plasma membrane	Sec15 like	49% 9.4e-48
Cdc42	YLR229C	MGG_00466.6	1328 (194)	Polarisome	Core: Miro like and Ras family, Small GTPbinding protein Rho small GTPase	90% 2.2e-85
Exo70	YJL085W	MGG_01760.6	1977 (630)	Subunit of the exocyst complex	EXO70 like	43% 7.9e-23
Myo5	YMR109W	MGG_06923.6	5277 (1590)	Route of secretory vesicle delivery	5'-SH3 like, Myosin head (motor domain), IQ Calmodulin, DIL-3'	55% 3.2e-115
Mss4/PI4PK	YDR208W	MGG_06572.6	4074 (1057)	Sterol-rich plasma membrane "Lipid rafts"	Core: Phosphatidylinositol 4 phosphate 5 kinase	71% 1.2e-107
Sec2	YNL272C	MGG_02923.6	2519 (669)	Site of exocytosis	5'-viralA-type inclusion protein repeat. GDP/GTP exchange factor	3.8e-22

Table 3.2. Primers used for cloning and sequencing of cellular markers of *M. oryzae*.

MG box No.	Primer Name	Sequence 5'-3'	Description
22.	Spa2 MGG_03703 <i>SacI</i> _F'	CGAGCTCTCTACCCCTGTAGGGCACTG	Spa2_1 kb promoter and coding sequence
23.	Spa2 MGG_03703 <i>Bam</i> HI_R'	CGCGGATCCTGAAAAGTCATCACCACCACC	with <i>SacI</i> - <i>Bam</i> HI restriction enzyme sites
24.	Spa2 857_MGG_03703	TGCTTCATTCTGCACCAGAC	For sequence from 857 bp forward
25.	Spa2 1501_MGG_03703	CTCCGAACCTCCACCTAAAT	For sequence from 1501 bp forward
26.	Spa2 2221_MGG_03703	AGCTGGAGGCTGTCCAAGAT	For sequence from 2221 bp forward'
27.	Spa2 2821_MGG_03703	TCCAGGTTGCCATCGATGAT	For sequence from 2821 bp forward
28.	Yup1 MGG_05428 <i>SacI</i> _F'	CGAGCTCTTGAGGTGCAATCGGATAC	Yup1_1 kb promoter and coding sequence
29.	Yup1 MGG_05428 <i>Bam</i> HI_R'	CGCGGATCCCAGCCCCAGCTTCCTC	
30.	Yup1 MGG_05428-	TCGCTACTTTGAGACGTCAC	For sequence from 801 bp forward
31.	Tub1 MGG_06650 <i>Eco</i> RI_F'	CCGGAATTCGACGAGACCAACCCTCTC	Tub1_1 kb promoter and coding sequence
32.	Tub1 MGG_06650 <i>Bgl</i> II_R'	GGAAGATCTGTACTCCGCCTCAATACCCTC	
33.	Myo5 MGG_06923 <i>Eco</i> RI_F'	CCGGAATTCGCCAGAGAGTTTCGTGCGCTAT	Myo5_1 kb promoter and coding sequence
34.	Myo5 MGG_06923 <i>Bam</i> HI_R'	CGCGGATCCTGCGCTGGCGCCGAT	
35.	PIP5K MGG_06572 <i>SacI</i> _F'	CGAGCTCTGCCGTGAGGTTGAAGTACAGAG	PIP5K_1 kb promoter and coding sequence
36.	PIP5K MGG_06572 <i>Nco</i> I_R'	CATGCCATGGTGTCCGGAGCGGGC	
37.	Spa2 MGG_03703 <i>Xba</i> I_F'	TGCTCTAGATCTACCCCTGTAGGGCACTG	Spa2_1 kb promoter and coding sequence
38.	Spa2 MGG_03703 <i>Pac</i> I_R'	CCTTAATTAATGAAAAGTCATCACCACCACC	with <i>Xba</i> I- <i>Pac</i> I restriction enzyme sites
40.	Spa2 MGG_03703 <i>Bam</i> HI_F'	CGCGGATCCATGAACGCTGCTGCCACC	Spa2_coding sequence
41.	Spa2 MGG_03703 <i>Sbf</i> I_R'	GGACGTCTGAAAAGTCATCACCACC	
42.	Tub1 MGG_06650 <i>Bgl</i> II_F'	GGAAGATCTATGCGCGAGATTATCAGC	Tub1_coding sequence
43.	Tub1 MGG_06650 <i>Pst</i> I_R'	CGACGTCGTACTCCGCCTCAATACC	
44.	F_ <i>Sac</i> I Cdc42:	GAGCTCACCATAACAAGAGCCCAGTGTTA	Cdc42_1 kb promoter and coding sequence
45.	R_ <i>Bam</i> HI Cdc42:	GGATCCAAGGATCAGGCACTTTTTGGATT	
46.	F_ <i>Sac</i> I Spa2:	GAGTCCTTGGGGGCTCAAAGTAACGG	1.5 kb promoter and Spa2 coding sequence
47.	R_ <i>Bam</i> HI Spa2:	GGATCCTGAAAAGTCATCACCACCACC	
49.	Sec15_ <i>Bam</i> HI_R'	GCGGATCCGCTGAAACCAAAACGAGAT	Sec15_1 kb promoter and coding sequence
50.	Sec15_ <i>Sac</i> I_F'	GAGTCACAATCGTGGGTGCATATTG	
51.	Exo70_ <i>Eco</i> RI_F'	CCGGAATTCAGCTTCGGGCATTTTG	Exo70_1 kb promoter and coding sequence
52.	Exo70_ <i>Bam</i> HI_R'	CGCGGATCCGTAAGGCTGG	
53.	Mlc1_ <i>Eco</i> RI_F'	CCGGAATTCCTCAAGTCTCGTTCC	Mlc1_1 kb promoter and coding sequence
54.	Mlc1_ <i>Bam</i> HI_R'	CATTCTGGCCAACGGATCCCG	

Table 3.3. Plasmids used for fungal transformation of *M. oryzae*.

Clone	Description
pBV176	0.5 kb <i>Bam</i> HI- <i>Pst</i> I fragment between P27_EGFP expression binary vector derived from pBHt2. Kanamycin and Hygromycin resistance
pBV403	EGFP expression binary vector derived from pBGt (Seogchan Kang, unpublished results), consisting of 2 kb P27 <i>AVR-Pita</i> SP:GFP (<i>Eco</i> RI- <i>Bam</i> HI fragment), EGFP (<i>Bam</i> HI- <i>Xba</i> I fragment of pBV126), and <i>N.crassa</i> β -tubulin terminator (<i>Sph</i> I- <i>Hind</i> III fragment) that were cloned in <i>Eco</i> RI- <i>Hind</i> III sites of pBGt. Kanamycin and Geneticin (G418) resistance
pBV367	mRFP expression binary vector derived from pBGt (Seogchan Kang, unpublished results), consisting of three modules of P27 (<i>Eco</i> RI- <i>Bam</i> HI fragment), mRFP (<i>Bam</i> HI- <i>Sph</i> I fragment of pBV192), and <i>N.crassa</i> β -tubulin terminator (<i>Sph</i> I- <i>Hind</i> III fragment) that were cloned in <i>Eco</i> RI- <i>Hind</i> III sites of pBGt. Kanamycin and G418 resistance
pBV565	2.0 kb <i>Yup1</i> MGG_05428.6, include 1 kb promoter and coding sequence, <i>Sac</i> I- <i>Bam</i> HI fragment into pBV403. Kanamycin and G418 resistance
pBV567	4.0 kb <i>SPA2</i> MGG_03703.6, include 1 kb promoter and coding sequence, <i>Sac</i> I- <i>Bam</i> HI fragment into pBV367. Kanamycin and G418 resistance
pBV568	3.3 kb <i>Tub1</i> MGG_06650.6, include 1 kb promoter and coding sequence, <i>Eco</i> RI- <i>Bgl</i> II (<i>Bam</i> HI site is lost) fragment into pBV367. Kanamycin and G418 resistance
pBV940	3.0 kb <i>SPA2</i> MGG_03703.6, coding sequence, <i>Bam</i> HI- <i>Sbf</i> I into pBV176, P27_EGFP. Kanamycin and Hygromycin resistance
pBV941	2.3 kb <i>Tub1</i> MGG_06650.6, coding sequence, <i>Bgl</i> II- <i>Pst</i> I into pBV176, P27_EGFP. Kanamycin and Hygromycin resistance.
pBV942	2.2 kb <i>Cdc42</i> MGG_00466.6, include 1 kb promoter and coding sequence, <i>Sac</i> I- <i>Bam</i> HI into pBV403, GFP. Kanamycin and G418 resistance
pBV943	2.2 kb <i>Cdc42</i> MGG_00466.6, include 1 kb promoter and coding sequence, <i>Sac</i> I- <i>Bam</i> HI into pBV367, mRFP. Kanamycin and G418 resistance
pBV944	4.5 kb <i>Spa2</i> MGG_03703.6, include 1.5 kb promoter and coding sequence, <i>Sac</i> I- <i>Bam</i> HI into pBV403, GFP. Kanamycin and G418 resistance
pBV945	4.5 kb <i>Spa2</i> MGG_03703.6, include 1.5 kb promoter and coding sequence, <i>Sac</i> I- <i>Bam</i> HI into pBV367, mRFP. Kanamycin and G418 resistance
pBV946	1.76 kb <i>Mlc1</i> MGG_09470.6, include 1 kb promoter and coding sequence, <i>Eco</i> RI- <i>Bam</i> HI into pBV403, GFP. Kanamycin and G418 resistance
pBV947	2.97 kb <i>Exo70</i> MGG_01760.6, include 1 kb promoter and coding sequence, <i>Eco</i> RI- <i>Bam</i> HI into pBV403, GFP. Kanamycin and G418 resistance

Table 3.4. Fungal transformants.

Name	Description [background strain; plasmid used]
KV118	Transformant containing a fusion of PWL2 promoter and coding sequence (PWL2 145 aa) with mRFP reporter gene [O-137; pBV 317]. Hygromycin resistance. Synonym CKF287
KV108	Transformant containing a fusion of MGG_05428.6, MoYup1, promoter and coding sequence with GFP reporter gene [KV118; pBV 403]. Geneticin (G418) resistance.
KV125	Transformant containing a fusion of MGG_09470.6, MoMlc1, promoter and coding sequence with GFP reporter gene [CP987; pBV 403]. G418 resistance.
KV126	Transformant containing a fusion of MGG_09470.6, MoMlc1, promoter and coding sequence with GFP reporter gene [KV118; pBV 403]. G418 resistance.
FP 143	Transformant containing a fusion of Snc1 with GFP [Guy11; unpublished] from Dr. Nicholas Talbot's Laboratory, Exeter University U.K. Sulfonylurea (Sur) resistance.
FP 144	Transformant containing a fusion of GFP with Spa2 [Guy11; unpublished] from Dr. Nicholas Talbot's Laboratory, Exeter University U.K. Sur resistance.

Table 3.5. FRAP experiment for MoMlc1:GFP recovery.

FRAP <i>in vitro</i> vegetative hypha - MoMlc1p:GFP at hyphal tip		
Time [s]	Intensity ROI 6 Ch2	Intensity ROI 6 ChD
0.000	109.8	160.2
0.572	55.4	160.8
1.971	79.6	160.7
3.370	90.9	160.2
4.769	96.0	161.2
6.168	94.1	161.0
7.567	92.0	161.2
8.966	91.2	161.1
10.365	98.9	160.3

FRAP <i>in planta</i> invasive hypha - MoMlc1p:GFP at primary hyphal tip		
Time [s]	Intensity ROI 8 Ch2	Intensity ROI 8 ChD
0.000	31.5	114.0
0.431	6.7	114.6
1.680	12.2	115.0
2.929	15.1	115.0
4.178	15.8	114.3
5.427	11.9	114.7
6.676	16.1	114.4
7.925	13.2	113.8
9.174	15.7	113.0
10.423	12.4	113.6
1800.0	28.2	113.0

Chapter 4 - Future Perspectives

The extraordinary biology exhibited by *Magnaporthe oryzae* during biotrophic invasion in the compatible interactions revealed a powerful manipulation of the host. Display of an arsenal of unique effector proteins with functional redundancy (Mosquera et al., 2009), and G-protein coupled receptors (GPCRs) (Dean et al., 2005), suggest an enhanced flexibility to counteract plant signaling in contrast to non-biotrophic pathogens. Some clues are given on how the fungal pathogens manipulate plant mechanisms of defense to avoid detection, most probably from the penetration stage. Is it possible that the fungus manages plant components for its own benefit? How do the plants develop *de novo* an extra membrane to enclose the fungus? Is the BIC an exchange space where the fungus protects its avirulence proteins from plant degradation? Is the BIC a special structure where the plant undergoes endocytosis to translocate fungal effector proteins into the cytoplasm in a signaling-dependent, regulated manner? There are still many questions to understand the mechanism(s) that regulates this interaction, but recent advances in understanding of the nature of this interface helps us to find better tools to facilitate uncovering these missing answers.

Live cell imaging of fluorescently-labeled effectors and effector candidates enabled an innovative strategy to decode the mechanism of secretion and translocation used in rice blast disease (Kankanala et al., 2007; Mosquera et al., 2009; Khang et al., 2010; Giraldo and Valent, Unpublished). Results from chapter 2 of four biotrophy-associated secreted (BAS) proteins suggest differences in function and localization between BAS1, as well as the BIC-localized AVR effectors, and BAS4. The BAS1 and BAS4 differential localization patterns can be useful to test if there is a particular mechanism for effector secretion and accumulation into BICs, which in turn directs regulated delivery of effectors inside the rice cytoplasm. Further studies in blast effector translocation will include BAS4 as a sensitive marker of EIHM intactness in order to guarantee observation of effector delivery by successful IH inside the host cells (Mosquera et al., 2009; Khang et al., 2010).

The secretion mechanism in filamentous fungi is highly conserved among eukaryotes. Thus, labeled *M. oryzae* orthologs of main cellular components of the secretion pathway facilitated visualization of their tracking and their localization with respect to BIC development.

These results support our hypothesis for the BIC's role in secretion of effectors (Giraldo et al, Unpublished). Results from chapter 3 are summarized in the Figure 3.15; the cartoon shows the model for *M. oryzae* spatially segregated secretion in bulbous invasive hyphae *in planta* during compatible interaction (Giraldo and Valent, Unpublished). Localization of the polarisome at a spatially distinct location from the vesicle supply center or "Seitenkörper" in the bulbous invasive hyphae supports the hypotheses: (1) The switch of growth from polarized to bulbous invasive hyphae is accompanied by a modification of the filamentous hyphal secretion mechanism; (2) There is a spatially-segregated mechanism for secretion of effectors into BICs; and (3) BICs are important in the efficient translocation of effectors to the rice cytoplasm (Giraldo et al, Unpublished). Labeling cellular components of the exocyst complex, such as Sec2, microtubules by alpha-tubulin and the actin cables by Lifeact will assist in understanding the role of BIC-associated cells in the secretion and accumulation of blast effectors in the BIC. Studying cellular components of the secretion machinery can help us to understand how differentiated IH grow *in planta*. In the same direction, labeling rice organelles and membranes will assist us to test if components of the plant endocytosis pathway play a role in the translocation of blast effectors relative to BICs, and will provide clues about the origin of the extrainvasive hyphal membrane (EIHM).

Determine if the rice blast cell-to-cell movement occurs through plasmodesmata

Our research has led us to hypothesize that the blast fungus co-opts the host plasmodesmata for cell-to-cell movement as well as for cell-to-cell trafficking of effectors into host cells before invasion. Interestingly, both BAS2 and BAS3 fluorescent-proteins accumulate at locations where IH have crossed the rice cell wall, suggesting they might play a role in cell-to-cell movement.

Co-localization of putative cell-to-cell movement proteins such as BAS2 and BAS3 with plasmodesmata markers via transient and stable expression of rice plasmodesmata components will represent a good strategy to test the hypothesis that *M. oryzae* moves cell-to-cell through the plasmodesmata during biotrophic invasion. A conserved plasmodesmata protein that specifically binds to 1,3- β -glucans (callose) has been identified (Simpson et al., 2009). This callose protein, which belongs to a family of small glycosylphosphatidylinositol (GPI)-linked proteins, could be

identified in the rice genome for transient and/or stable rice transformation (Oparka et al., 1997; Oparka et al., 1999; Zambryski and Crawford, 2000; Simpson et al., 2009) to facilitate further co-localization studies.

In addition, complementation assays using viral movement proteins can be useful to provide evidence about their function in modifying the plasmodesmatal permeability, or to indicate if they use a different strategy. Analysis in this direction will provide evidence to validate the hypothesis that rice blast moves cell-to-cell using plasmodesmatal channels (Kankanala et al., 2007).

Determine the protein or complex of proteins that interact with known effectors and BAS proteins *in planta*

Interaction between proteins is distinct from the interaction of a protein and a non-protein molecule, which usually is a relationship like an enzyme with its substrate. Protein-protein interaction generally occurs for two different purposes: first, to assist the other protein in accomplishing a biochemical function or regulation of cellular processes; and second, to modify the role of the other protein (Cagney, 2009). Because of these two main goals involved in the protein-protein interaction, comprehensive efforts have begun to map interaction networks beginning with model systems such as the budding yeast, *Saccharomyces cerevisiae*, for which a detailed protein-protein interaction networks map has been acquired from large genome-scale studies (Drees et al., 2001; Zhang et al., 2009; Costanzo et al., 2010). Based on *S. cerevisiae*, Costanzo et al (2010) provided a functionally unbiased genetic interaction map for interpretation of chemical-genetic interactions for a eukaryotic cell. Advances in yeast provide the starting point for similar studies in other fungal-model systems, and currently researchers have a set of affinity tags appropriate for protein recovery fused to the N- or C-terminus of individual proteins.

To our knowledge, there is no study on systematic characterization of the protein-protein interactome in filamentous fungi. The use of affinity purification and proteomic analysis by mass spectrometry of effectors and BAS proteins from inoculated rice with *M. oryzae* can generate potential interacting proteins with *in planta*-secreted proteins. Studies in this field will be the first step towards the study of the protein-protein interaction networks of pathogenicity factors in plant pathogenic fungi. Identification of proteins interacting *in planta* with BIC

localized proteins can help us to identify other component proteins of the BICs and support our understanding about its role during compatible interactions. This strategy might also identify the virulence target effectors and provide molecular understanding of how these pathogen molecules promote successful infection.

References

- Altschul, S.F., Madden, T.L., Schaffer, A.A., Zhang, J., Zhang, Z., Miller, W., and Lipman, D.J.** (1997). Gapped BLAST and PSI-BLAST: a new generation of protein database search programs. *Nucleic Acids Research* **25**, 3389-3402.
- Araujo-Palomares, C.L., Riquelme, M., and Castro-Longoria, E.** (2009). The polarisome component SPA-2 localizes at the apex of *Neurospora crassa* and partially colocalizes with the Spitzenkörper. *Fungal Genetics and Biology* **46** (8), 551-63.
- Armstrong, M.R., Whisson, S.C., Pritchard, L., Bos, J.I.B., Venter, E., Avrova, A.O., Rehmany, A.P., Böhme, U., Brooks, K., Cherevach, I., Hamlin, N., White, B., Fraser, A., Lord, A., Quail, M., Churcher, C., Hall, N., Berriman, M., Huang, S., Kamoun, S., Beynon, J.L., and Birch, P.R.J.** (2005). An Ancestral Oomycete Locus Contains Late Blight Avirulence Gene *Avr3a*, Encoding a Protein that is Recognised in the Host Cytoplasm. *Proceedings of the National Academy of Sciences USA* **102**, 7766-7771.
- Atkinson, H.A., Daniels, A., and Read, N.D.** (2002). Live-cell imaging of endocytosis during conidial germination in the rice blast fungus, *Magnaporthe grisea*. *Fungal Genetics and Biology* **37**, 233-244.
- Ballini, E., Morel, J.-B., Droc, G., Price, A., Courtois, B., Notteghem, J.-L., and Tharreau, D.** (2008). A Genome-Wide Meta-Analysis of Rice Blast Resistance Genes and Quantitative Trait Loci Provides New Insights into Partial and Complete Resistance. *MPMI* **21**, 859-868.
- Bartnicki-Garcia, S., Hergert, F., and Gierz, G.** (1989). Computer-simulation of fungal morphogenesis and the mathematical basis for hyphal (tip) growth. *Protoplasma* **153**, 46-57.
- Bartnicki-Garcia, S., Bartnicki, D., Gierz, G., Lopez-Franco, R., and Bracker, C.E.** (1995). Evidence that Spitzenkörper behavior determines the shape of a fungal hypha - a test of the hyphoid model. *Exp Mycol* **19**, 153-159.

- Basse, C.W., Stumpferl, S., and Kahmann, R. (2000).** Characterization of a *Ustilago maydis* gene specifically induced during the biotrophic phase: evidence for negative as well as positive regulation. *Mol Cell Biol* **20**, 329-339.
- Basse, C.W., Kolb, S., and Kahmann, R. (2002).** A maize-specifically expressed gene cluster in *Ustilago maydis*. *Mol Microbiol* **43**, 75-93.
- Berepiki, A., Lichius, A., Shoji, J.-Y., Tilsner, J., and Read, N.D. (2010).** F-Actin Dynamics in *Neurospora crassa*. *Eukaryotic Cell* **9**, 547-557.
- Berruyer, R., Poussier, S., Kankanala, P., Mosquera, G., and Valent, B. (2006).** Quantitative and qualitative influence of inoculation methods on *in planta* growth of rice blast fungus. *Phytopathology* **96**, 346-355.
- Bhattacharjee, S., Hiller, N.L., Liolios, K., Win, J., and Kanneganti, T.-D. (2006).** The Malarial Host-Targeting Signal Is Conserved in the Irish Potato Famine Pathogen. *PLoS Pathog* **2**, 0453-0465.
- Bielli, P., Casavola, E.C., Biroccio, A., Urbani, A., and Ragnini-Wilson, A. (2006).** GTP drives myosin light chain 1 interaction with the class V myosin Myo2 IQ motifs via a Sec2 Rab GEF mediated pathway. *Molecular Microbiology* **59**, 1576-1590.
- Birch, P.R.J., Rehmany, A.P., Pritchard, L., Kamoun, S., and Beynon, J.L. (2006).** Trafficking Arms: Oomycete Effectors Enter Host Plant Cells. *Trends in Microbiology* **14**, 8-11.
- Böhnert, H.U., Fudal, I., Dioh, W., Tharreau, D., Notteghem, J.-L., and Lebrun, M.-H. (2004).** A Putative Polyketide Synthase/Peptide Synthetase from *Magnaporthe grisea* Signals Pathogen Attack to Resistant Rice. *The Plant Cell* **16**, 2499-2513.
- Bolte, S., Talbot, C., Boutte, Y., Catrice, O., Read, N.D., and Satiat-Jeunemaitre, B. (2004).** FM-dyes as experimental probes for dissecting vesicle trafficking in living plant cells. *Journal of Microscopy* **214**, 159-173.
- Bourett, T.M., and Howard, R.J. (1990).** *In vitro* development of penetration structures in the rice blast fungus *Magnaporthe grisea*. *Canadian Journal of Botany* **68**, 329-342.
- Bourett, T.M., Sweigard, J.A., Czymmek, K.J., Carroll, A., and Howard, R.J. (2002).** Reef coral fluorescent proteins for visualizing fungal pathogens. *Fungal Genetics and Biology* **37**, 211-220.

- Boyko, V., Ferralli, J., Ashby, J., Schellenbaum, P., and Heinlein, M.** (2000). Function of microtubules in intercellular transport of plant virus RNA. *Nature Cell Biol.* **2**(11), 826-32.
- Bryan, G.T., Jia, Y., Farrall, L., Wu, K.-S., Hershey, H.P., McAdams, S.A., Faulk, K.N., Donaldson, G.K., Tarchini, R., and Valent, B.** (2000a). Molecular characterization of resistance gene /avirulence gene interactions in the rice blast system. In *Biology of Plant-Microbe Interactions*, P.J.G.M. de Wit, T. Bisseling, and W.J. Stiekema, eds (St. Paul, Minnesota: International Society for Molecular Plant-Microbe Interactions), pp. 35-39.
- Bryan, G.T., Wu, K., Farrall, L., Jia, Y., Hershey, H.P., McAdams, S.A., Faulk, K.N., Donaldson, G.K., Tarchini, R., and Valent, B.** (2000b). A single amino acid difference distinguishes resistant and susceptible alleles of the rice blast resistance gene *Pi-ta*. *The Plant Cell* **12**, 2033-2045.
- Cagney, G.** (2009). Interaction networks: Lessons from large-scale studies in yeast. *Proteomics* **9**, 4799-4811.
- Campbell, R.E., Tour, O., Palmer, A.E., Steinbach, P.A., Baird, G.S., Zacharias, D.A., and Tsien, R.Y.** (2002). A monomeric red fluorescent protein. *Proc. Natl. Acad. Sci.* **99**, 7877-7882.
- Carbó, N., and Pérez-Martín, J.** (2008). Spa2 is required for morphogenesis but it is dispensable for pathogenicity in the phytopathogenic fungus *Ustilago maydis*. *Fungal Genetics and Biology* **45**, 1315-1327.
- Casavola, E.C., Catucci, A., Bielli, P., Pentima, A.D., Porcu, G., Pennestri, M., Cicero, D.O., and Ragnini-Wilson, A.** (2008). Ypt32p and Mlc1p bind within the vesicle binding region of the class V myosin Myo2p globular tail domain. *Mol. Microbiol.* **67**, 1051-1066.
- Catanzariti, A.-M., Dodds, P.N., Lawrence, G.J., Ayliffe, M.A., and Ellisa, J.G.** (2006). Haustorially Expressed Secreted Proteins from Flax Rust Are Highly Enriched for Avirulence Elicitors. *The Plant Cell* **18**, 243-256.
- Catanzariti, A.-M., Dodds, P.N., Ve, T., Kobe, B., Ellis, J.G., and Staskawicz, B.J.** (2010). The AvrM Effector from Flax Rust Has a Structured C-Terminal Domain and Interacts Directly with the M Resistance Protein. *Molecular Plant-Microbe Interactions* **23**, 49-57.

- Chalfie, M., and Kain, S.** (1998). Green Fluorescent Protein: Properties, Applications, and Protocols. (New York: Wiley-Liss).
- Chisholm, S.T., Coaker, G., Day, B., and Staskawicz, B.J.** (2006). Host-Microbe Interactions: Shaping the Evolution of the Plant Immune Response. *Cell* **124**, 803-814.
- Chiu, W.-L., Niwa, Y., Zeng, W., Harano, T., Kobayashi, H., and Sheen, J.** (1996). Engineered GFP as a vital reporter in plants. *Current Biology* **6**, 325-330.
- Chumley, F.G., and Valent, B.** (1990). Genetic analysis of melanin-deficient, nonpathogenic mutants of *Magnaporthe grisea*. *Mol. Plant-Microbe Interact.* **3**, 135-143.
- Conesa, A., Punt, P.J., Luijk, N.v., and Hondel, C.A.M.J.J.v.d.** (2001). The secretion pathway in filamentous fungi: A biotechnological view. *Fungal Genetics and Biology* **33**, 155–171.
- Correa-Victoria, F.J., Zeigler, R., S., and Levy, M.** (1994). Virulence characteristics of genetic families of *Pyricularia grisea* in Colombia. In Rice blast disease, R.S. Zeigler, S.A. Leong, and P.S. Teng, eds (Wallingford, UK.: CAB International), pp. 211-229.
- Correll, J.C., Harp, T.L., Guerber, J.C., Zeigler, R.S., Liu, B., Cartwright, R.D., and Lee, F.N.** (2000). Characterization of *Pyricularia grisea* in the United States using independent genetic and molecular markers. *Phytopathology* **90**, 1396-1404.
- Costanzo, M., Baryshnikova, A., Bellay, J., Kim, Y., Spear, E.D., Sevier, C.S., Ding, H., Koh, J.L.Y., Toufighi, K., Mostafavi, S., Prinz, J., Onge, R.P.S., VanderSluis, B., Makhnevych, T., Vizeacoumar, F.J., Alizadeh, S., Bahr, S., Brost, R.L., Chen, Y., Cokol, M., Deshpande, R., Li, Z., Lin, Z.-Y., Liang, W., Marback, M., Paw, J., Luis, B.-J.S., Shuteriqi, E., Tong, A.H.Y., Dyk, N.v., Wallace, I.M., Whitney, J.A., Weirauch, M.T., Zhong, G., Zhu, H., Houry, W.A., Brudno, M., Ragibizadeh, S., Papp, B., Pál, C., Roth, F.P., Giaever, G., Nislow, C., Troyanskaya, O.G., Bussey, H., Bader, G.D., Gingras, A.-C., Morris, Q.D., Kim, P.M., Kaiser, C.A., Myers, C.L., Andrews, B.J., and Boone, C.** (2010). The genetic landscape of a cell. *Science* **327**, 425-431.
- Couch, B.C., and Kohn, L.M.** (2002). A multilocus gene genealogy concordant with host preference indicates segregation of a new species, *Magnaporthe oryzae*, from *M. grisea*. *Mycologia* **94**, 683-693.

- Crampin, H., Finley, K., Gerami-Nejad, M., Court, H., Gale, C., Berman, J., and Sudbery, P.** (2005). *Candida albicans* hyphae have a Spitzenkörper that is distinct from the polarisome found in yeast and pseudohyphae. *Journal of Cell Science* **118**, 2935-2947.
- Cutler, S.R., Ehrhardt, D.W., and Somerville, C.R.** (2000). Random GFP::cDNA fusions enable visualization of subcellular structures in cells of *Arabidopsis* at a high frequency. *Proceedings of the National Academy of Sciences* **97**, 3718-3723.
- Czymmek, K.J., Bourett, T.M., Sweigard, J.A., Carroll, A., and Howard, R.J.** (2002). Utility of cytoplasmic fluorescent proteins for live-cell imaging of *Magnaporthe grisea* in planta. *Mycologia* **94**, 280-289.
- Dean, R.A., Talbot, N.J., Ebbole, D.J., Farman, M.L., Mitchell, T.K., Orbach, M.J., Thon, M., Kulkarni, R., Xu, J.-R., Pan, H., Read, N.D., Lee, Y.-H., Carbone, I., Brown, D., Oh, Y.Y., Donofrio, N., Jeong, J.S., Soanes, D.M., Djonovic, S., Kolomiets, E., Rehmeier, C., Li, W., Harding, M., Kim, S., Lebrun, M.-H., Bohnert, H., Coughlan, S., Butler, J., Calvo, S., Ma, L.-J., Nicol, R., Purcell, S., Nusbaum, C., Galagan, J.E., and Birren, B.W.** (2005). The genome sequence of the rice blast fungus *Magnaporthe grisea*. *Nature* **434**, 980-986.
- DeJong, J.C., McCormack, B.J., Smirnov, N., and Talbot, N.J.** (1997). Glycerol generates turgor in rice blast. *Nature* **389**, 244-245.
- Denecke, J., Botterman, J., and Deblaere, R.** (1990). Protein Secretion in Plant Cells Can Occur via a Default Pathway. *The Plant Cell* **2**, 51-59.
- DeWit, P.J.G.M.d., Mehrabi, R., Burg, H.A.V.D., and Stergiopoulos, I.** (2009). Fungal effector proteins: past, present and future. *Molecular Plant Pathology* **10**, 735-747.
- Dodds, P.N., Lawrence, G.J., Catanzariti, A.-M., Ayliffe, M.A., and Ellis, J.G.** (2004). The *Melampsora lini* AvrL567 Avirulence Genes Are Expressed in Haustoria and Their Products Are Recognized inside Plant Cells. *The Plant Cell* **16**, 755-768.
- Dodds, P.N., Lawrence, G.J., Catanzariti, A., Teh, T., Wang, C.I., Ayliffe, M.A., Kobe, B., and Ellis, J.G.** (2006). Direct protein interaction underlies gene-for-gene specificity and coevolution of the flax resistance genes and flax rust avirulence genes. *Proc. Natl. Acad. Sci.* **103**, 8888-8893.
- Dou, D., Kale, S.D., Wang, X., Jiang, R.H.Y., Bruce, N.A., Arredondo, F.D., Zhang, X., and Tyler, B.M.** (2008). RXLR-mediated entry of *Phytophthora sojae* effector Avr1b into

- soybean cells does not require pathogen-encoded machinery. *The Plant Cell* **20**, 1930-1947.
- Drees, B.L., Sundin, B., Brazeau, E., Caviston, J.P., Chen, G.-C., Guo, W., Kozminski, K.G., Lau, M.W., Moskow, J.J., Tong, A., Schenkman, L.R., III, A.M., Brennwald, P., Longtine, M., Bi, E., Chan, C., Novick, P., Boone, C., Pringle, J.R., Davis, T.N., Fields, S., and Drubin, D.G.** (2001). A protein interaction map for cell polarity development. *The Journal of Cell Biology* **154**, 549-571.
- Ebbole, D.J.** (2007). *Magnaporthe* as a Model for Understanding Host-Pathogen Interactions. *Annual Review of Phytopathology* **45**, 437-456.
- FAO, F.a.A.O.** (2003). *World Agriculture Towards 2015/2030. An FAO Perspective*, J. Bruinsma, ed.
- FAO, F.A.A.O.O.T.U.N.** (2006). Part II. *World and Regional Review: Facts and Figures*. (Rome: Editorial Production and Design Group Publishing Management Service - FAO).
- FAO, F.A.A.O.O.T.U.N.** (2009). *Undernourishment around the world*. (Rome: Electronic Publishing Policy and Support Branch Communication Division FAO).
- Farman, M.L., and Leong, S.A.** (1998). Chromosome walking to the *AVRI-CO39* avirulence gene of *Magnaporthe grisea*. Discrepancy between the physical and genetic maps. *Genetics* **150**, 1049-1058.
- Fedorkin, O.N., Solovyev, A.G., Yelina, N.E., Jr, A.A.Z., Zinovkin, R.A., Mäkinen, K., Schiemann, J., and Morozov, S.Y.** (2001). Cell-to-cell movement of potato virus X involves distinct functions of the coat protein. *Journal of General Virology* **82**, 449-458.
- Fischer-Parton, S., Parton, R.M., Hickey, P.C., Dijksterhuis, J., Atkinson, H.A., and Read, N.D.** (2000). Confocal microscopy of FM4-64 as a tool for analysing endocytosis and vesicle trafficking in living fungal hyphae. *Journal of Microscopy* **198**, 246-259.
- Flor, H.H.** (1971). Current status of the gene-for-gene concept. *Annual Review of Phytopathology* **9**, 275-296.
- Gerbens-Leenesa, W., Hoekstra, A.Y., and Meerb, T.H.v.d.** (2009). The water footprint of bioenergy. *PNAS* **106**, 10219-10223.
- Gilbert, M.J., Thornton, C.R., Wakley, G.E., and Talbot, N.J.** (2006). A P-type ATPase required for rice blast disease and induction of host resistance. *Nature* **440**, 535-539.

- Giraldo, M.C., and Valent, B.** (Unpublished). Spitzenkörper and polarisome of *Magnaporthe oryzae* during biotrophic rice invasion.
- Giraldo, M.C et al.**, (Unpublished). Spitzenkörper and polarisome of *Magnaporthe oryzae* during biotrophic rice invasion.
- Gow, N.A.R., Brown, A.J.P., and Odds, F.C.** (2002). Fungal morphogenesis and host invasion. *Current Opinion in Microbiology* **5**, 366-371.
- Gurunathan, S., Chapman-Shimshoni, D., Trajkovic, S., and Gerst, J.E.** (2000). Yeast Exocytic v-SNAREs Confer Endocytosis. *Mol. Biol. Cell* **11**, 3629-3643.
- Hahn, M., Neef, U., Struck, C., Göttfert, M., and Mendgen, K.** (1997). A putative amino acid transporter is specifically expressed in haustoria of the rust fungus *Uromyces fabae*. *Molecular Plant Microbe Interactions* **10**, 438-445.
- Hamer, J.E., Howard, R.J., Chumley, F.G., and Valent, B.** (1988). A mechanism for surface attachment in spores of a plant pathogenic fungus. *Science* **239**, 288-290.
- Harris, S.D., Read, N.D., Roberson, R.W., Shaw, B., Seiler, S., Plamann, M., and Momany, M.** (2005). Polarisome meets Spitzenkorper: microscopy, genetics, and genomics converge. *Eukaryotic Cell* **4**, 225–229.
- Heath, M.C., Valent, B., Howard, R.J., and Chumley, F.G.** (1990a). Interactions of two strains of *Magnaporthe grisea* with rice, goosegrass, and weeping lovegrass. *Canadian Journal of Botany* **68**, 1627-1637.
- Heath, M.C., Valent, B., Howard, R.J., and Chumley, F.G.** (1990b). Correlations between cytologically detected plant - fungal interactions and pathogenicity of *Magnaporthe grisea* toward weeping lovegrass. *Phytopathology* **80**, 1382-1386.
- Heath, M.C., Howard, R.J., Valent, B., and Chumley, F.G.** (1992). Ultrastructural interactions of one strain of *Magnaporthe grisea* with goosegrass and weeping lovegrass. *Canadian Journal of Botany* **70**, 779-787.
- Howard, R.J., and Valent, B.** (1996). Breaking and Entering: Host penetration by the fungal rice blast pathogen *Magnaporthe grisea*. *Annual Review of Microbiology* **50**, 491-512.
- Howard, R.J., Ferrari, M.A., Roach, D.H., and Money, N.P.** (1991). Penetration of hard substrates by a fungus employing enormous turgor pressures. *Proc. Natl. Acad. Sci.* **88**, 11281-11284.

- Hulbert, S.H., Webb, C.A., Smith, S.M., and Sun, Q.** (2001). Resistance gene complexes: evolution and utilization. *Annual Review of Phytopathology* **39**, 285-312.
- Jia, Y., McAdams, S.A., Bryan, G.T., Hershey, H.P., and Valent, B.** (2000). Direct interaction of resistance gene and avirulence gene products confers rice blast resistance. *The EMBO Journal* **19**, 4004-4014.
- Jia, Y., Wang, Z., Fjellstrom, R.G., Moldenhauer, K.A.K., Azam, M.A., Correll, J., Lee, F.N., Xia, Y., and Rutger, J.N.** (2004). Rice *Pi-ta* gene confers resistance to the major pathotypes of the rice blast fungus in the United States. *Phytopathology* **94**, 296-301.
- Jiang, R.H.Y., Weide, R., Vondervoort, P.J.I.v.d., and Govers, F.** (2006). Amplification generates modular diversity at an avirulence locus in the pathogen *Phytophthora*. *Genome Research* **16**, 827-840.
- Johnston, G.C., Prendergast, J.A., and Singer, R.A.** (1991). The *Saccharomyces cerevisiae* MYO2 gene encodes an essential myosin for vectorial transport of vesicles. *J. Cell Biol.* **113**, 539-551.
- Jones, J.D.G., and Dangl, J.L.** (2006). The plant immune system. *Nature* **444**, 323-329.
- Jones, L.A., and Sudbery, P.E.** (2010). Spitzenkörper, Exocyst, and Polarisome Components in *Candida albicans* Hyphae Show Different Patterns of Localization and Have Distinct Dynamic Properties. *Eukaryotic Cell* **9**, 1455-1465.
- Kamoun, S.** (2007). Groovy times: filamentous pathogen effectors revealed *Current Opinion in Plant Biology* **10**, 358-365.
- Kämper, J., Kahmann, R., Bolker, M., Ma, L.-J., Brefort, T., Saville, B.J., Banuett, F., Kronstad, J.W., Gold, S.E., Muller, O., Perlin, M.H., Wosten, H.A.B., de Vries, R., Ruiz-Herrera, J., Reynaga-Pena, C.G., Snetselaar, K., McCann, M., Perez-Martin, J., Feldbrugge, M., Basse, C.W., Steinberg, G., Ibeas, J.I., Holloman, W., Guzman, P., Farman, M., Stajich, J.E., Sentandreu, R., Gonzalez-Prieto, J.M., Kennell, J.C., Molina, L., Schirawski, J., Mendoza-Mendoza, A., Greilinger, D., Munch, K., Rossel, N., Scherer, M., Vranes, M., Ladendorff, O., Vincon, V., Fuchs, U., Sandrock, B., Meng, S., Ho, E.C.H., Cahill, M.J., Boyce, K.J., Klose, J., Klosterman, S.J., Deelstra, H.J., Ortiz-Castellanos, L., Li, W., Sanchez-Alonso, P., Schreier, P.H., Hauser-Hahn, I., Vaupel, M., Koopmann, E., Friedrich, G., Voss, H., Schluter, T., Margolis, J., Platt, D., Swimmer, C., Gnirke, A., Chen, F., Vysotskaia, V.,**

- Mannhaupt, G., Guldener, U., Munsterkotter, M., Haase, D., Oesterheld, M., Mewes, H.-W., Mauceli, E.W., DeCaprio, D., Wade, C.M., Butler, J., Young, S., Jaffe, D.B., Calvo, S., Nusbaum, C., Galagan, J., and Birren, B.W.** (2006). Insights from the genome of the biotrophic fungal plant pathogen *Ustilago maydis*. *Nature* **444**, 97-101.
- Kankanala, P., Czymmek, K., and Valent, B.** (2007). Roles for rice membrane dynamics and plasmodesmata during biotrophic invasion by the blast fungus. *The Plant Cell* **19**, 19.
- Keitt, G.W.** (1915). Simple Technique for Isolating Single Spore Strains of Certain Types of Fungi. *Phytopathology* **5**, 266-269.
- Kemen, E., Kemen, A.C., Rafiqi, M., Hempel, U., Mendgen, K., Hahn, M., and Voegelé, R.T.** (2005). Identification of a Protein from Rust Fungi Transferred from Haustoria into Infected Plant Cells. *MPMI* **18**, 1130-1139.
- Khang, C.H., Park, S.-Y., Lee, Y.-H., and Kang, S.** (2005). A dual selection based, targeted gene replacement tool for *Magnaporthe grisea* and *Fusarium oxysporum*. *Fungal Genetics and Biology* **42**, 483-492.
- Khang, C.H., Berruyer, R., Giraldo, M.C., Kankanala, P., Park, S.-Y., Czymmek, K., Kang, S., and Valent, B.** (2010). Translocation of *Magnaporthe oryzae* effectors into rice cells and their subsequent cell-to-cell movement. *The Plant Cell* **22**, 16.
- Khush, G.S.** (2005). What it will take to Feed 5.0 Billion Rice consumers in 2030. *Plant Molecular Biology* **59**, 1-6.
- Knop, M., Miller, K.J., Mazza, M., Feng, D., Weber, M., Keränen, S., and Jäntti, J.** (2005). Molecular Interactions Position Mso1p, a Novel PTB Domain Homologue, in the Interface of the Exocyst Complex and the Exocytic SNARE Machinery in Yeast. *Molecular Biology of the Cell* **16**, 4543-4556.
- Koga, H., and Nakayachi, O.** (2004). Morphological studies on attachment of spores of *Magnaporthe grisea* to the leaf surface of rice. *Journal of General Plant Pathology* **70**, (1), 11-15, DOI: 10.1007/s10327-003-0085-4.
- Koga, H., Dohi, K., Nakayachi, O., and Mori, M.** (2004). A novel inoculation method of *Magnaporthe grisea* for cytological observation of the infection process using intact leaf sheaths of rice plants. *Physiological and Molecular Plant Pathology* **64**, 67-72.

- Krishnamurthy, K., Heppler, M., Mitra, R., Blancaflor, E., Payton, M., Nelson, R.S., and Verchot-Lubicz, J.** (2003). The Potato virus X TGBp3 protein associates with the ER network for virus cell-to-cell movement. *Virology* **309**, 135-151.
- Kulkarni, R.D., Thon, M.R., Pan, H.Q., and Dean, R.A.** (2005). Novel G-protein-coupled receptor-like proteins in the plant pathogenic fungus *Magnaporthe grisea*. *Genome Biol.* **6**, R24.
- Kuratsu, M., Taura, A., Shoji, J., Kikuchi, S., Arioka, M., and Kitamoto, K.** (2007). Systematic analysis of SNARE localization in the filamentous fungus *Aspergillus oryzae*. *Fungal Genetics and Biology* **44**, 1310-1323.
- Leach, J.E., Vera Cruz, C.M., Bai, J., and Leung, H.** (2001). Pathogen fitness penalty as a predictor of durability of disease resistance genes. *Annual Review of Phytopathology* **39**, 187-224.
- Leung, H., Borromeo, E.S., Bernardo, M.A., and Notteghem, J.L.** (1988). Genetic analysis of virulence in the rice blast fungus *Magnaporthe grisea*. *Phytopathology* **78**, 1227-1233.
- Lew, D.J., and Reed, S.I.** (1995). Cell cycle control of morphogenesis in budding yeast. *Curr. Opin. Genet. Dev.* **5**, 17-23.
- Li, W., Wang, B., Wu, J., Lu, G., Hu, Y., Zhang, X., Zhang, Z., Zhao, Q., Feng, Q., Zhang, H., Wang, Z., Wang, G., Han, B., Wang, Z., and Zhou, B.** (2009). The *Magnaporthe oryzae* Avirulence Gene *AvrPiz-t* Encodes a Predicted Secreted Protein That Triggers the Immunity in Rice Mediated by the Blast Resistance Gene *Piz-t*. *Mol Plant Microbe Interact.* **22**, 411-420.
- Lipatova, Z., Tokarev, A.A., Jin, Y., Mulholland, J., Weisman, L.S., and Segev, N.** (2008). Direct Interaction between a Myosin V Motor and the Rab GTPases Ypt31/32 Is Required for Polarized Secretion. *Molecular Biology of the Cell* **19**, 4177-4187.
- Lodish, H., Berk, A., Kaiser, C.A., Krieger, M., Scott, M.P., Bretscher, A., Ploegh, H., and Matsudaria, P.** (2008). Vesicular traffic, secretion, and endocytosis. In *Molecular Cell Biology*, K. Ahr, ed (New York, England: W. H. Freeman and Company), pp. 579.
- Lopez-Franco, R., Bartnicki-Garcia, S., and Bracker, C.E.** (1994). Pulsed growth of fungal hyphal tips. *Proc Natl Acad Science* **91**, 12228-12232.
- Maruyamaa, J., Kikuchia, S., and Kitamoto, K.** (2006). Differential distribution of the endoplasmic reticulum network as visualized by the BipA-EGFP fusion protein in hyphal

- compartments across the septum of the filamentous fungus, *Aspergillus oryzae* Fungal Genetics and Biology **43**, 642-654.
- Mellersh, D.G., and Heath, M.C.** (2001). Plasma membrane-cell wall adhesion is required for expression of plant defense responses during fungal penetration. *The Plant Cell* **13**, 413-424.
- Meyer, V., Arentshorst, M., Hondel, C.A.M.J.J.v.d., and Ram, A.F.** (2008). The polarisome component SpaA localises to hyphal tips of *Aspergillus niger* and is important for polar growth. *Fungal Genetics and Biology* **45**, 152-164.
- Mosquera, G., Giraldo, M.C., Khang, C.H., Coughlan, S., and Valent, B.** (2009). Interaction transcriptome analysis identifies *Magnaporthe oryzae* BAS1-4 as biotrophy-associated secreted proteins in rice blast disease. *The Plant Cell* **21**, 1273–1290
- Mosquera, G.M.** (2007). Analysis of the interaction transcriptome during biotrophic invasion of rice by the blast fungus, *Magnaporthe oryzae*. PhD Thesis, Department of Plant Pathology (Manhattan Kansas State University).
- Mullins, E.D., Chen, X., Romaine, P., Raina, R., Geiser, D.M., and Kang, S.** (2001). *Agrobacterium*-mediated transformation of *Fusarium oxysporum*: An efficient tool for insertional mutagenesis and gene transfer. *Phytopathology* **91**, 173-180.
- Oparka, K.J., Prior, D.A.M., Santa Cruz, S., Padgett, H.S., and Beachy, R.N.** (1997). Gating of epidermal plasmodesmata is restricted to the leading edge of expanding infection sites of tobacco mosaic virus (TMV). *The Plant Journal* **12**, 781-789.
- Oparka, K.J., Roberts, A.G., Boevink, P., Santa Cruz, S., Roberts, I., Pradel, K.S., Imlau, A., Kotlizky, G., Sauer, N., and Epel, B.** (1999). Simple, but not branched, plasmodesmata allow the nonspecific trafficking of proteins in developing tobacco leaves. *Cell* **97**, 743-754.
- Orbach, M.J., Farrall, L., Sweigard, J.A., Chumley, F.G., and Valent, B.** (2000). A Telomeric Avirulence Gene Determines Efficacy for the Rice Blast Resistance Gene *Pita*. *The Plant Cell* **12**, 2019-2032.
- Patkar, R.N., Suresh, A., and Naqvi, N.I.** (2010). MoTea4-Mediated polarized growth is essential for proper asexual development and pathogenesis in *Magnaporthe oryzae*. *Eukaryotic Cell* **9** (7), 1029-1038.

- Perfect, S.E., and Green, J.R.** (2001). Infection structures of biotrophic and hemibiotrophic fungal plant pathogens. *Molecular Plant Pathology* **2**, 101-108.
- Punt, P.J., Seiboth, B., Weenink, X.O., Zeijl, C.v., Lenders, M., Konetschny, C., Ram, A.F., Montijn, R., Kubicek, C.P., and Hondel, C.A.v.d.** (2001). Identification and characterization of a family of secretion-related small GTPase-encoding genes from the filamentous fungus *Aspergillus niger*: a putative SEC4 homologue is not essential for growth. *Mol Microbiol.* **41**, 513-525.
- Ravindran, S., and Boothroyd, J.C.** (2008). Secretion of Proteins into Host Cells by Apicomplexan Parasites. *Traffic* **9**, 647-656.
- Read, N.D., and Hickey, P.C.** (2001). The Vesicle trafficking network and tip growth in fungal hyphae. In *Cell Biology of plant and fungal tip growth*, A. Geitman, ed (Amsterdam: The Netherlands: IOS Press), pp. 137-147.
- Rehmany, A.P., Gordon, A., Rose, L.E., Allen, R.L., Armstrong, M.R., Whisson, S.C., Kamoun, S., Birch, P.R.J., and Beynon, J.L.** (2005). Differential recognition of highly divergent downy mildew avirulence gene alleles by RPP1 genes from two *Arabidopsis* lines. *The Plant Cell* **17**, 1839-1850.
- Rep, M., van der Does, H.C., Meijer, M., van Wijk, R., Houterman, P.M., Dekker, H.L., de Koster, C.G., and Cornelissen, B.J.C.** (2004). A small, cysteine-rich protein secreted by *Fusarium oxysporum* during colonization of xylem vessels is required for I-3-mediated resistance in tomato. *Molecular Microbiology* **53**, 1373-1383.
- Rho, H.-S., Kang, S., and Lee, Y.-H.** (2001). *Agrobacterium tumefaciens*-mediated Transformation of the Plant Pathogenic Fungus, *Magnaporthe grisea*. *Mol. Cells* **12**, 407-411.
- Ridout, C.J., Skamniotia, P., Porritta, O., Sacristana, S., Jones, J.D.G., and Brown, J.K.M.** (2006). Multiple Avirulence Paralogues in Cereal Powdery Mildew Fungi May Contribute to Parasite Fitness and Defeat of Plant Resistance *The Plant Cell* **18**, 2402-2414.
- Riedl, J., Crevenna, A.H., Kessenbrock, K., Yu, J.H., Neukirchen, D., Bista, M., Bradke, F., Jenne, D., Holak, T.A., Werb, Z., Sixt, M., and Wedlich-Soldner, R.** (2008). Lifeact: a versatile marker to visualize F-actin. *Nat. Methods* **5**, 605-607.

- Rooney, H.C.E., Klooster, J.W.v.t., Hoorn, R.A.L.v.d., Joosten, M.H.A.J., Jones, J.D.G., and DeWit, P.J.G.M.d.** (2005). *Cladosporium Avr2* Inhibits Tomato Rcr3 Protease Required for Cf-2–Dependent Disease Resistance. *Science* **308**, 1783-1786.
- Saitou, N., and Nei, M.** (1987). The neighbor-joining method: a new method for reconstructing phylogenetic trees. *Mol. Evol. Biol* **4**, 406-425.
- Sakamoto, M.** (1949). On the new method of sheath-inoculation of rice plants with blast fungus, *Pyricularia oryzae* Cav. for the study of the disease-resistant nature of the plant. *Bull Inst Agric Res Tohoku Univ.*, **1**, 120-129.
- Samaj, J., Baluska, F., Voigt, B., Schlicht, M., Volkmann, D., and Menzel, D.** (2004). Endocytosis, actin cytoskeleton, and signaling. *Plant Physiology* **135**, 1150-1161.
- Segev, N.** (2001). Ypt/Rab GTPases: Regulators of Protein Trafficking. *Sci. STKE*. doi:10.1126/stke.2001.100.re11.
- Simpson C., Thomas C., Findlay K., Bayer E., Maule A. J.** (2009). An Arabidopsis GPI-anchor plasmodesmal neck protein with callose binding activity and potential to regulate cell-to-cell trafficking. *Plant Cell* **21**, 581-594.
- Sheu, Y.J., Santos, B., Fortin, N., Costigan, C., and Snyder, M.** (1998). Spa2p interacts with cell polarity proteins and signaling components involved in yeast cell morphogenesis. *Mol. Cell. Biol.* **18**, 4053-4069.
- Shinsuke, M., Kotaro, M., Hideki, K., Keisuke, O., Taketo, A., Nobuko, Y., Satoru, F., Junko, S., Kazuyuki, H., Yoshikatsu, F., Toshihiko, N., Fusao, T., and Teruo, S.** (2009). Molecular cloning and characterization of the *AVR-Pia* locus from a Japanese field isolate of *Magnaporthe oryzae*. *Molecular Plant Pathology* **10**, 361-374.
- Shivas, J.M., Morrison, H.A., Bilder, D., and Skop, A.R.** (2010). Polarity and endocytosis: reciprocal regulation. *Trends in Cell Biology* **20**, 445-452.
- Shoji, J.-y., Arioka, M., and Kitamoto, K.** (2008). Dissecting cellular components of the secretory pathway in filamentous fungi: insights into their application for protein production. *Biotechnol Lett.* **30**, 7-14.
- Soderlund, C., Haller, K., Pampanwar, V., Ebbole, D., Farman, M., Orbach, M., Wang, G-L., Wing, R., Xu, J-R., Brown, D., Mitchell, T., and Dean, R.** (2006). MGOS: A Resource for Studying *Magnaporthe grisea* and *Oryza sativa* Interactions. *MPMI* **19**, 1055-1061.

- Söllner, T., Whiteheart, S.W., Brunner, M., Erdjument-Bromage, H., Geromanos, S., Tempst, P., and Rothman, J.E.** (1993). SNAP receptors implicated in vesicle targeting and fusion. *Nature* **362**, 318-324.
- Steinberg, G.** (2007a). Hyphal Growth: a Tale of Motors, Lipids, and the Spitzenkorper. *Eukaryotic Cell* **6**, 351-360.
- Steinberg, G.** (2007b). On the move: endosomes in fungal growth and pathogenicity. *Nature Reviews Microbiology* **5**, 309-316.
- Sudbery, P., and Court, H.** (2007). Polarised Growth in Fungi. In *The Mycota VIII. Biology of the Fungal Cell*, Howard/Gow, ed (Springer-Verlag Berlin Heidelberg), pp. 135-164.
- Sweigard, J.A., Carroll, A.M., Kang, S., Farrall, L., Chumley, F.G., and Valent, B.** (1995). Identification, cloning, and characterization of *PWL2*, a gene for host species specificity in the rice blast fungus. *The Plant Cell* **7**, 1221-1233.
- Talbot, N.J.** (2003). On the Trail of a Cereal Killer: Exploring the Biology of *Magnaphorthe grisea*. *Ann Rev Microbiol* **57**, 177-202.
- Tian, M., Benedetti, B., and Kamoun, S.** (2005). A Second Kazal-Like Protease Inhibitor from *Phytophthora infestans* Inhibits and Interacts with the Apoplastic Pathogenesis-Related Protease P69B of Tomato1. *Plant physiology* **138**, 1785-1793.
- Tian, M., Win, J., Song, J., Hoorn, R.v.d., Knaap, E.v.d., and Kamoun, S.** (2007). A *Phytophthora infestans* Cystatin-Like Protein Targets a Novel Tomato Papain-Like Apoplastic Protease. *Plant physiology* **143**, 364-377.
- Tong, A.H.Y., Evangelista, M., Parsons, A.B., Xu, H., Bader, G.D., Pagé, N., Robinson, M., Raghbizadeh, S., Hogue, C.W.V., Bussey, H., Andrews, B., Tyers, M., and Boone, C.** (2001). Systematic Genetic Analysis with Ordered Arrays of Yeast Deletion Mutants. *Science* **294**, 2364-2368.
- Valent, B.** (1990). Rice blast as a model system for plant pathology. *Phytopathology* **80**, 33-36.
- Valent, B.** (1997). The Rice Blast Fungus, *Magnaporthe grisea*. In *Plant Relationships*, Carrol/Tudzynski, ed (Berlin Heidelberg: Springer-Verlag), pp. 37-54.
- Valent, B., and Khang, C.H.** (2010). Recent advances in rice blast effector research. *Current Opinion in Plant Biology* **13**, 434-441.

- Valent, B., Farrall, L., and Chumley, F.G.** (1991). *Magnaporthe grisea* genes for pathogenicity and virulence identified through a series of backcrosses. *Genetics* **127**, 87-101.
- Valkonen, M.** (2003). Functional studies of the secretory pathway of filamentous fungi. The effect of unfolded protein response on protein production. In ESPOO 2003 (Helsinki, Finland: University of Helsinki).
- Valkonen, M., Kalkman, E.R., Saloheimo, M., Penttila, M., Read, N.D., and Duncan, R.R.** (2007). Spatially segregated SNARE protein interactions in living fungal cells. *The Journal of Biological Chemistry* **282**, 22775-22785.
- Veses, V., and Gow, N.A.R.** (2009). Pseudohypha budding patterns of *Candida albicans*. *Medical Mycology* **47**, 268 - 275.
- Wagner, W., Bielli, P., Wacha, S., and Ragnini-Wilson, A.** (2002). Mlc1p promotes septum closure during cytokinesis via the IQ motifs of the vesicle motor Myo2p. *EMBO J.* **21**, 6397-6408.
- Waignann, E., Lucas, W.J., Citovsky, V., and Zambryski, P.** (1994). Direct functional assay for tobacco mosaic virus cell-to-cell movement protein and identification of a domain involved in increasing plasmodesmal permeability. *Proc. Natl Acad. Sci.* **91**, 1433-1437.
- Wedlich-Soldner, R., Bolker, M., Kahmann, R., and Steinberg, G.** (2000). A putative endosomal t-SNARE links exo- and endocytosis in the phytopathogenic fungus *Ustilago maydis*. *The EMBO* **19**, 1974-1986.
- Whisson, S.C., Boevink, P.C., Moleleki, L., Avrova, A.O., Morales, J., Gilroy, E.M., Armstrong, M.R., Grouffaud, S., West, P.v., Chapman, S., Hein, I., Toth, I.K., Pritchard, L., and Birch, P.R.J.** (2007). A translocation signal for delivery of oomycete effector proteins inside host plant cells. *Nature* **450**, 115-118.
- Wilson, C., Bellen, H.J., and Gehring, W.J.** (1990). Position effects on eukaryotic gene expression. *Annu. Rev. Cell Bio* **6**, 679-714.
- Wilson, R.A., and Talbot, N.J.** (2009). Under pressure: investigating the biology of plant infection by *Magnaporthe oryzae*. *Nature Reviews Microbiology* **7**, 185-195
- Yan, X., Gonzales, R.A., and Wagner, G.J.** (1997). Gene fusions of signal sequences with a modified β -glucuronidase gene results in retention of the β -glucuronidase protein in the secretory pathway/plasma membrane. *Plant physiology* **115**, 915-924

- Yi, M., Chi, M.-H., Khang, C.H., Park, S.-Y., Kang, S., Valent, B., and Lee, Y.-H.** (2009). The ER Chaperone LHS1 Is Involved in Asexual Development and Rice Infection by the Blast Fungus *Magnaporthe oryzae*. *The Plant Cell* **21** (2), 681-95.
- Yoshida, K., Saitoh, H., Fujisawa, S., Kanzaki, H., Matsumura, H., Yoshida, K., Tosa, Y., Chuma, I., Takano, Y., Win, J., Kamoun, S., and Terauchia, R.** (2009). Association Genetics Reveals Three Novel Avirulence Genes from the Rice Blast Fungal Pathogen *Magnaporthe oryzae*. *The Plant Cell* **21**, 1573-1591.
- Zambryski, P., and Crawford, K.** (2000). Plasmodesmata: Gatekeepers for cell-to-cell transport of developmental signals in plants. *Annu. Rev. Cell Dev. Biol.* **16**, 393-421.
- Zhang, H., Chen, J., Wang, Y., Peng, L., Dong, X., Lu, Y., Keating, A.E., and Jiang, T.** (2009). A computationally guided protein-interaction screen uncovers coiled-coil interactions involved in vesicular trafficking. *Journal of Molecular Biology* **392**, 228-241.
- Zheng, W., Chen, J., Liu, W., Zheng, S., Zhou, J., Lu, G., and Wang, Z.** (2007). A Rho3 Homolog Is Essential for Appressorium Development and Pathogenicity of *Magnaporthe grisea*. *Eukaryotic Cell* **6**, 2240-2250.
- Zheng, W., Zhao, Z., Chen, J., Liu, W., Ke, H., Zhou, J., Lu, G., Darvill, A.G., Albersheim, P., Wu, S., and Wang, Z.** (2009). A Cdc42 ortholog is required for penetration and virulence of *Magnaporthe grisea*. *Fungal Genet Biol.* **46**, 450-460.